UCRL 9023

UNIVERSITY OF CALIFORNIA

Ernest O. Lawrence Radiation Laboratory

DOWNFLOW BOILING AND NONBOILING HEAT TRANSFER IN A UNIFORMLY HEATED TUBE

TWO-WEEK LOAN COPY

This is a Library Circulating Copy which may be borrowed for two weeks. For a personal retention copy, call Tech. Info. Division, Ext. 5545

DISCLAIMER

This document was prepared as an account of work sponsored by the United States Government. While this document is believed to contain correct information, neither the United States Government nor any agency thereof, nor the Regents of the University of California, nor any of their employees, makes any warranty, express or implied, or assumes any legal responsibility for the accuracy, completeness, or usefulness of any information, apparatus, product, or process disclosed, or represents that its use would not infringe privately owned rights. Reference herein to any specific commercial product, process, or service by its trade name, trademark, manufacturer, or otherwise, does not necessarily constitute or imply its endorsement, recommendation, or favoring by the United States Government or any agency thereof, or the Regents of the University of California. The views and opinions of authors expressed herein do not necessarily state or reflect those of the United States Government or any agency thereof or the Regents of the University of California.

UCRL-9023
Chemistry-Gen. UC-4
TID-4500 (15th Ed.)

UNIVERSITY OF CALIFORNIA
Lawrence Radiation Laboratory
Berkeley, California

Contract No. W-7405-eng-48

DOWNFLOW BOILING AND NONBOILING HEAT TRANSFER IN A UNIFORMLY HEATED TUBE

Robert LeRoy Sani

(M. S. Thesis)

January 4, 1960

Printed for the U. S. Atomic Energy Commission

Printed in USA. Price $2.50. Available from the
Office of Technical Services
U. S. Department of Commerce
Washington 25, D.C.

Table of Contents

	page
Nomenclature	iv
I. Abstract	1
II. Introduction	2
A. General	2
B. Forced-Convection Boiling of Saturated Liquids	3
a. Dengler	3
b. Mumm	5
c. Schrock and Grossman	6
C. Local Pressure Gradients in Forced-Convection Vaporization	7
III. Experimental Equipment	9
A. Flow System	9
B. Test Section	11
C. Power Supply	12
D. Instrumentation	12
a. Temperature Measurement	12
b. Pressure Measurement	14
c. Power Supply	16
d. Flow-Rate Measurement	17
IV. Experimental Procedure	18
V. Calculation Procedures	20
A. Inner Wall Temperature	20
B. Nonboiling Heat Transfer Calculations	21
C. Boiling Heat Transfer Calculations	23

Table of Contents (Continued)

page

D. Local Fluid Properties 24

E. Local Total Pressure Gradients 24

VI. Discussion 26

A. Nonboiling Heat Transfer 26

B. Boiling Heat Transfer 27

C. Entrance Effect 31

D. Local Total Pressure Gradients 34

E. Amplitude and Frequency of Local Pressure Fluctuations 35

VII. Conclusions 37

VIII. Graphical Results 39

IX. Appendices 54

A. Determination of Inner Wall Temperature 54

B. Tabulated Results 59

Table I 60

Table II 61

C. Sample Calculations 79

a. Vapor Mass Fraction 79

b. Martinelli Parameter 84

c. Boiling Heat Transfer Coefficients 84

d. Nonboiling Heat Transfer Coefficient (Boiling Runs) 85

e. Boiling Number 86

X. Bibliography 87

NOMENCLATURE

Symbol	Definition	Unit
A	Area	ft^2
Bo	Boiling Number $q/h_{fg}G_T$	dimensionless
C	Specific Heat	BTU/lb °F
D	Inside Diameter	ft
E	Voltage Drop	volts
f	Blasius Friction Factor	dimensionless
g	Acceleration of Gravity	ft /sec^2
g_c	Conversion Factor	ft lb_m/sec^2 lb_f
G	Mass Flux	lb /sec ft^2
h	Specific Enthalpy or	BTU/lb
	Heat-Transfer Coefficient	BTU/hr ft^2 °F
J	Joule's Constant	ft lb /BTU
k	Thermal Conductivity	BTU/hr ft °F
ℓ	Distance from Entrance of Heated Section	ft
L	Total Length of Heated Section	ft
m	Mass Flow Rate	lb /sec
Nu	Nusselt Number	dimensionless
p	Pressure	psia
P	Electrical Power	kilowatts
Pr	Prandtl Number	dimensionless
q	Heat Flux	BTU/hr ft^2
Q	Total Heat Input	BTU/hr
r	Radius	ft
R	Electrical Resistance	ohms

NOMENCLATURE (Continued)

Symbol	Definition	Unit
Re	Reynolds Number	dimensionless
R_ℓ	Liquid Holdup	dimensionless
T	Temperature	°F
ΔT	Temperature Difference = $(T_i - T_b)$	°F
v	Specific Volume	ft^3/lb
V	Velocity or Volume	ft /sec ; ft^3
x	Quality (mass fraction of vapor)	dimensionless
X_{tt}	Martinelli Parameter = $(\mu_f/\mu_g)^{0.1}(v_f/v_g)^{0.5}(1-x/x)^{0.9}$	dimensionless
α	Linear Temperature Coefficient of Thermal Conductivity	$°F^{-1}$
γ	Linear Temperature Coefficient of Electrical Resistance	$°F^{-1}$
	Density	lb/ft^3
μ	Viscosity	centipoise
σ	Surface Tension	lb /ft

Subscripts

b	Evaluated at bulk fluid properties
B	Boiling
f	Properties of saturated liquid
fg	Difference in property between saturated liquid and vapor
g	Properties of saturated vapor
i	Inner wall

NOMENCLATURE (Continued)

Subscripts

ℓ	Property evaluated on basis of local liquid flow rate
o	Outer wall or property evaluated on basis of total mass flow rate.
T	total
w	Property evaluated at inner wall temperature
m	Mean value
1	Property preceding flashing valve

Superscripts

0	First approximation
1	Second approximation

DOWNFLOW BOILING AND NONBOILING HEAT TRANSFER IN A UNIFORMLY HEATED TUBE

Robert LeRoy Sani

Lawrence Radiation Laboratory and Department of Chemistry
University of California, Berkeley, California

January 4, 1960

I. ABSTRACT

Local heat-transfer coefficients in forced convection, downflow boiling, and nonboiling have been measured by use of an electrically heated type-304 stainless steel tube (0.7194 in. i.d. x 0.7502 in. o.d. x 68.0 in. long). Average forced-convection heat-transfer coefficients in turbulent one-phase flow and local total pressure gradients in two-phase flow were also determined.

Data have been obtained for the boiling of distilled water with mass fluxes of 51 to 165 lb /sec ft.^{2}, heat fluxes from $13.8 \cdot 10^3$ to $49.8 \cdot 10^3$ BTU/hr ft ^{2}, pressures from 15.8 to 30.9 psia, and qualities up to 14%.

The boiling heat transfer data were compared to the correlations proposed by Mumm, Dengler, Rohsenow, and Grossman and Schrock. No attempt was made to formulate a new correlation because of the limited range of conditions investigated. The nonboiling heat transfer data were compared to the Dittus-Boelter and Sieder-Tate correlations. The local total pressure gradients in two-phase flow were correlated by the Martinelli parameter, X_{tt}, for turbulent two-phase flow.

II. INTRODUCTION

A. General

Recently attention has been focused on the problem of removing tremendous quantities of heat from small spaces. Conventional heat-transfer methods do not even approach the solution to this problem. A solution to the problem seems to lie in the realm of forced-convection boiling heat transfer. Heat-transfer processes which involve a change in phase can accommodate very large heat fluxes. Until recently little attention had been directed to boiling of saturated liquids (net boiling) in forced convection. This is a very complex problem. Even the flow mechanism encountered in isothermal two-phase flow isn't understood. In the two-phase flow of a liquid and its vapor an additional degree of freedom, the quality of the mixture, is encountered. When heat transfer which effects a phase change is superimposed on this complex flow mechanism, the analytical complexity of the problem becomes intractable.

Downflow systems operated at moderate pressures are important in the food industry and in one of the proposed processes for the conversion of sea water to fresh water. The food industry uses downflow evaporators in the concentration of juices. Prolonged retention of the juices at high temperatures is injurious to their flavor. The short retention time in downflow evaporators causes minimum flavor damage. For desalting of sea water to be economically feasible, multiple-effect evaporation units must be used, and effective use must be made of the surface available for heat transfer. The staging of units means that

small temperature driving forces will be encountered. In an upflow system inefficient use of heat-transfer surface is caused by the hydrostatic head, which prevents boiling in the lower sections of the evaporator. This has led to the use of downflow systems.

Previous work in this field has mainly been directed to upflow systems which were operated at elevated pressures and large heat fluxes. This work was undertaken to extend this to a downflow system operated over a range of low heat fluxes and low pressures.

B. Forced-Convection Boiling of Saturated Liquids

The three notable works published in the field of forced-convection boiling of water were due to Dengler (1), Mumm (11), and Schrock and Grossman (13).

a. Dengler

Dengler's upflow system consisted of a 1-in. i.d., 20-ft. vertical copper tube. Five steam jackets were spaced along the tube and twenty-one thermocouples were embedded in the tube wall. Local static pressures were obtained by a manometer system, and local heat fluxes were determined by collecting condensate. Saturated feed was introduced to the test section and the mass flow rate was varied from $2.4 \cdot 10^2$ to $5.5 \cdot 10^3$ lb /hr. The outlet pressure varied from 7.2 to 29 psia. The mass fraction of vapor (quality) was varied from 0 to 100%. The local volumetric fraction of liquid was determined by a radioactive tracer technique. It was postulated that the local heat-transfer coefficients at low flow rates and qualities were governed by

the combined influence of boiling and forced convection. As the linear velocity of the vapor-liquid mixture increased, the nucleate boiling mechanism was suppressed and the forced convection heat transfer mechanism was the dominant factor. The correlation in the region of suppressed nucleate boiling was

$$\frac{h_B}{h_0} = 3.5\, X_{tt}^{-0.5} ;$$

h_0 is the nonboiling heat-transfer coefficient calculated from the Dittus-Boelter relationship,

$$h_0 = 0.023 \frac{k_\ell}{D} Re_{T,\ell}^{0.8}\, Pr_\ell^{0.4} .$$

The physical properties were those of the liquid state evaluated at the local saturation temperature, and the Reynolds number, DG_T/μ_ℓ, was based on the total mass flow rate.

X_{tt} is the Lockhart-Martinelli parameter defined by

$$X_{tt} = \left(\frac{V_f}{V_g}\right)^{0.5} \left(\frac{\mu_f}{\mu_g}\right)^{0.1} \left(\frac{1-x}{x}\right)^{0.9} .$$

This was originally developed for the correlation of pressure drop in two-phase, two-component flow. Its possibility as a correlating parameter for heat transfer in two-phase flow was suggested by Lockhart and Martinelli (9).

In the entrance regions of the test section Dengler observed h_B/h_0 values which were larger than those predicted by the correlation. Dengler postulated that this was the region in which the nucleate boiling mechanism was predominant. The boiling was suppressed as the linear velocity of the liquid increased. A temperature difference to initiate nucleate boiling, ΔT_1, was defined by

$$\Delta T_i = 10\left(\frac{G_T V_\ell}{R_\ell}\right)^{0.3} .$$

This was applied as a criterion for nucleate boiling Dengler obtained no correlation between the liquid velocity and ΔT_i when a fog flow model was used. ΔT_i was then nondimensionalized in an arbitrary manner, and the data were correlated by dividing h_B/h_0 by the factor

$$0.673\left[(T_w - T_b - \Delta T_i)\left(\frac{dp}{dT}\right)_{sat.}\frac{D}{\sigma}\right]^{0.1}$$

when this group was greater than one. The form of the factor seems inappropriate and its significance vague. It did succeed in reducing the scatter of the data.

b. Mumm

Mumm's system consisted of an electrically heated, horizontal, type-347 stainless steel tube which was 0.465 in. i.d. and 7 ft long. Local heat-transfer coefficients were measured for exit qualities up to 60%. The investigation covered a range of pressures from 45 to 200 psia, heat fluxes from $5 \cdot 10^4$ to $2.5 \cdot 10^5$ BTU/hr ft^2, and mass flow rates from 70 to 280 lb per sec ft.^{2} The data for qualities less than 40% were correlated by

$$Nu_B = \left[4.3 + 5\cdot 10^{-4}\left(\frac{V_{fg}}{V_f}\right)^{1.64} X\right]\left(\frac{q}{G_T h_{fg}}\right)^{0.464} Re_\ell^{0.808} ,$$

with a standard deviation of ±10%.

c. Schrock and Grossman

The upflow system of Schrock and Grossman consisted of an electrically heated 1/8-in. i.d. type-347 stainless steel tube which was 20 in. long. Local heat-transfer coefficients were measured for qualities from 0 to 50% at heat fluxes of $6 \cdot 10^4$ to $6 \cdot 10^5$ BTU/hr ft^2, pressures from 50 to 200 psia, and mass fluxes of 255 to 605 lb/sec ft^2. The data were correlated in two flow regimes. For very low vapor qualities where nucleate boiling was considered predominant, the data were correlated by

$$\frac{h_B}{h_\ell} = 1.15 \cdot 10^{-5}\, q \; .$$

Since the scatter of the data in this region was large, the validity of this correlation seems dubious. At higher qualities the high values of the heat-transfer coefficients were attributed to forced convection due to high vapor velocities and mass transfer from the annular liquid layer to the vapor core. The data were correlated by

$$\frac{h_B}{h_\ell} = 2.5\, X_{tt}^{-0.75} \; ,$$

where h_ℓ is the local nonboiling heat-transfer coefficient calculated from the Dittus-Boelter correlation. The physical properties were assumed to be those of the liquid state at the prevailing saturation temperature. The Reynolds number was evaluated at the local liquid mass flow rate and not the total mass flow rate as used by Dengler; X_{tt} is the Lockhart-Martinelli parameter.

Schrock and Grossman (14) have recently extended their reported experimental data. The new data indicated the importance of the boiling number which was defined by Mumm (11). At very high boiling numbers the heat-transfer coefficient proved to be nearly independent of the Martinelli parameter. As the boiling number was decreased the heat-transfer coefficients became more dependent upon the Martinelli parameter. All their experimental data were correlated by

$$\frac{Nu_B}{Pr_\ell^{1/3} Re_\ell^{0.8}} = 1.7 \cdot 10^2 \left[\left(\frac{q}{h_{fg} G_T} \right) + 1.5 \cdot 10^{-4} \; X_{tt}^{-2/3} \right],$$

with a standard deviation of ±35%.

C. Local Pressure Gradients in Forced-Convection Vaporization

The most extensive investigation in this field is due to Grossman and Schrock (6). They obtained data for 1/8 to 1/2-in. i.d. electrically heated stainless steel tubes 15 and 20 in. in length. The system was the same one discussed in Section B. They investigated mass fluxes of 200 to 700 lb /sec ft^2, heat fluxes of $1 \cdot 10^5$ to $8 \cdot 10^5$ BTU/hr ft^2, exit qualities up to 50%, and pressures from 50 to 400 psia. A correlation was obtained between the local total pressure gradient and the Lockhart-Martinelli parameter. Their data were correlated to ±15%. By assuming a slip-flow model and using Dengler's holdup data, the Lockhart-Martinelli correlation for frictional pressure drop in two-phase flow was verified. A better correlation was obtained for the local total pressure gradient than for the local frictional pressure gradient. This was due in part to the

inapplicability of the slip-flow model. The advantage of this type of correlation over previously suggested ones (10) is that it greatly simplifies design calculations.

III. EXPERIMENTAL EQUIPMENT

A. Flow System

The flow system consisted of a semi-closed loop. Two vented 50-gallon stainless steel barrels were used for storing the distilled water. One was placed on a Toledo dial scale to facilitate the measurement of a mass flow rate. By an auxiliary piping and valve arrangement either one of the barrels could be used as a source for the feed pump. A filter constructed from small-mesh stainless steel screen was inserted in the system between the feed barrels and the feed pump. The feed pump was a Waukeshaw 10 DO stainless steel gear pump with a rating of 4000 lb /hr at 60 psig discharge pressure and 700 rpm. The speed of the pump was controlled by a Reeves Vari-speed Motodrive. A surge tank was installed near the pump's discharge end to smooth out any pressure fluctuations induced in the feed by the pump.

Two steam preheaters connected in series were used to preheat the feed to the desired temperature. Each preheater contained a bundle of four 1/4-in. o.d. copper tubes which were 10 ft long. The steam pressure in the first preheater was manually controlled by means of a Spence pressure regulator. The steam pressure in the second preheater was controlled by a Taylor diaphragm valve model 4VQ255. The diaphragm valve was actuated by a Taylor indicating pressure controller model 162RM123, which had proportional and reset modes. The sensing element of the controller, an Accuratus temperature-compensated stainless steel thermometer, was inserted in the flow circuit

at the outlet of the second preheater.

The flashing valve consisted of a globe valve which was controlled from the main control panel. On the downstream side of the flashing valve a high-pressure Pyrex sight glass was installed so that a visual inspection of the two-phase flow pattern could be made. The distilled water was degassed before each run by causing hot, high-pressure water to flash when passed through the flashing valve.

The vapor-liquid mixture was separated by means of an insulated cyclone separator. Negligible entrainment of the liquid in the vapor stream was encountered, as proven by tests. Soluble salts were dissolved in the liquid phase, and then an analysis for the salts was performed on the vapor-phase condensate. Such tests showed that under the vapor-liquid loads experienced in this work there was negligible entrainment. A two-pass condenser in which cooling water was run through six 1-in. o.d. copper tubes was attached to the vapor outlet of the condenser. On the liquid outlet an intercooler had to be installed to stop cavitation from occuring in the liquid return pump.

Through a solenoid valve arrangement the vapor condensate and liquid flows to the feed barrel could be diverted into separate 50-gallon stainless steel barrels located on beam balances. This was done to obtain the mass flow rates of the vapor condensate and liquid streams.

All interconnecting piping was of 304 stainless steel. The test section and all interconnecting piping from the flashing

valve to the test section was heavily insulated. Figure 1 is a flow diagram and Figures 2 to 5 are photographs of the installed equipment. The insulation was a 7-in. layer of glass wool.

B. Test Section

The test section was constructed of 304 stainless steel tubing which had a 0.7502-in. o.d. and a 0.0154-in. wall thickness. Two copper sleeves were silver-soldered on the test section to provide adequate electrical connection. These sleeves insured a uniformly distributed current density at the entrance and exit of the test section.

Nine pressure taps were distributed along the test section. They were constructed by silver-soldering 1-in. x 3/16-in. stainless steel tubes to the test section, and then drilling a 0.040-in. (No. 60 drill size) hole through the test section wall. These were electrically isolated from the rest of the pressure-measuring circuit by 3-in. sections of 1/4-in. i.d. Fisher-Porter glass pipe.

Sixteen copper-constantan thermocouples were spaced approximately every 6 in. along the test section. They were fabricated by soldering the junctions directly to the outer tube wall. The thermocouple wires were wrapped around the tube three times before leading the wires to the measuring circuit. This was done to eliminate the effect of longitudinal heat conduction along the thermocouple wires. The thermocouple wires were then taped to the test section with pressure-sensitive high-temperature glass tape.

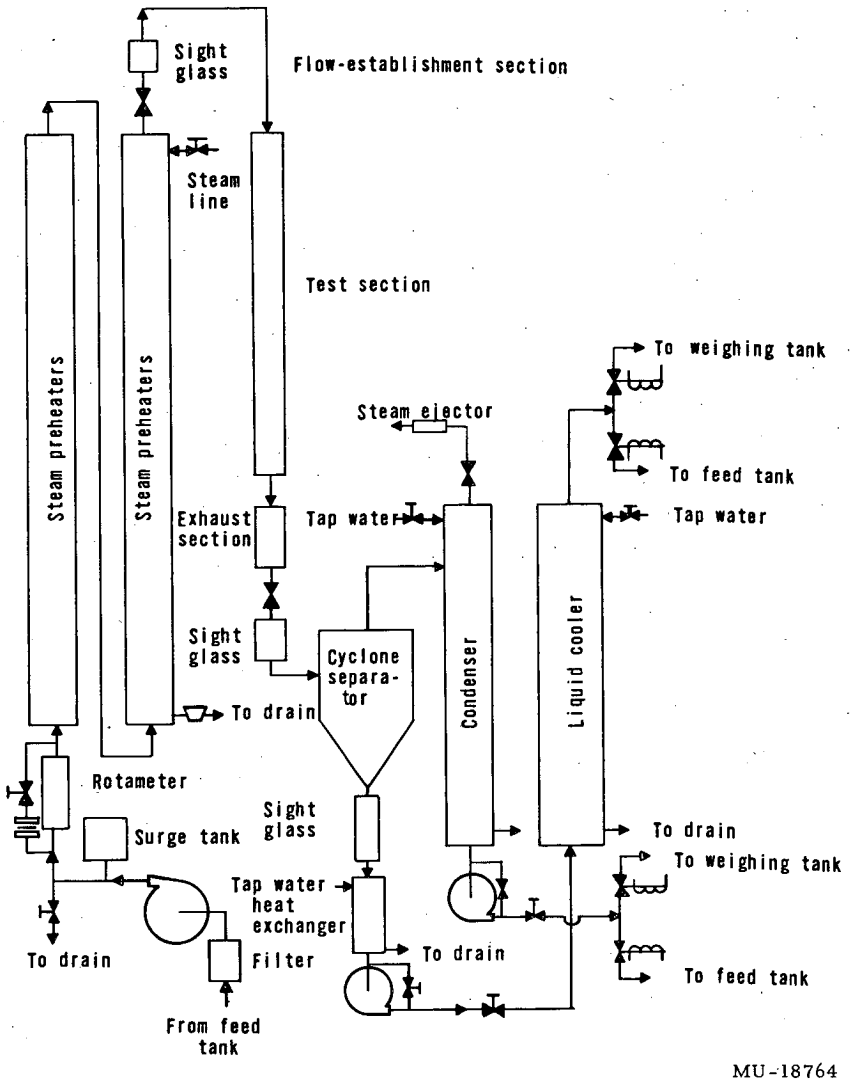

Fig. 1. Schematic diagram of flow system.

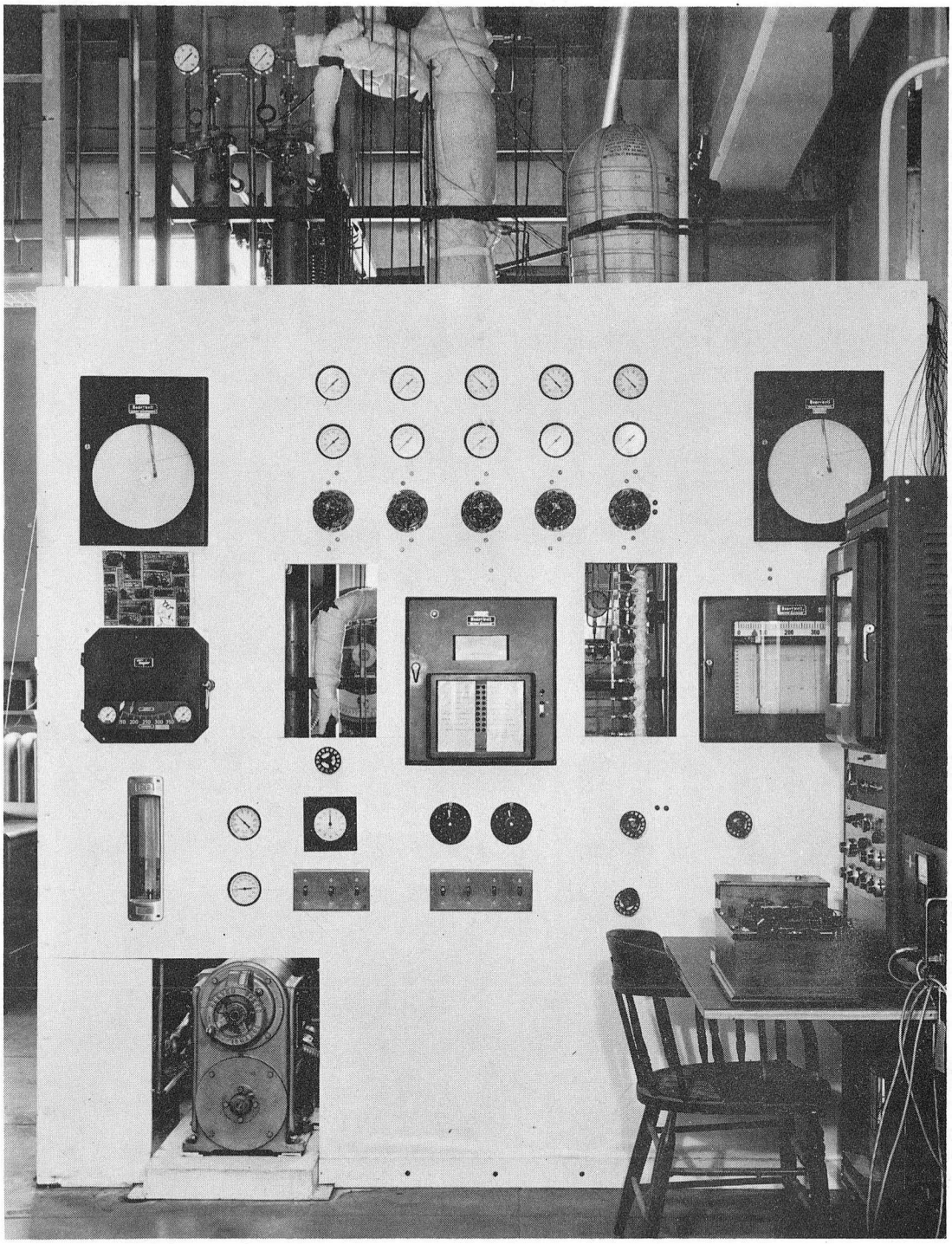

ZN-2311

Fig. 2. Control panel.

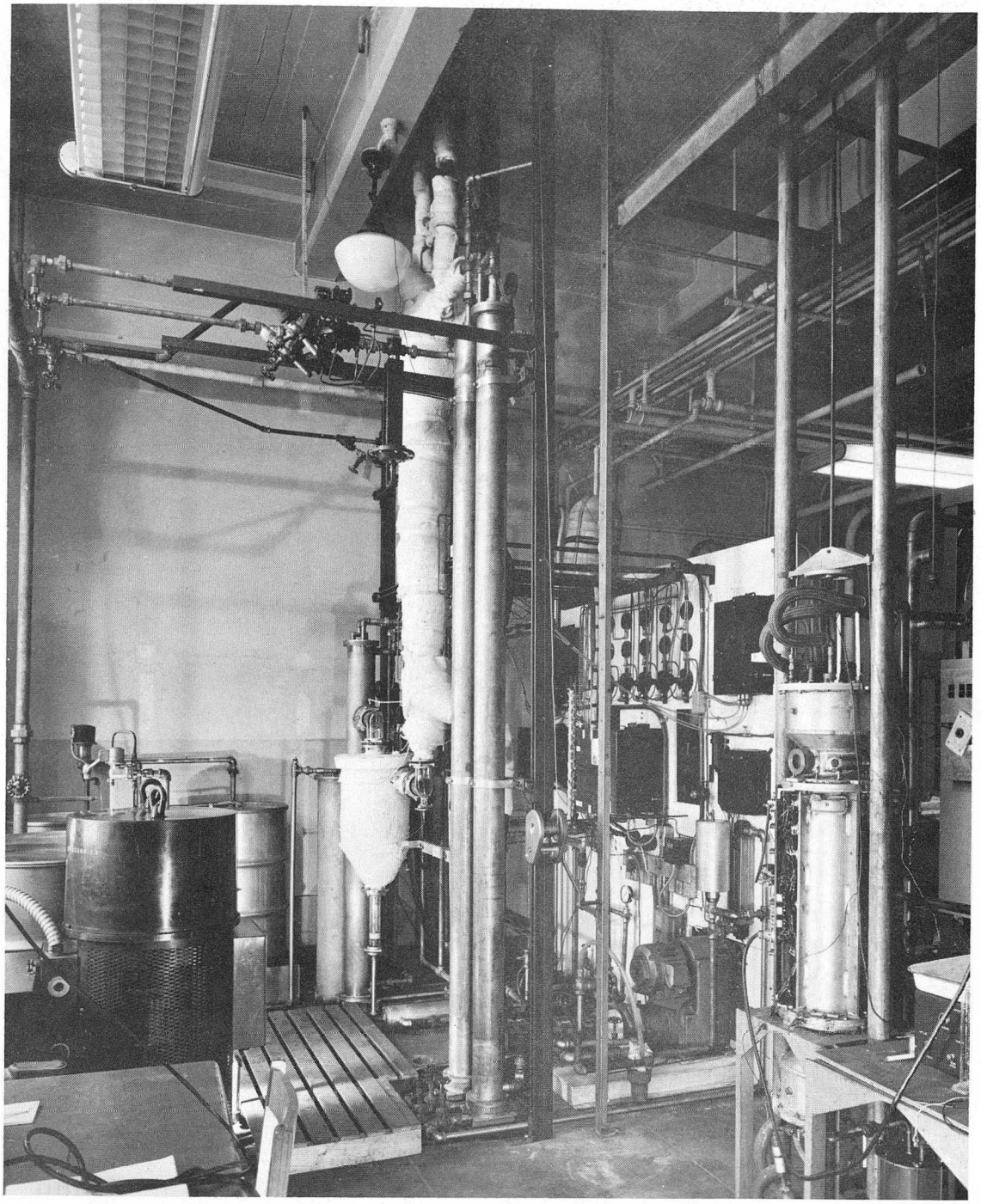

ZN-2312

Fig. 3. Flow system.

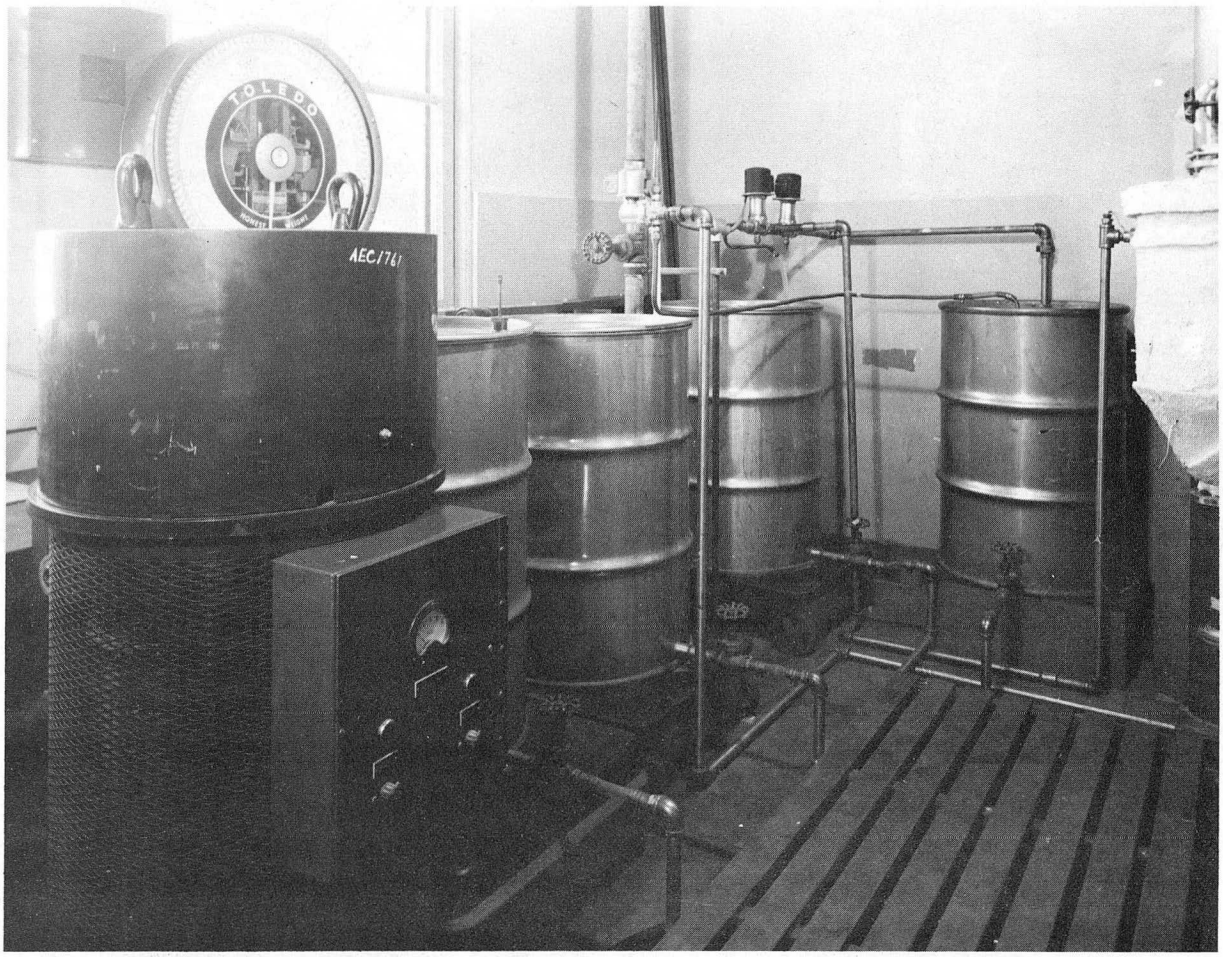

ZN-2313

Fig. 4. Storage tanks and power supply.

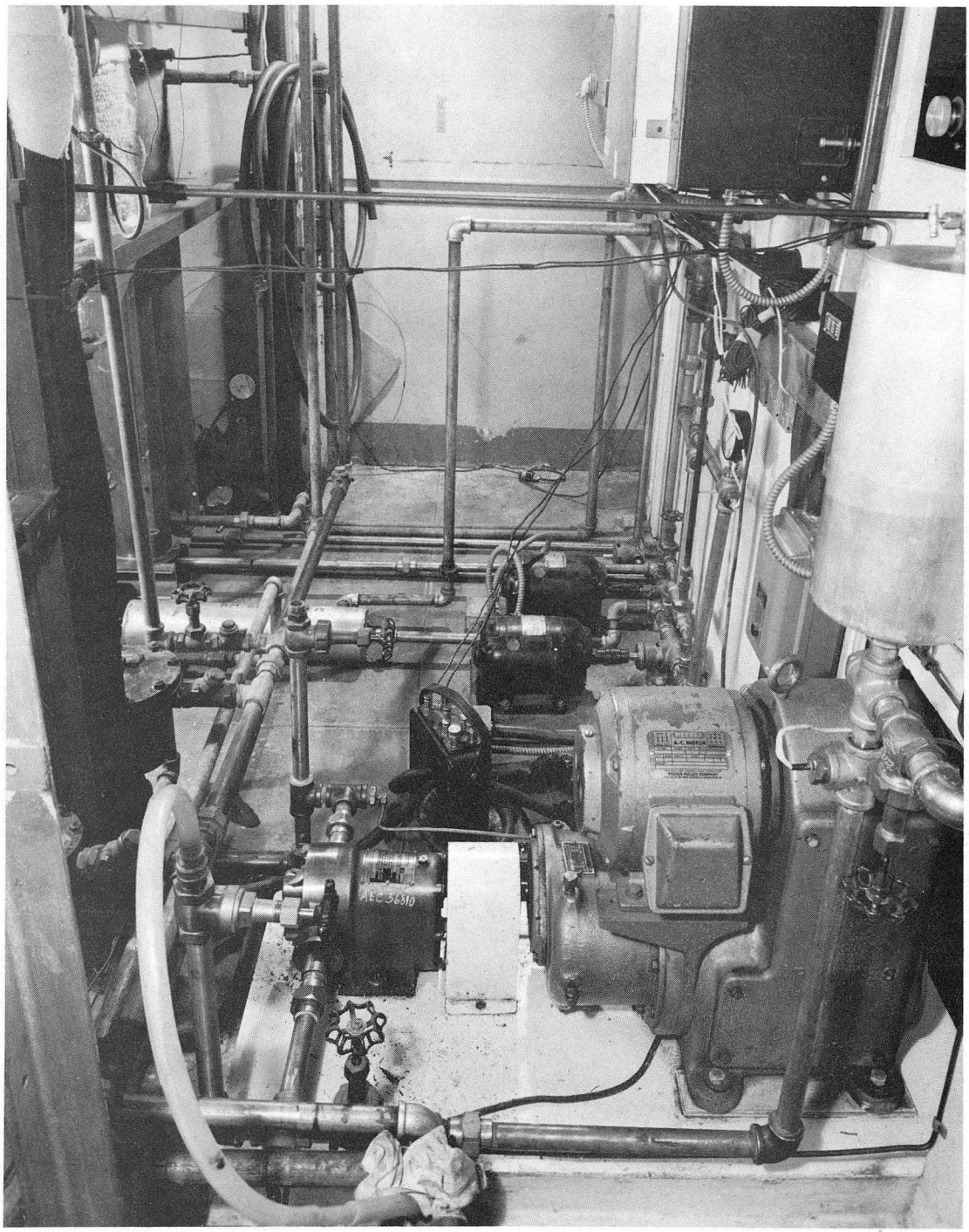

ZN-2314

Fig. 5. Pumping installation.

The test section was connected to the auxiliary flow system by stainless steel conical fittings. These fittings were silver-soldered on the ends of the test section. Teflon gaskets were used to electrically isolate the test section.

Thermal insulation was effected by first wrapping the test section with a 3/4-in. layer of Johns-Manville asbestos woven tape and then with a 7-in. layer of glass wool insulation.

The bottom of the test section was securely anchored, and a hook was attached to the top so that a vertical force could be applied to prevent buckling.

See Figures 6 and 7 for complete details of the construction of the test section, Figures 8 and 9 for photographs.

C. Power Supply

An air-cooled stepdown transformer was used to supply power to the test section. It could deliver a maximum of 25 kva. With 230 v, 150 amp on its primary the transformer would deliver 40 v, 875 amp at its secondary. The voltage to the primary of the step-down transformer was regulated by a General Electric induction regulator. The voltage regulator operated at 60-cycle, single-phase, 25-kva continuous duty with a 240-v primary voltage. The output voltage of the regulator was varied continuously over its output range by means of an electric motor.

D. Instrumentation

a. Temperature Measurement

Iron-constantan thermocouples were placed in insulated

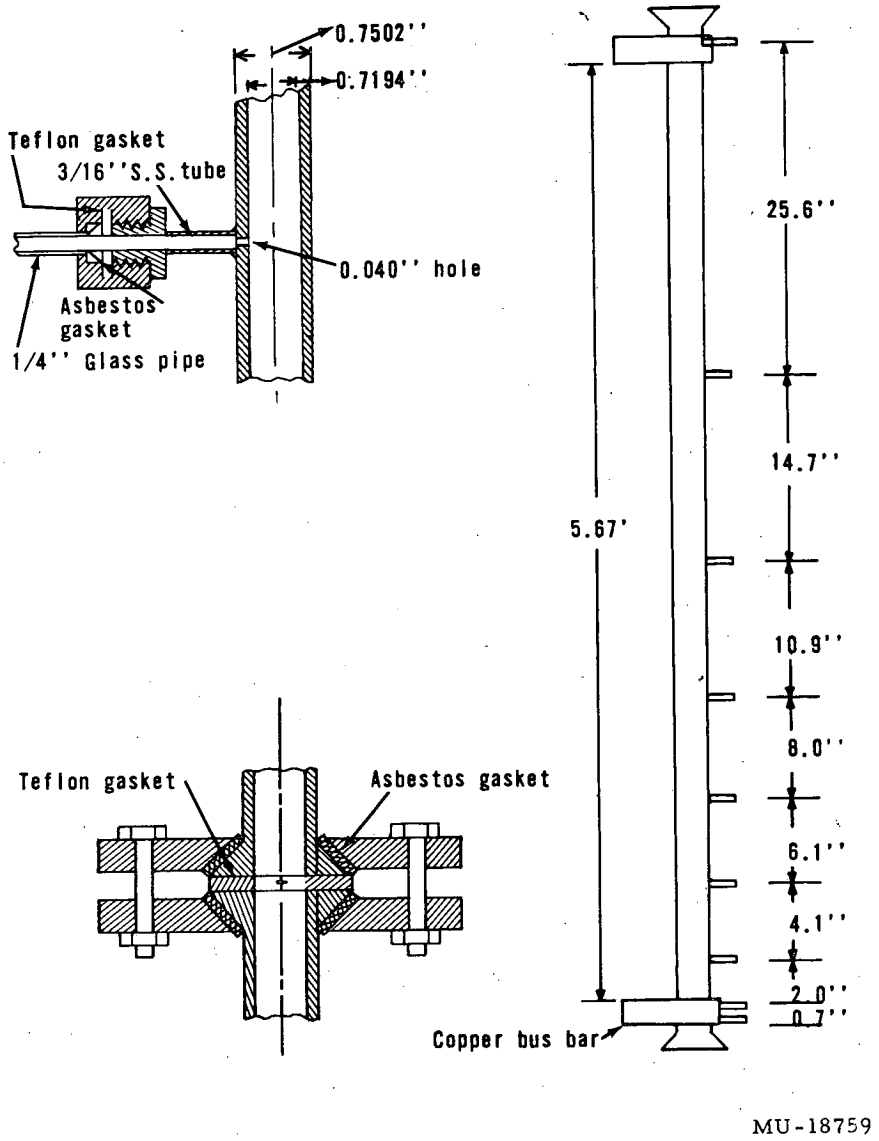

Fig. 6. Detail of test section.

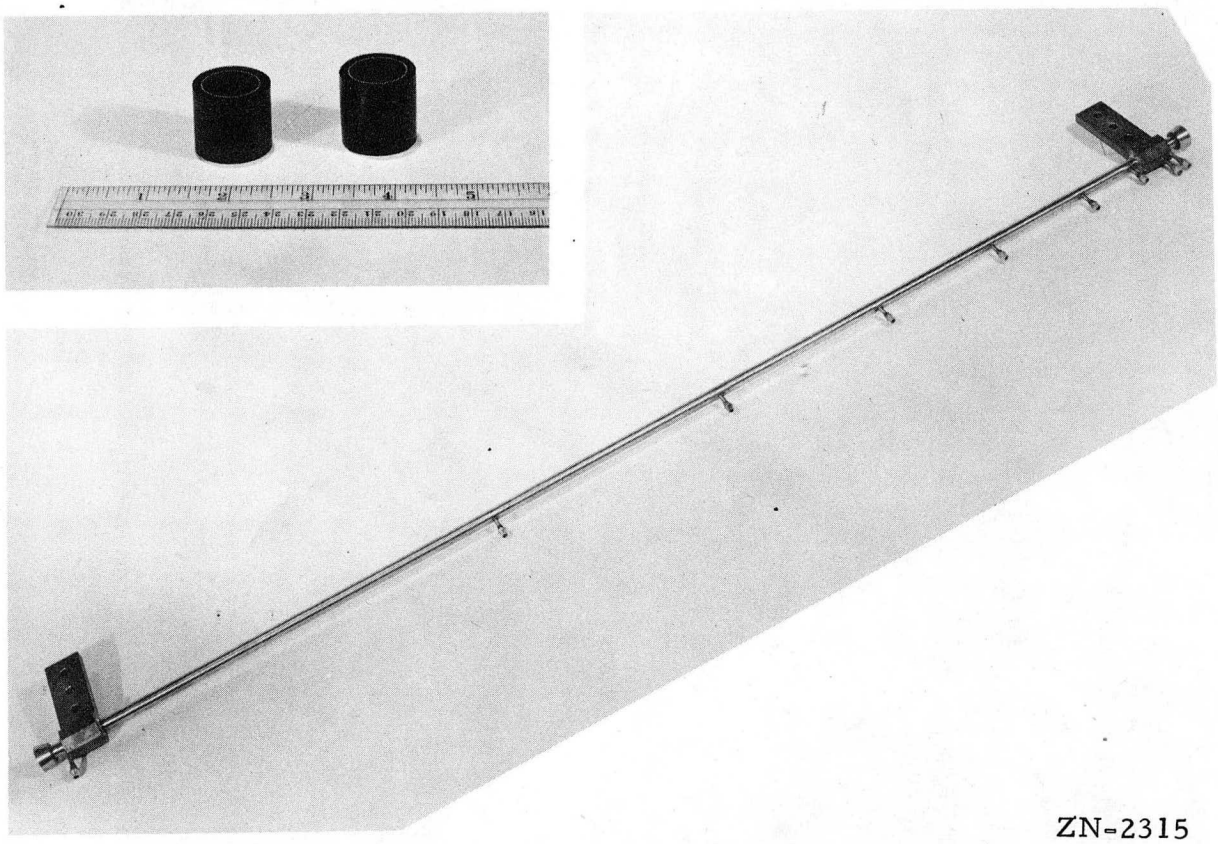

ZN-2315

Fig. 7. Test section.

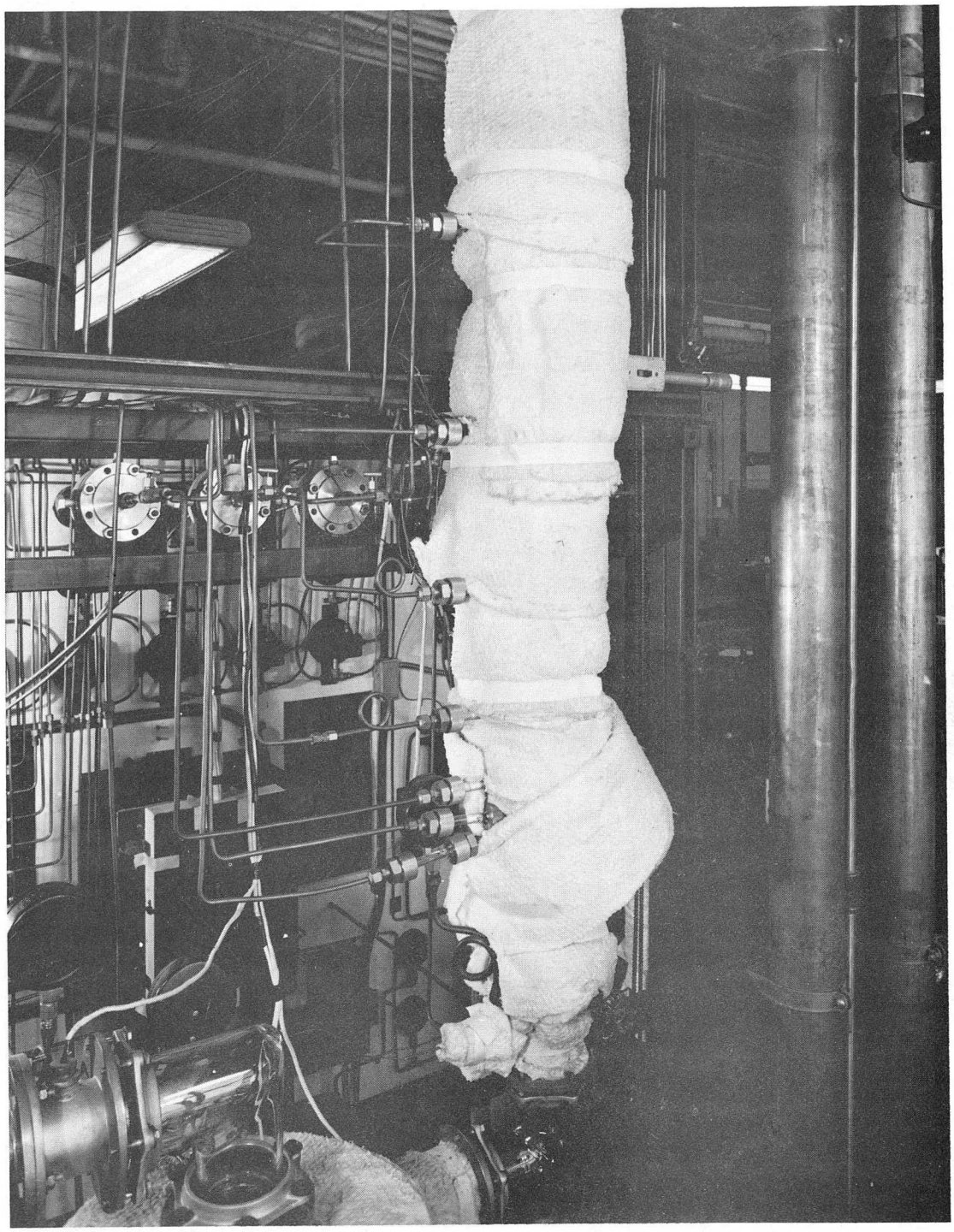

ZN-2316

Fig. 8. Test section installation.

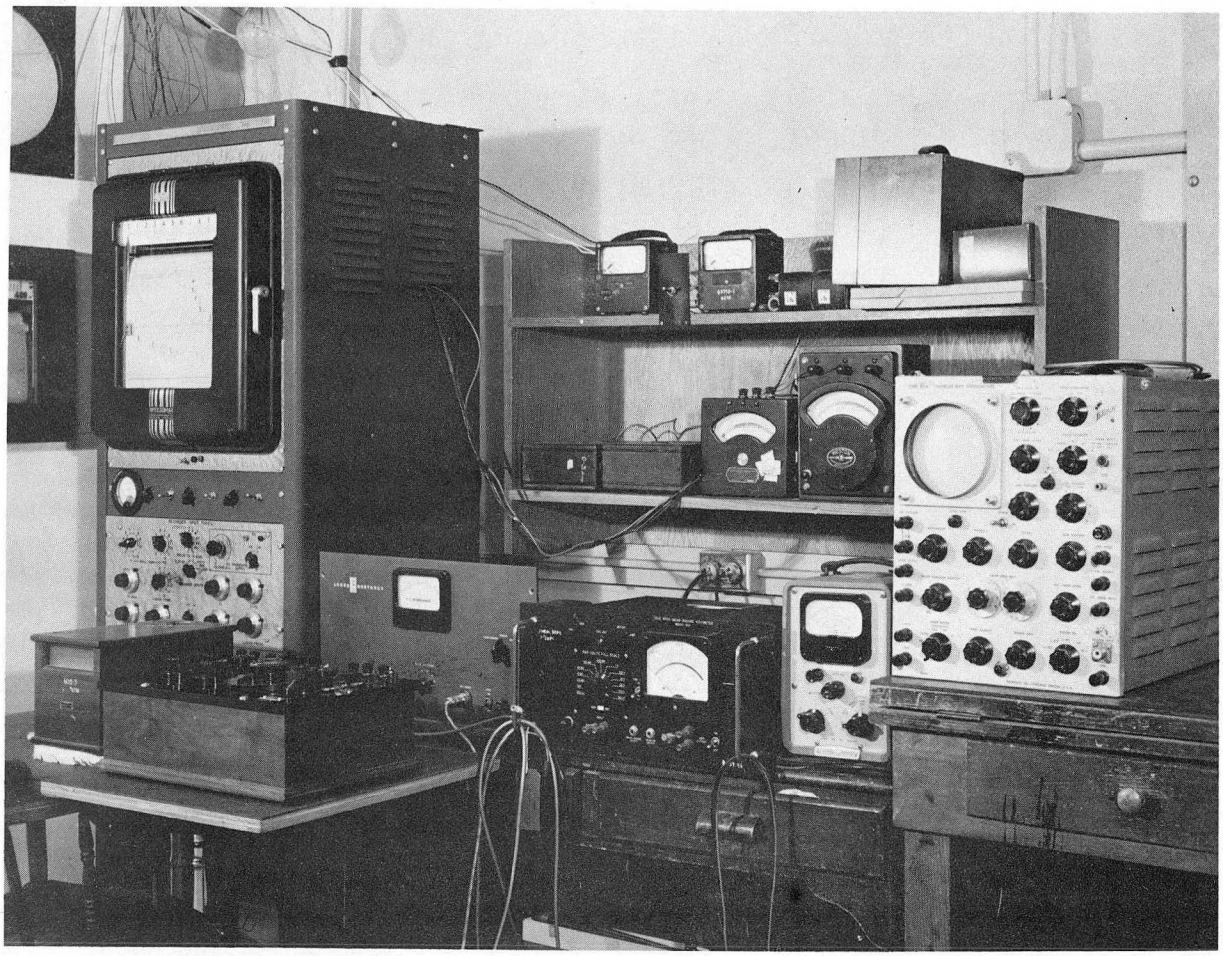

ZN-2317

Fig. 9. Instrumentation.

stainless steel wells at major points in the flow system. The thermocouple wells protruded into the fluid stream for at least 3 in. in the direction of flow. These were used to keep a check on the thermal conditions throughout the system. The thermocouple wires were led to an insulated junction box. The box had a thick copper cover and back to eliminate temperature gradients across the thermocouple terminal strip. From the terminal strip the thermocouple wires were led to an 18-point Minneapolis Honeywell-Brown model 156 x 62P18 temperature indicator. The indicator had a range of 0-400°F and an accuracy of 1/5 of 1% of span. Leeds and Northrup 11-point thermocouple switches were attached to two of the eighteen points. This enabled the instrument to accomodate all the thermocouples. A six-point Minneapolis Honeywell-Brown model 153X-G2-PG-X-23 temperature recorder was attached to certain key thermocouples. It was used in the determination of steady-state conditions.

All the copper-constantan thermocouples were fabricated from matched Leeds and Northrup thermocouple wire. The thermocouples which were soldered to the test section and those in the insulated thermocouple wells before and after the flashing valve were led directly to a heavily insulated copper box. This box also held a bucking voltage and span-adjust circuit. The thermocouple emf could be reduced by a bucking voltage and displayed on a 0-1-mv Leeds and Northrup Speedomax-G recorder or read directly on a precision Rubicon laboratory type B potentiometer. The bucking voltage circuit was designed so that the bucking voltage could be read on the 0-1-mv recorder. See Figure 10 for details of the circuit.

A direct electrical circuit between ground and the test section resulted when a thermocouple was switched into the recorder circuit. This impeded the operation of the recorder. This was remedied by operating the recorder with a floating ground. A 60-cycle pickup problem was also encountered until one side of the main transformer was tied to ground.

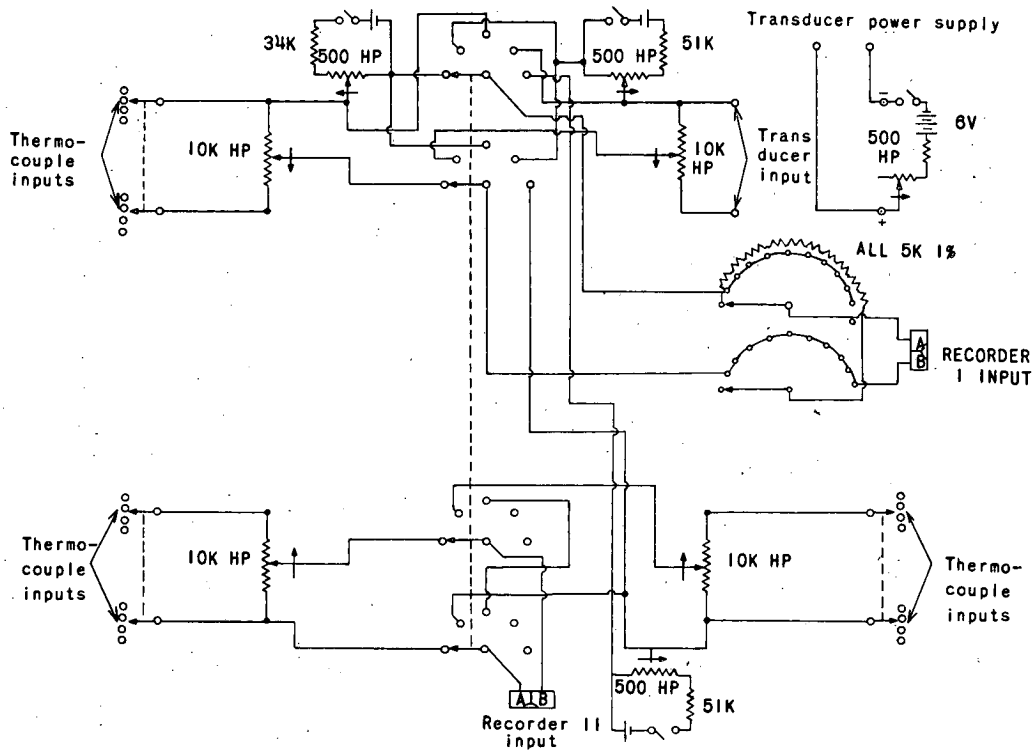

MU-18761

Fig. 10. Schematic diagram of recorder input circuit.

The Speedomax-G recorder was used to observe temperature and pressure fluctuations. All quantitative temperature measurements were made on the precision Rubicon potentiometer.

Since the thermocouples were in electrical contact with the test section, their cold junctions had to be electrically isolated from one another. This was accomplished by individually sealing the cold junctions in small glass capillary tubes. The ice bath was located in a large Dewar flask.

The thermocouples were calibrated in place by filling the test section with steam. Condensate and inerts were bled out the bottom of the test section. The bleed valve was adjusted until it performed the above duties while causing a negligible pressure drop across the test section. After a few hours the thermocouple and pressure readings were recorded. Over the range of temperatures encountered in this work, the measured and thermodynamically determined (assuming saturated steam) temperatures agreed to less than 0.2°F. No corrections were applied to the Leeds and Northrup table. This also verified the adequacy of the test-section insulation.

b. Pressure Measurement

A pressure manifold was connected to the 3-in. sections of glass pipe by 1/4-in. o.d. copper tubing. A needle valve was installed in each line immediately preceding its attachment to the manifold. The manifold was constructed from a 30-in. length of 1-in. i.d. brass tubing which was closed at both ends and mounted vertically. It was provided with a vent valve at the top and a connection with the main flow circuit. With this

arrangement all the air could be flushed out of the system before making pressure measurements. A Consolidated Electrodynamics model 4-313 transducer was attached to the center of the manifold. The transducer was calibrated by a dead-weight gage. The transducer was excited with a stable three-volt battery source. Its output was run through a bucking voltage circuit and displayed on a 0-1-mv Leeds and Northrup Speedomax-G recorder. The bucking voltage was also read on the recorder after first being run through a voltage-divider network. This system was used in the calibration of the transducer so that the small voltage drop incurred in the voltage-divider network was incorporated in the calibration curve. The calibration curve was linear.

Since the most stable exciting voltage will eventually drift, a procedure was developed to eliminate this effect. Before each run the barometric pressure was independently determined. The transducer was then opened to atmosphere and the exciting voltage was adjusted until the transducer's output corresponded to the voltage determined from the calibration curve. In this manner the pressure could be measured to less than ±0.1 psia.

Temperature gradients across the transducer's case caused erratic operation. This was corrected by two system modifications. The transducer and pressure manifold were insulated, and a head tank of room-temperature distilled water was used to fill the manifold.

The root-mean-square (rms) value and the frequency spectrum of the pressure fluctuations were measured in certain runs. The transducer's output was bucked, and the remaining signal was amplified by a Leeds and Northrup type 9835-A amplifier. The amplified signal could be visually observed on a Tektronix type 511-A oscilloscope, or its rms value could be read from a Ballantine model-320 true root-mean-square voltmeter. For the frequency-spectrum analysis the voltage amplifier output was fed directly to a Hewlett-Packard model 300-A harmonic wave analyzer. Only qualitative results were obtained from the wave analyzer. The main frequencies were low, and the sensitivity of the instrument was poor in this range. (Figure 14 is a plot of the pressure fluctuations encountered in some typical runs.)

c. Power Measurement

Four equally spaced voltage taps were soldered to the test section. Calibrated Weston voltmeters, models 341 and 155, with a least count of 0.05 volt and 0.5 volt, respectively, were attached to these voltage taps by short lengths of low-resistance copper wire.

Before being connected to the test section, the main power inputs were run through a Weston model 327 current transformer. This transformer had the following ampere ranges: 1200/600/400/300/200/100/50/20/10 primary to 5 secondary. At 60 cycles the characteristics of this transformer were such that the ratio-correction factor, 0.9998, and the phase-angle-correction factor, leading 0°1', were negligible. The secondary

of the current transformer was connected to a calibrated Weston model 155 ammeter which had a least count of 0.05 ampere. With this load the maximum error in the secondary of the current transformer was 0.0035 amperes. In actual amperage through the test section this amounted to 0.28% of the total current.

The voltmeters could be switched out of the voltage-measuring circuit and a calibrated Weston model 432 wattmeter could be used to measure the power dissipated between taps. The average power factor as well as the power dissipated per unit length were obtained. See Figure 11 for details of the circuit.

d. Flow Rate Measurement

The flow rate was metered by a calibrated Fisher-Porter rotameter and by weight measurement. Through a solenoid valve arrangement the flow could be quickly switched from the feed-tank circuit to the weighing-tank circuit. A weight rate of liquid and vapor condensate was obtained in this manner. The mass flow rate could also be determined by a direct measurement on the feed barrel. The maximum difference in flow rates obtained by these independent measurements was 1%. See Figure 1 for details of the flow circuit.

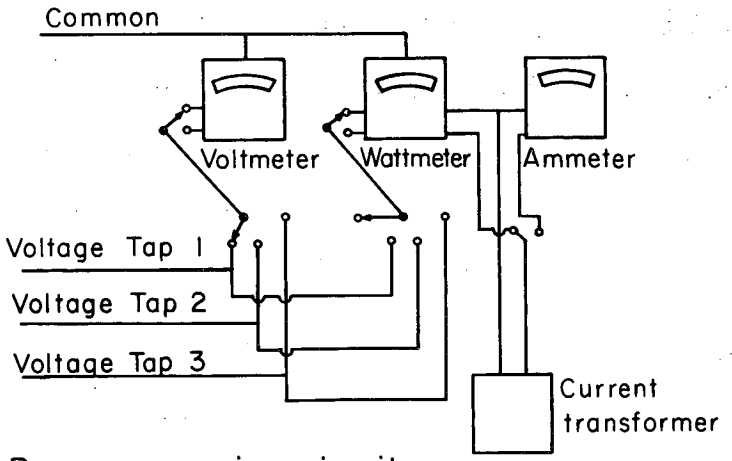

Power-measuring circuit

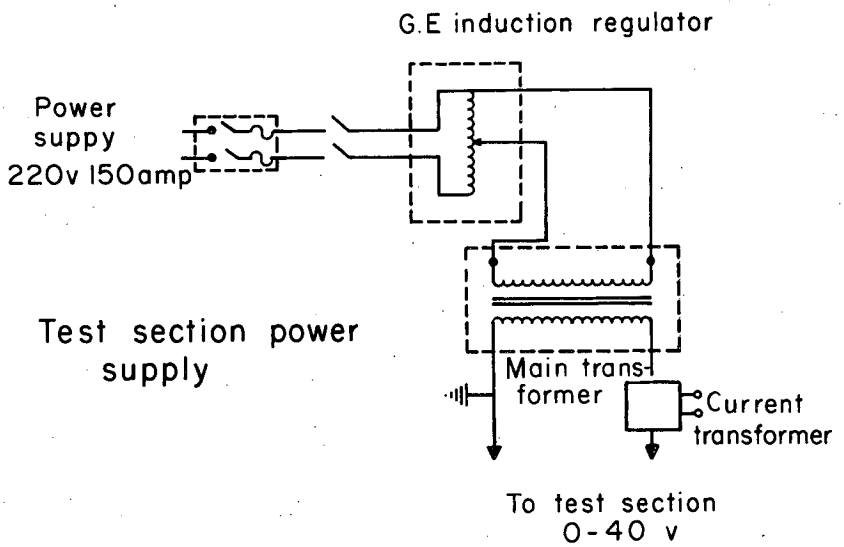

MU-18766

Fig. 11. (above) Power-measuring circuit
(below) Test-section power supply.

IV. EXPERIMENTAL PROCEDURE

Prior to making an experimental run all the air was driven out of the pressure manifold and its auxiliary lines. The feed was then degassed for about 30 minutes. This consisted of preheating the distilled water enough so that it flashed when passed through the flashing valve.

The quality of the mixture entering the test section was controlled by the amount which was allowed to flash. The approximate amount of preheating for the desired quality entering the test section was calculated before a run. By these calculations the experimental conditions could be approximately set. The flashing valve was closed to raise the pressure in the second preheater 10 psia above the saturation pressure of the preheated liquid. The closing of the flashing valve was done concurrently with the advancement of the pump speed in order to maintain the desired mass flow rate. Then the temperature controller was set to maintain the desired preheat temperature of the liquid stream issuing from the second preheater.

The test-section power was then turned on and adjusted to the desired level. The increased quality in the test section raised the back pressure so that a slight adjustment of the feed rate was necessary. The flow was very stable and reproducible except at very low vapor fractions and power inputs, where "slugging" occurred.

Forty-five minutes after startup a quasi-steady state was reached. At this time experimental data were recorded. Outside

tube wall temperatures and all other fluid temperatures which were necessary in later calculations were measured on a Rubicon precision potentiometer. All pressures of interest were measured by means of a pressure transducer and recorded on a Leeds and Northrup recorder. After each run the liquid legs of the auxiliary piping from the test section to the pressure manifold were recorded. In this manner compensation for the density of the liquid in these lines was effected. That the lines were always completely filled with liquid was established by visual inspection through the small sections of glass pipe. Atmospheric pressure was read on a barometer and recorded.

At frequent intervals the flow system was cleaned with a solution of tri-sodium phosphate. The test section was cleaned by a soft bristled test tube brush dipped in a suspension of Bon Ami. After these operations the system was thoroughly rinsed with distilled water. The flow storage system was then recharged with fresh distilled water.

V. CALCULATION PROCEDURES

A. Calculation Procedures

Since the inner wall temperature of the tube could not be measured directly without disturbing the flow, the outer tube wall temperature was measured. With a heat-transfer process occurring there is a temperature drop through the wall which is a function of the amount of heat transferred. The pertinent heat-conduction equation was solved in order to determine the temperature drop through the tube wall. The basic assumptions made were:

1. Linear dependence of thermal conductivity and electrical conductivity upon temperature.
2. Circular symmetry.
3. Negligible longitudinal heat conduction.
4. Adiabatic outer tube wall.
5. Negligible electrical capacitance and inductance effects.

The derivation of the equation and the justification of the assumptions are given in Appendix B. The solution obtained was:

$$T(r_1,\alpha,\gamma) = \overset{0}{T}(r_1) + \frac{\alpha}{2}\left\{T_o^2+\overset{0}{T}{}^2(r_1)\right\} + \gamma\left[\left\{T_o^2-T_o\overset{0}{T}(r_1)\right\}\right.$$

$$- \frac{A^2r_o^4}{16}\ln\frac{r_o}{r_1} - \frac{A^2r_o^2r_1^2}{8}\ln\frac{r_o}{r_1} + \frac{A^2r_o^2}{16}\left(r_o^2-r_1^2\right)$$

$$\left. + \frac{A^2}{64}\left(r_o^4-r_1^4\right)\right] + \ldots,$$

where

$$\overset{o}{T} = \frac{A}{4}\left(r_o^2 - r_1^2\right) - \frac{Ar_o^2}{2} \ln \frac{r_o}{r_1} + T_o \ ,$$

$$A = \frac{E^2}{Vk_oR_o} \ .$$

The maximum tube wall temperature drop was 3°F. The lowest film temperature drop, $T_1 - T_b$, which was encountered concurrently with the maximum tube wall temperature drop, was 10°F. If the correction due to the temperature drop through the tube wall were neglected, a maximum error of 23% would have resulted in the heat transfer coefficient.

The temperature drop through the tube wall was subsequently evaluated for this particular test section (and plotted in Figure 26) to facilitate the reduction of data.

B. Nonboiling Heat-Transfer Calculations

The inner wall temperature of the tube was obtained (from Figure 26) after having experimentally determined the outer tube wall temperature. A plot of inner wall temperature versus distance from the entrance of the heated section was made. After an initial thermal entrance region which lasted for approximately 16 diameters, the slope of this line was nearly constant. In the constant-slope region the thermal boundary layer was assumed to be completely established. In Ref. 12 it was shown that in the range of Peclet numbers involved in this study axial conduction in the fluid was negligible. With this condition and the condition of uniform axial generation of heat (which was justified by Figure 12), the bulk temperature

of the fluid is a linear function of the distance from the entrance of the heated section. The bulk fluid temperature was obtained by plotting the inlet and outlet bulk fluid temperatures at their respective tube positions and then connecting these two points by a straight line. In this manner local values of the bulk fluid temperature were determined. In the region of the plot where the slope of the inner wall temperature of the tube was constant the temperature difference between the inner wall and the bulk fluid also was constant. This is the region where the heat-transfer coefficient was calculated. It was calculated from the defining equation:

$$h = \frac{q}{(T_i - T_b)} .$$

The experimentally determined heat-transfer coefficients were compared to the Dittus-Boelter correlation,

$$\frac{hD}{k} = 0.023\ Re^{0.8} Pr^{0.4} ,$$

and the Sieder-Tate correlation,

$$\frac{hD}{k} = 0.027\ Re^{0.8} Pr^{0.33} \left(\frac{\mu_w}{\mu_b}\right)^{0.14} .$$

In these relationships all the fluid properties were evaluated at the bulk fluid temperature except μ_w in the Sieder-Tate relationship, which was evaluated at the inner wall temperature. (The results are plotted in Figures 15 and 16.)

Local heat-transfer coefficients were also calculated for one run and compared to those theoretically predicted by R. Siegel and E. M. Sparrow (15). The comparison is shown in Figure 17.

C. Boiling Heat Transfer Calculations

The temperature of the inner wall was obtained in the same manner as in the nonboiling runs. The local axial static pressure was assumed to be independent of radial position, and the two-phase mixture was assumed to be in thermodynamic equilibrium. To support this assumption the temperature and pressure of the bulk fluid stream were measured independently at a point near the entrance of the test section. The measured temperature and the temperature obtained from the static-pressure measurement by assuming thermodynamic equilibrium were always in agreement within the experimental accuracy of the measurements. This supports the validity of the previous assumptions if one further assumes that the boiling heat transfer process does not materially affect the establishment of thermodynamic equilibrium. These assumptions were also made in references 1, 6, 9, 10, and 12. The bulk fluid temperatures were then obtained from the pressure measurements with the help of the Keenan and Keyes steam tables (7). For each run local heat transfer coefficients at five different tube locations were calculated from the defining equation,

$$h_B = \frac{q}{(T_i - T_b)} .$$

The first location was one foot from the entrance of the heated section and succeeding locations were at one-foot intervals.

D. Local Fluid Properties

The local fluid properties in the two-phase flow regime were calculated by writing an energy balance over the region bounded by a point immediately preceding the flashing valve and the position of interest in the test section. The velocities of the two phases were assumed to be equal (fog flow model), and the spatial generation of heat was assumed uniform. Using Linning's slip-flow model (8) as a basis, calculations were made which indicated that in the region of vapor qualities encountered in this study, even with an appreciable amount of slip (the vapor velocity was assumed to be nine times that of the liquid) between the two phases, the error in the vapor quality was small. With these assumptions the energy balance was

$$h-h_1 = \frac{V^2-V_1^2}{2gJ} + \left(\frac{Q_T}{L}\right)\frac{\ell}{m} - \frac{1}{J}(Z-Z_1) = h_f + xh_{fg} - h_1 \ .$$

Since the velocity depends on the vapor quality, which is an unknown, an iterative procedure was employed. As a first approximation the kinetic energy term was neglected, and the quality x was calculated. Then the kinetic energy term was evaluated, using this quality. A second approximation to the quality was generated by placing this kinetic energy term into the original energy balance. Since the qualities of interest in this study were small, one iteration was all that was necessary.

E. Local Total Pressure Gradients

The local two-phase-flow pressure gradients were determined graphically. The experimental static pressure was plotted and

then a plastic straight edge was visually adjusted until the tangent to the curve was obtained. The local pressure gradients for each run were then plotted versus length in order to check their consistency. In every instance a smooth curve could be placed through these points, which indicated the procedure was reliable. (The plot of static pressure and pressure gradient versus length for run 57 is shown in Figures 28 and 29.)

The local two-phase pressure gradients were nondimensionalized by dividing them by the local liquid frictional pressure gradient, which was calculated from the following relationship:

$$\left(\frac{dp}{d\ell}\right)_\ell = \frac{fG_\ell^2 V_\ell}{2gD} .$$

The friction factor, f, was calculated from the relationship

$$f = 0.3164\left(\frac{G_\ell D}{\mu_\ell}\right)^{-1/4} ,$$

which is the Blasius formula for a smooth tube.

VI. DISCUSSION

A. Nonboiling Heat Transfer

The average heat transfer coefficients for turbulent one-phase flow were correlated by the Dittus-Boelter and Sieder-Tate correlations to ±8.7% and ±3.7% respectively. The Sieder-Tate correlation was superior because of its ability to correlate runs with large $(T_i - T_b)$. This was due to the viscosity term which was added to compensate for temperature effects in the thermal boundary layer. In this range of Grashof and Reynolds numbers, Eckert, Diaguila, and Curren (5) have shown that the superposition of natural convection effects on forced convection is negligible. As was expected, the data compared favorably to these correlations.

Under conditions where the axial and radial variations of fluid properties with temperature were negligible, the local nonboiling heat transfer coefficients compared favorably with those theoretically predicted by Siegel and Sparrow (16). The condition of constant fluid properties was met by running at high mass fluxes, low heat inputs, and bulk fluid temperatures greater than 150°F. At these temperatures the temperature gradient of the viscosity of water is much smaller than it is at room temperature. (Figure 17 shows the comparison between the measured and theoretically predicted entrance region for a run at Pr = 1.86 and Re = $9.8 \cdot 10^4$.) In runs where the condition of constant fluid properties was not met, the thermal entrance region showed more Reynolds-number dependence than predicted by Siegel and Sparrow (16). In this case the entrance

region compared more favorably to the theoretically predicted one of Diessler (2). The main interest in the entrance region in turbulent one-phase flow was to aid in understanding the one encountered in two-phase flow. A thorough investigation of this region was beyond the scope of this work.

B. Boiling Heat Transfer

Visual inspection was made of the two-phase flow pattern entering the test section. At large qualities the flow was mist-annular with wavy fluctuations riding on the vapor-liquid interface. As the quality was lowered there was a gradual change in flow pattern. A train of vapor bubbles with liquid entrained between them was visible at qualities near 1%.

In Figure 18 the net boiling data are plotted in terms of the Rohsenow parameters, $(q_B/\mu_\ell h_{fg})\sqrt{(g/\rho_\ell-\rho_v)}$ and $(C\Delta T/h_{fg})Pr^{1.7}$. The correlation is unsatisfactory. In the derivation of the Rohsenow correlation the characteristic constant in the equation depends on the fluid and surface properties. The present test section was constructed of 304 stainless steel. The data lie in the region of the curve obtained from Rohsenow's data for a 0.18-in. i.d. nickel tube. The applicability of the correlation to this investigation seems dubious. In Rohsenow's investigation and in the present study the surface was kept clean, and the distilled water was degassed. It doesn't seem probable that the deviations can be attributed to these factors. The data for an individual run tend to spread horizontally because of changes in the parameter $(C\Delta T/h_{fg})Pr^{1.7}$ which are not reflected in the slowly changing parameter

$(q_B/\mu_\ell h_{fg})\sqrt{(\sigma/\rho_\ell-\rho_v)}$. This horizontal spread can be characterized by the Martinelli parameter. As the Martinelli parameter of a data point increases the deviation from the Rohsenow correlation becomes greater. The parameters used in the Rohsenow correlation seem to be necessary but insufficient to characterize forced-convection net boiling.

The data are compared to Mumm's correlation (11) in Figure 19. The spread in the data is large. There is a definite trend in the data for each separate run. This indicates that although the parameters used by Mumm are important in characterizing the heat transfer, the groupings of variables and their exponents seem to be inappropriate.

Figure 20 shows that the present data lie below the Dengler correlation (1). This might be attributed to the inaccuracy of Dengler's local heat fluxes, which were determined by measurement of condensate. A definite correlation of the present data is visible in Figure 20, which indicates the Martinelli parameter is an important parameter in characterizing the heat-transfer process.

The comparison of the data to the Schrock and Grossman correlation No. 1 (B) was good. The comparison is shown in Figure 21. The parameters h_B/h_ℓ and X_{tt} correlate the data to ±20%. The data smoothly join the Schrock and Grossman correlation at higher values of X_{tt} because the Schrock and Grossman correlation was based on their data at low X_{tt}.

By assuming a simplified model it can be shown that a certain value of h_B/h_ℓ is approached as X_{tt} gets large. The

velocities of the liquid and vapor phases become equal when slugging occurs. The vapor slug pushes the upstream liquid out the end of the tube. The "boiling heat transfer coefficient," h_B, will approximately equal one calculated from the Dittus-Boelter equation in which the Reynolds number is based on the increased velocity which exists due to vapor formation. Slugging is an unsteady and complicated phenomenon. This simplified model gives a qualitative bound on h_B/h_ℓ as X_{tt} gets large. Calculations based on this simplified model yielded $h_B/h_\ell \approx 1.6$ at an X_{tt} of 15. The data tend in this direction. This model wouldn't apply at very large heat fluxes.

When Grossman and Schrock (14) analyzed their recent data a definite trend was found in the high X_{tt} range. There was a systematic deviation from the correlation. A set of curves resembling a friction-factor plot was obtained. Boiling number appeared as a parameter analogous to the relative roughness on a friction-factor plot. As the boiling number became larger the heat-transfer coefficient became less dependent on X_{tt}. The Grossman-Schrock correlation No. 2 was developed in an effort to combine these effects. See Section II-C. It correlated their data to ±35%. The form of this equation implies that the boiling effect and the forced-convection effect are additive.

The boiling-number range of this study was in the region where the heat-transfer coefficient was dependent upon X_{tt}. This was verified in this study. Although the parameters correlated 95% of the present data to ±15%, the comparison between this correlation and the data wasn't too favorable.

Figure 22 shows that the present data lie approximately 200% above the Schrock and Grossman correlation. In this figure the correlation obtained from the data of Morgan et al. for a downflow system is shown. It lies between the present data and the Schrock and Grossman correlation. This indicates that the deviation from the correlation is not solely due to a basic difference in upflow and downflow if the data of Morgan et al. are reliable.

The most pronounced difference in conditions investigated by this author and by Schrock and Grossman was the pressure range. Schrock and Grossman operated at pressures from twice to thirteen times those encountered in this study. At low pressures the specific volume change on vaporization is from two to four times that at high pressures. The difference between the data and correlation might be attributed to a need for more pressure dependence in the correlation.

The boiling number, $q/h_{fg}G_T$, can be considered as the ratio of the perpendicular mass flux to the total mass flux. It seems to the author that q/h_{fg} is not the important perpendicular mass flux. A quantity with more physical significance would be $qv_g/h_{fg}v_f$. A boiling number based on this mass flux would be $qv_g/h_{fg}v_fG_T$. The term $qv_g/h_{fg}v_f$ is the mass flux of liquid which is caused by vapor generation. This term does not allow for the mass flux of liquid due to flashing. The significance of the boiling number does not depend on the presence of nucleate boiling at the inner wall. It can characterize the disturbances caused at the vapor-liquid interface due to

vaporization. It is interesting to note that a boiling number formed on this basis was fundamental in characterizing the pressure fluctuations. Not enough experimental data have been obtained in this study to investigate the significance of this group.

A sacrifice in accuracy was made when Schrock and Grossman incorporated the boiling and forced convection effects in their correlation No. 2. Their "friction factor" type correlation, which is a plot resembling a familiar friction-factor plot, is the best available correlation for forced-convection net boiling of water. The boiling number defined by Mumm doesn't have as much physical significance as the proposed modified boiling number. A more general correlation might be obtained by using the modified boiling number.

C. Entrance Effect

A large, reproducible entrance effect was observed in forced-convection net boiling. The effect was more pronounced than the one encountered in one-phase flow. Figure 23 shows data obtained for a series of runs in which the inlet quality was decreased (increased inlet value of the Martinelli parameter) while the total mass flux and heat flux were held constant. The entrance effect always resulted in boiling heat transfer coefficients which were higher than those predicted from a Schrock-Grossman-type correlation of the remaining data.

The effect was not caused by axial conduction. An experiment was performed with adiabatic two-phase flow. Tube wall

and bulk fluid temperatures were measured. These measurements proved that axial conduction in the tube wall was negligible. The entrance effect varied at a constant heat flux. This indicates that the effect was not due to nonuniform heat generation. This was also substantiated by other measurements which are mentioned in Appendix A.

The entrance effect had two characteristic regions. The two regions were characterized by their position with respect to the observed maximum in the inner wall temperature. The initial entrance region preceded the maximum and the terminal entrance region immediately followed the maximum. The initial entrance effect had the following behavior:

1. slight increase in magnitude and no effect on thermal entrance length as the heat flux was increased,

2. decrease in magnitude and no effect on thermal entrance length as total mass flux was increased,

3. large increase in magnitude and thermal entrance length as inlet value of Martinelli parameter was decreased.

Figure 23 clearly illustrates the behavior described in 3 and the initial and terminal entrance regions. The main effect observed in the terminal entrance region was that its length of influence decreased as the heat flux was increased. In the initial entrance region the length of influence refers to the tube position at which the maximum inner wall temperature was reached and in the terminal entrance region it refers to the length of tube over which high boiling heat transfer coefficients were obtained.

Dengler observed heat-transfer coefficients in the entrance region which were too high and attributed them to the presence of nucleate boiling. He reasoned that increased liquid velocity suppressed the boiling mechanism. See Section II-A. In the range of conditions studied the data indicate that this is erroneous. If a nucleate boiling effect was predominant in the entrance region of the tube one would expect that at a constant, high value of the Martinelli parameter (indicating a low liquid velocity) the length of the entrance effect would increase as the heat flux was increased. An increase in heat flux increases the degree of superheat, $T_i - T_b$, which should increase the nucleate boiling effect. In this study the Martinelli parameter could be varied by adjusting the quality of the mixture entering the test section. The Martinelli parameter was varied in runs at three different heat fluxes. The total length of the entrance effect, initial plus terminal, decreased as the heat flux was increased while the Martinelli parameter was held constant. This indicates that nucleate boiling is not the mechanism which increases the heat-transfer coefficients in the entrance region. Calculations based on Dengler's holdup data indicated that the difference in the velocity of the liquid entering and leaving the test section was small. It seems unlikely that if nucleate boiling occurred in the entrance region, it could be suppressed at some later axial position, as Dengler proposed.

The properties of the entrance effect observed in this study seem to indicate that it originates from an interaction

between the increased turbulence in the liquid annulus due to interfacial shear and the development of the thermal boundary layer. More experimental work is needed to verify this interaction. As the magnitude of the entrance effect can have an appreciable influence on design calculations, a more thorough study of this region is warranted.

D. Local Total Pressure Gradients

The local total pressure gradients were correlated by means of the Martinelli parameter. The correlation is plotted in Figures 24 and 25. Figure 25 is a good test of the experimental data, since the ordinate and abscissa of the conventional Lockhart-Martinelli type correlation are squared. Since 95% of the data are correlated to ±20%, the validity of this correlation is substantiated. The conventional Lockhart-Martinelli-type correlation shown in Figure 24 correlated the data to ±6%. Most of the scatter in data occurred at X_{tt} values greater than one. Martinelli and Lockhart (9) observed the same effect. This could possibly be attributed to a transition region in the hydrodynamical character of the flow. In Figure 24 the present data are compared with the curve that Schrock and Grossman (6) obtained in an upflow system. The present data lie 10% higher.

A gravity field accelerates the liquid annulus in a downflow system. It has the opposite effect on an upflow system. Due to this effect the liquid holdup in a downflow system could be expected to be smaller. This would account for the difference between the two systems. There is also a difference

due to the sign of the static-pressure-drop term. The difference opposes the trend seen in Figure 24 . The effective density of the mixture is small. The gravity head is small compared to the total pressure drop. The gravity head exerts a small influence on the total until the Martinelli parameter becomes large.

Schrock and Grossman (6) investigated 1/8-in.- to 1/2-in.-diameter test sections over a wide range of conditions. All their data were correlated to ±15%. On the basis of their results the validity of the present pressure-drop correlation over a wider range of conditions seems justifiable.

E. Amplitude and Frequency of Local Pressure Fluctuations

The pressure fluctuations for a series of runs are shown in Figure 19 . The shape of the curves is the same at a total mass flux of 110 lb /sec ft^2. The hump in the curves becomes more pronounced and the initial value of the fluctuations become larger as the inlet quality is decreased. In each run the fluctuations become larger as the quality increased. The trend seems reasonable as an increase in these variables causes an increase in the specific volume change on vaporization.

At a constant total mass flux a relationship exists between the fluctuations, Martinelli parameter, and the modified boiling number, $qv_g/h_{fg}v_fG_T$. This substantiates the significance of the modified boiling number in characterizing the flashing or vaporization process. A thorough investigation of pressure fluctuations should be undertaken. This would lead to a better understanding of the heat-transfer process.

Qualitative measurements of the frequency spectrum of the pressure fluctuations were made with a harmonic wave analyzer. The observed wave form was very random. Its main components were at frequencies less than 30 cycles/sec. Frequencies of 1 cycle/sec were observed in the slugging region. This indicated that the simplified slugging model is qualitatively correct. The components at 60 and 120 cycles/sec were small compared to the main components. This indicates that the use of alternating current does not affect the vapor generation.

Frequencies observed in pool boiling are approximately 1000 cycles/sec. No high frequencies were observed. This indicates that either there was no pool-type boiling or that forced-convection effects were predominant. The same conclusion would be obtained from the "friction factor" type heat transfer correlation proposed by Schrock and Grossman (14).

VII. CONCLUSIONS

1. The best correlation of the boiling heat transfer data was obtained by the following Schrock-Grossman type of correlation:

$$\frac{Nu_B}{Re^{0.8}Pr^{1/3}} = 3.4 \cdot 10^2 \left(\frac{q}{h_{fg}G_T} + 1.5 \cdot 10^{-4}\, X_{tt}^{-2/3} \right).$$

This correlated 95% of the data to ±15%. There was a 200% deviation between this correlation and the one obtained by Schrock and Grossman for upflow. The deviation might be attributed to a need for more pressure dependence in the correlation. To introduce this pressure dependence a modified boiling number, $qv_g/h_{fg}v_fG_T$, was proposed.

2. The local total pressure gradients in forced vaporization were correlated by the Martinelli parameter. The following correlation represented the data to ±20%:

$$\frac{(dp/d\ell)_{tpt}}{(dp/d\ell)_{\ell}} = 30\, X_{tt}^{-1.39} .$$

3. Nonboiling heat transfer coefficients were correlated by the Dittus-Boelter and Sieder-Tate correlations to ±8.7% and ±3.7% respectively.

4. Main frequencies of pressure fluctuations observed in forced vaporization were below 30 cycles/sec. It was concluded that either nucleate boiling didn't occur or that forced-convection effects were predominant.

5. A large thermal entrance region was observed in forced vaporization. Its origin was not due to nucleate boiling. It was postulated that it was due to an interaction between the increased turbulence in the liquid annulus due to interfacial shear and the thermal boundary layer.

VIII. GRAPHICAL RESULTS

Fig. No.		page
	A. General	
12	Power Dissipated Along Tube	40
13	Thermal Conductivity of 304 Stainless Steel	41
14	Pressure Fluctuations and Heat-Transfer Coefficients Along Tube	42
	B. Heat Transfer	
15	Comparison of Present Data with Dittus-Boelter Correlation	43
16	Comparison of Present Data with Dieder-Tate Correlation	44
17	Comparison of Present Data with Siegel-Sparrow Theoretical Equation	45
18	Correlation of Present Data Using Rohsenow Parameters	46
19	Comparison of Present Data with Mumm's Correlation	47
20	Comparison of Present Data with Dengler's Correlation	48
21	Comparison of Present Data with Grossman-Schrock Correlation Number 1	49
22	Comparison of Present Data with Grossman-Schrock Correlation Number 2	50
23	Entrance Effect	51

VIII. GRAPHICAL RESULTS (Continued)

Fig. No.		page
	C. Pressure Drop	
24	Comparison of Pressure-Drop Data with Grossman-Schrock Correlation	52
25	Correlation of Local Pressure Gradients	53

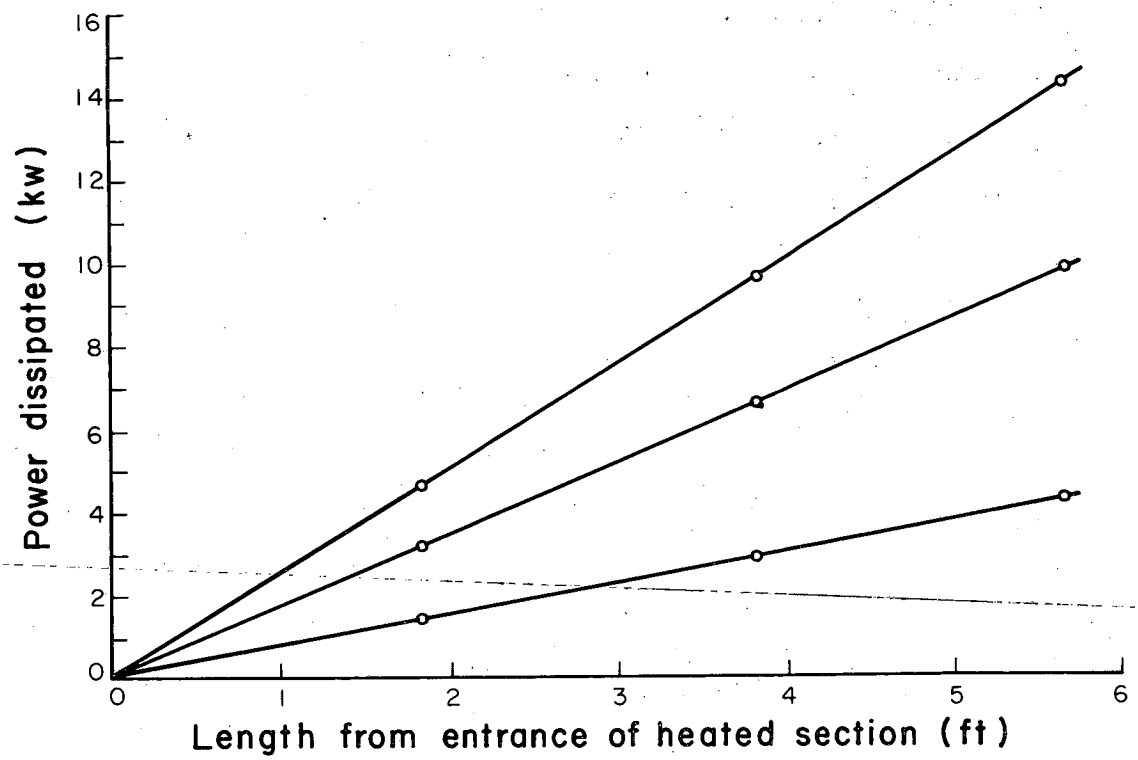

MU-18767

Fig. 12. Power dissipated along tube.

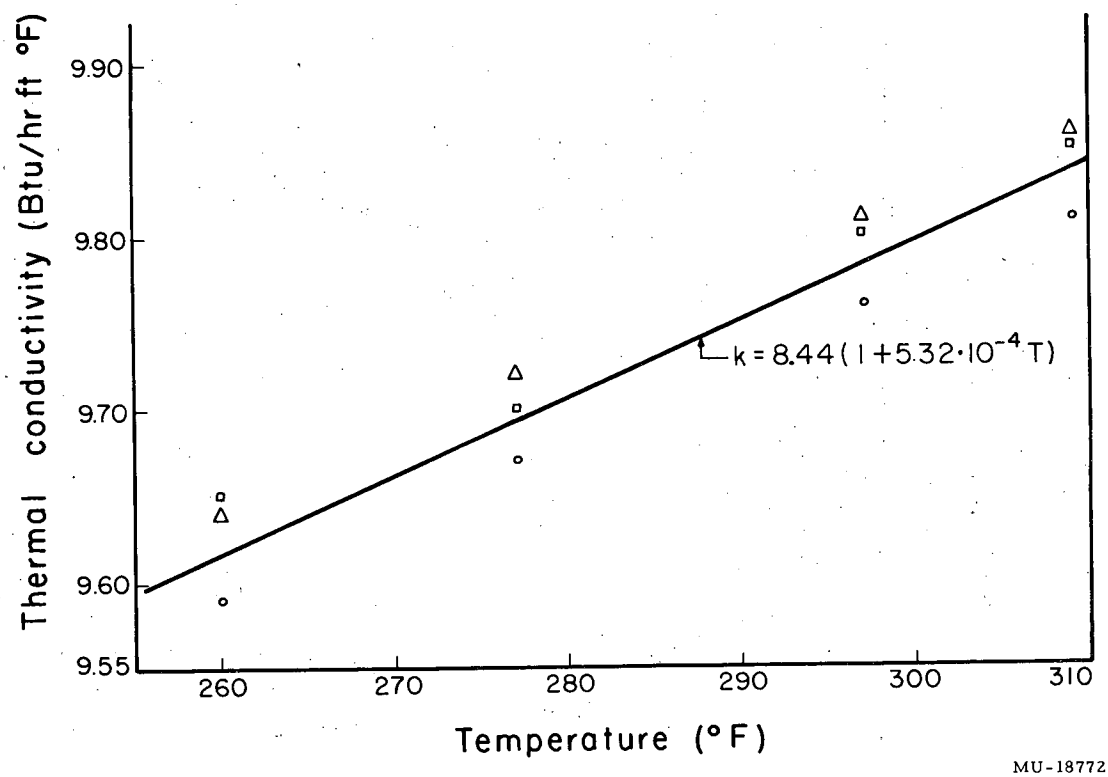

Fig. 13. Thermal conductivity of 304 stainless steel.
△ National Bureau of Standards.
□ Dickerson and Welsh, Trans. ASME 80, 746-754 (1958).
○ Metals Handbook, Section 20, 20-26 (1939).

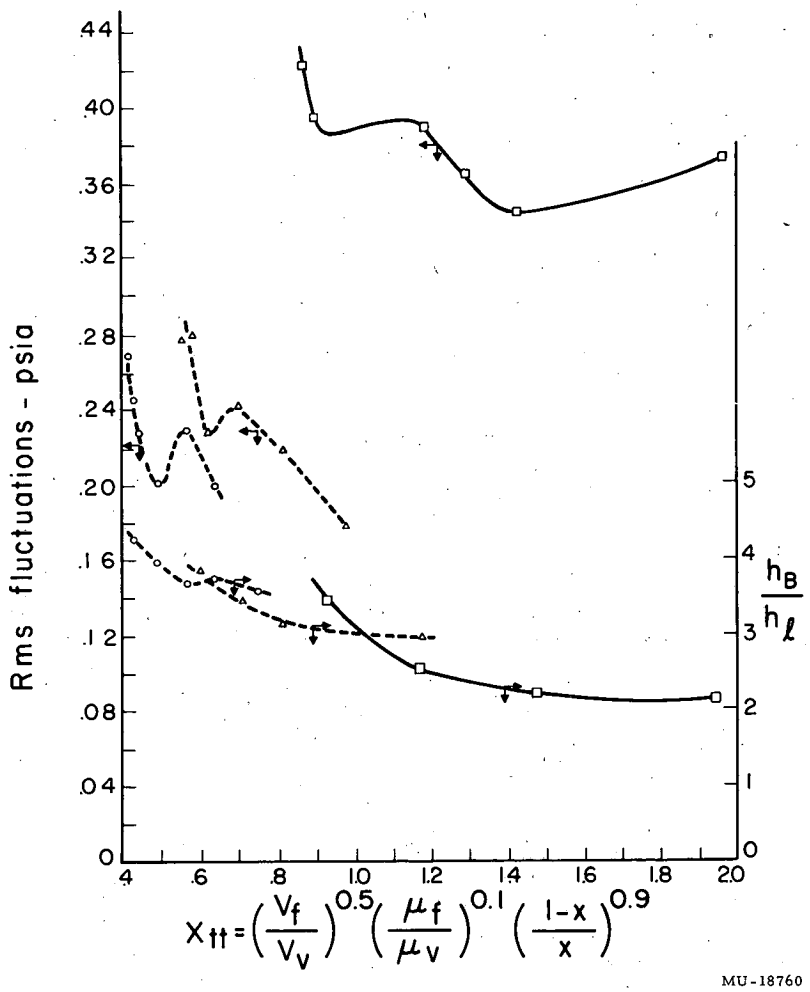

Fig. 14. Pressure fluctuations and heat-transfer coefficients along tube.

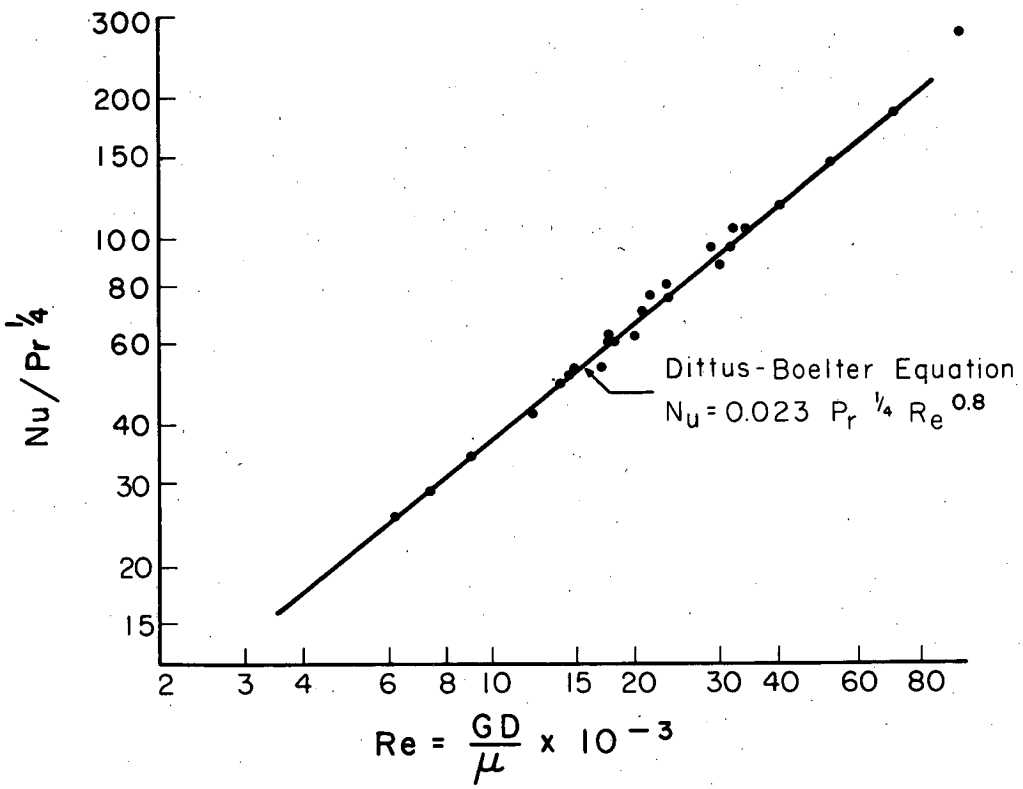

MU-18774

Fig. 15. Comparison of present data with Dittus-Boelter correlation.

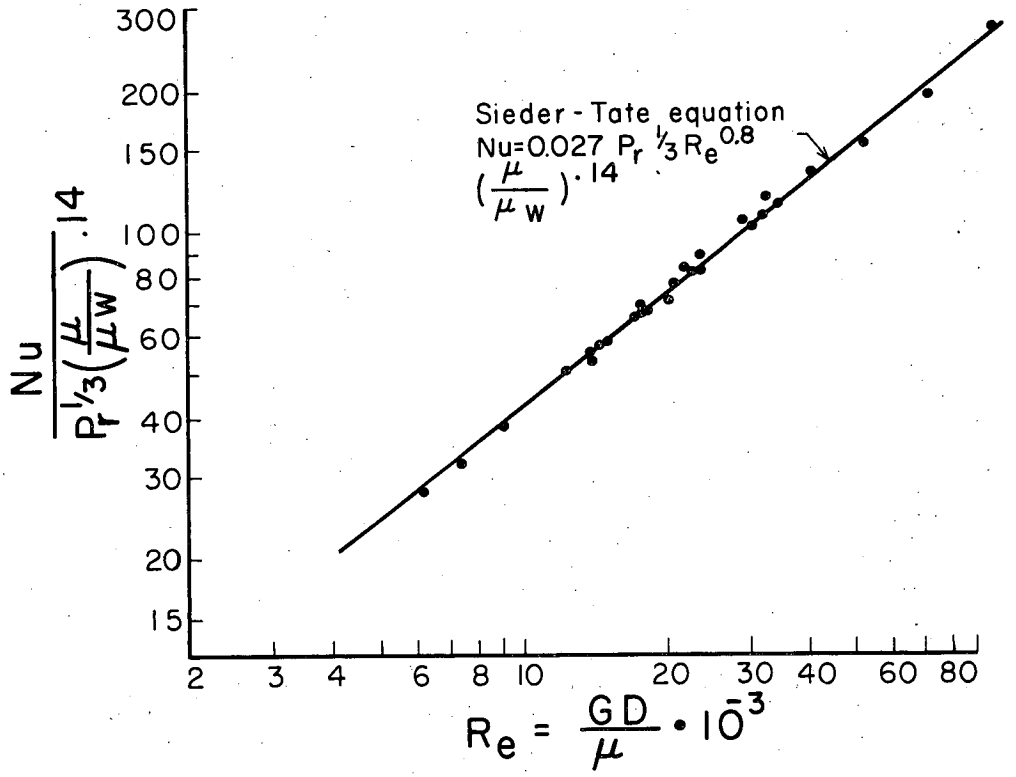

MU-18763

Fig. 16. Comparison of present data with Sieder-Tate correlation.

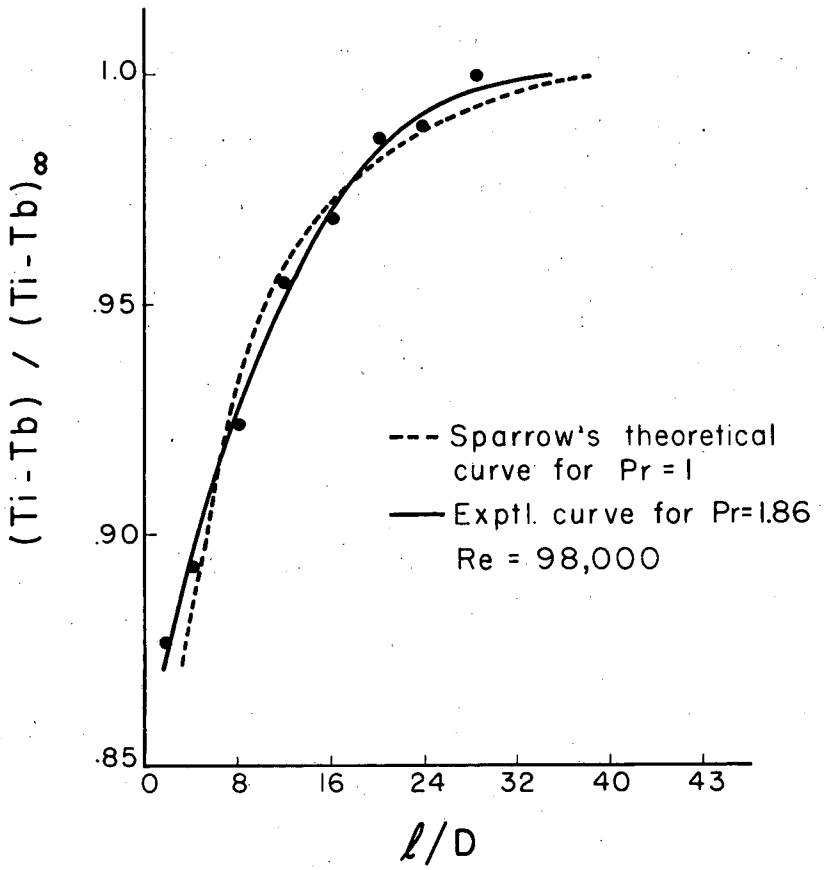

MU-18775

Fig. 17. Comparison of present data with Siegel-Sparrow theoretical equation.

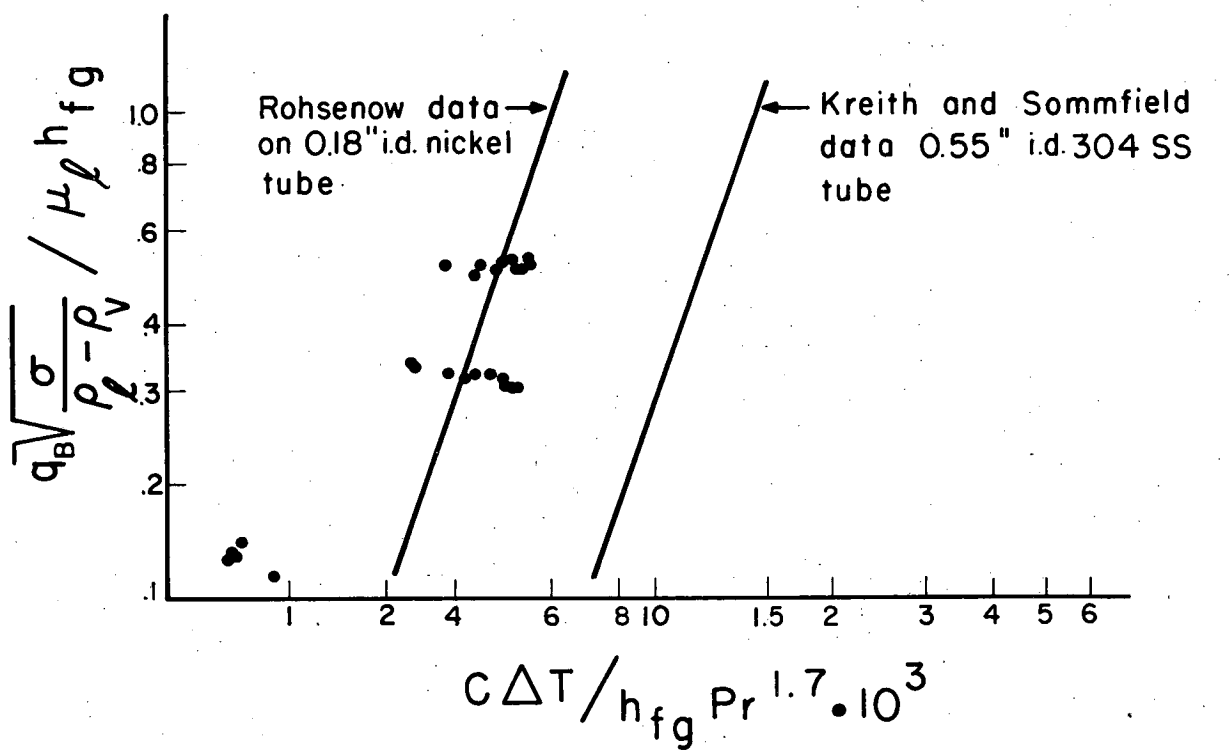

MU-18762

Fig. 18. Correlation of present data using Rohsenow parameters.

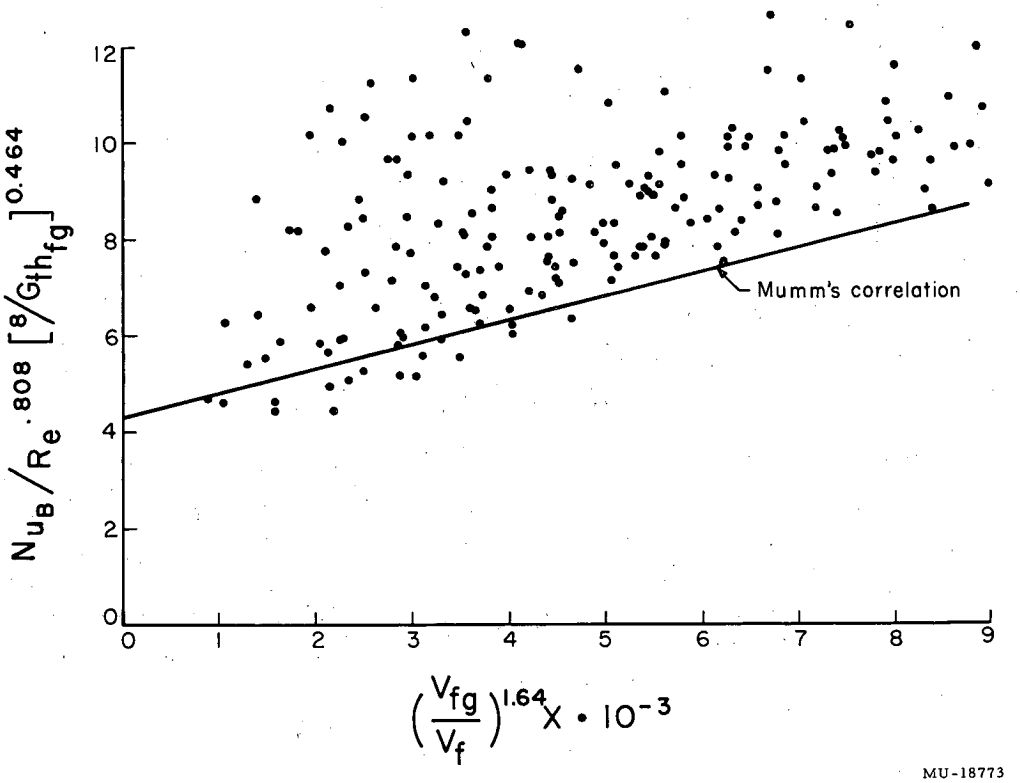

Fig. 19. Comparison of present data with Mumm's correlation.

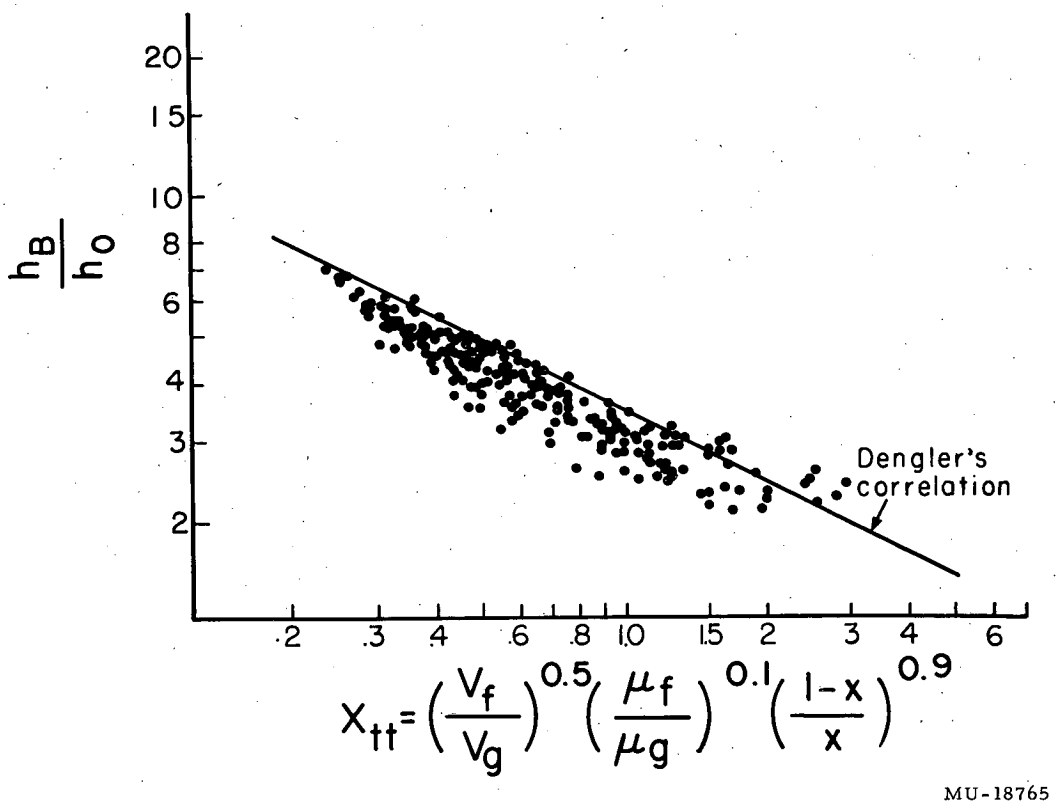

Fig. 20. Comparison of present data with Dengler's correlation.

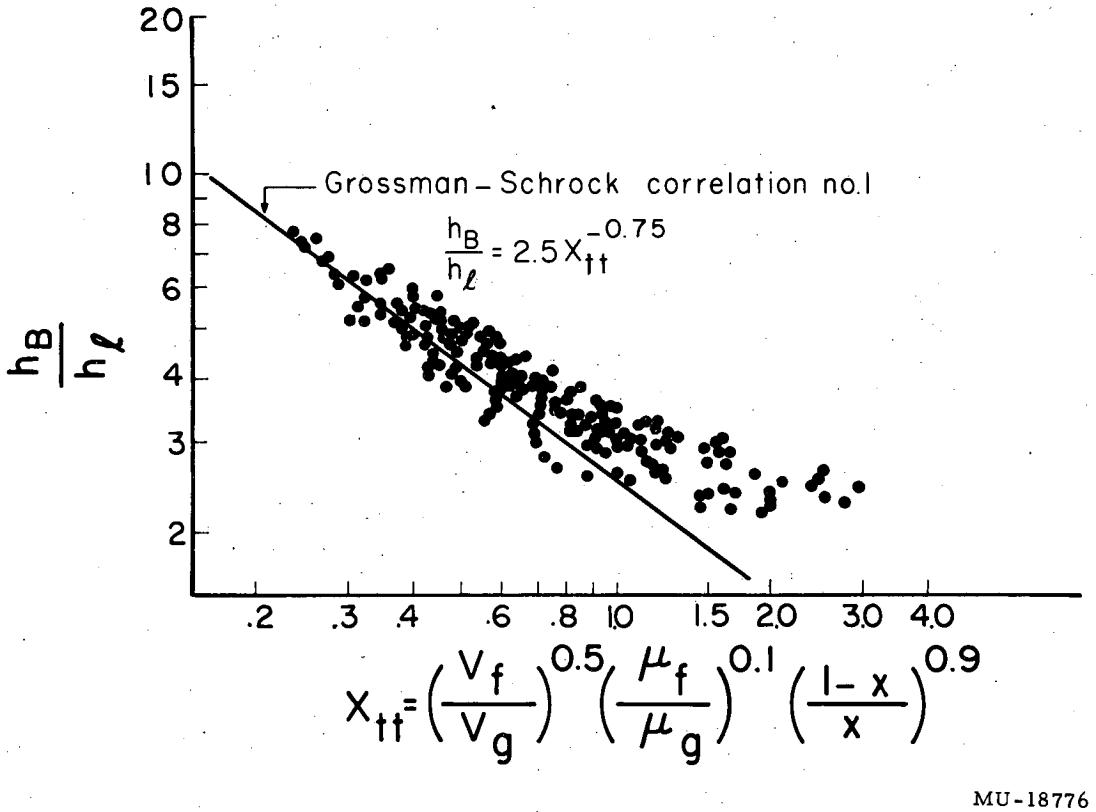

MU-18776

Fig. 21. Comparison of present data with Grossman-Schrock correlation No. 1.

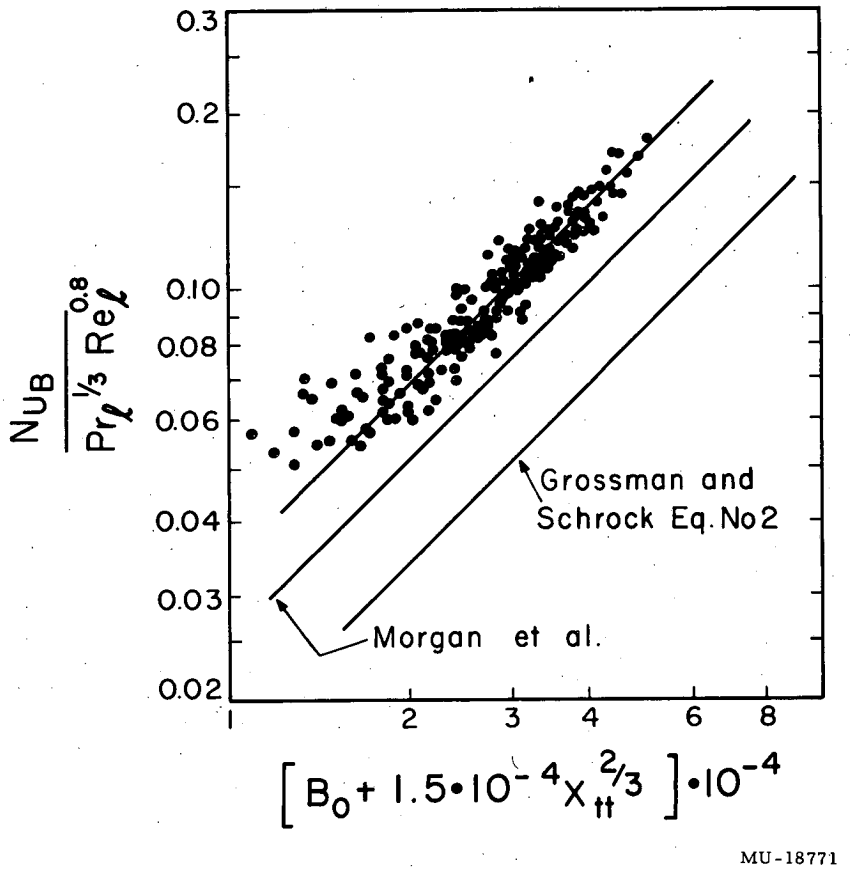

Fig. 22. Comparison of present data with Grossman-Schrock correlation No. 2.

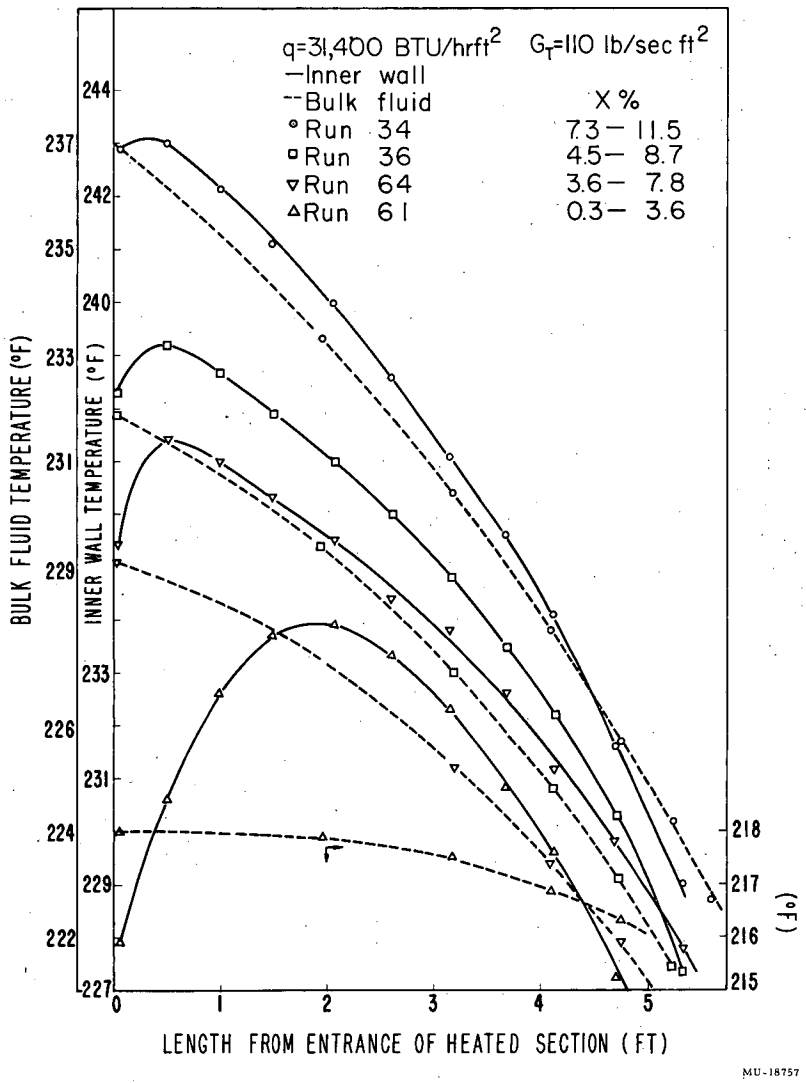

Fig. 23. Entrance effect.

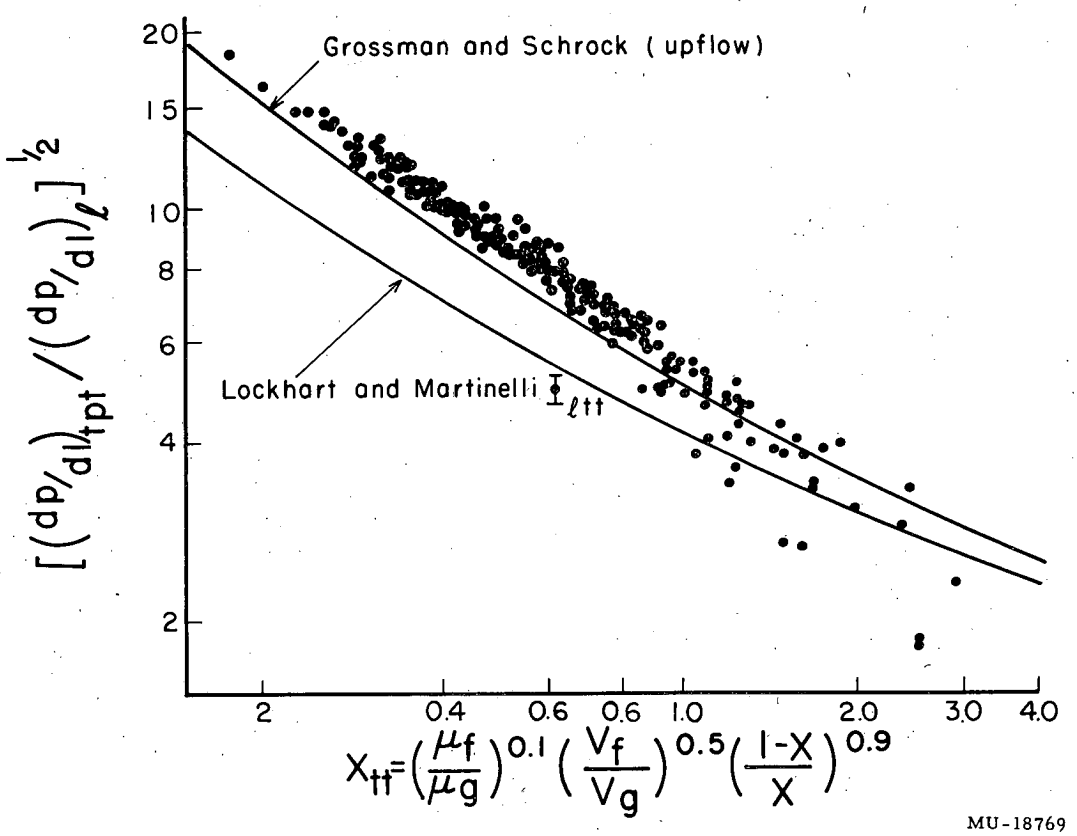

Fig. 24. Comparison of pressure-drop data with Grossman-Schrock correlation.

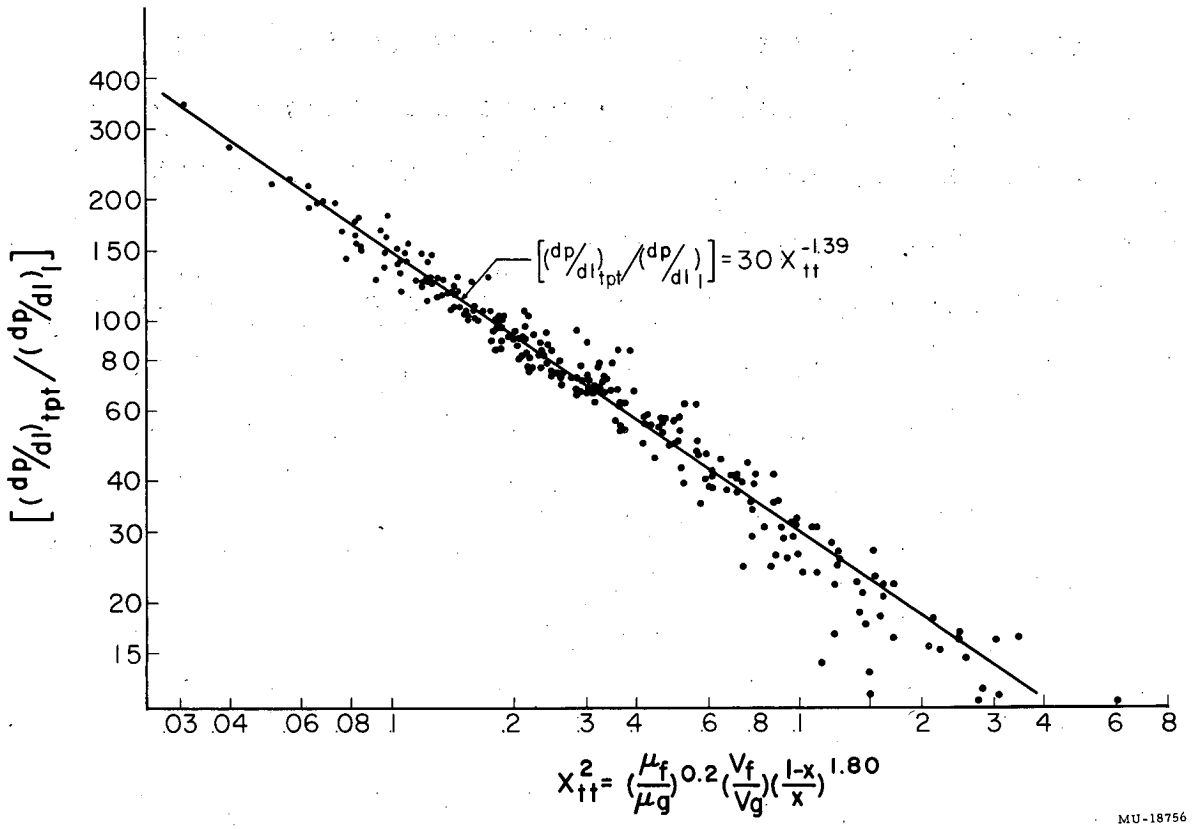

Fig. 25. Correlation of local pressure gradients.

Acknowledgment

The author wishes to gratefully acknowledge the financial assistance of the Lawrence Radiation Laboratory of the University of California, under a contract with the U. S. Atomic Energy Commission.

Grateful appreciation is also extended to Professor L. A. Bromley for his encouragement and valuable advice and to Rodger Wright for his help during the course of this investigation.

IX. APPENDICES

Appendix A - Determination of Inner Wall Temperature

The following assumptions were made in deriving the pertinent heat-conduction equation:

1. Linear dependence of thermal conductivity and electrical resistivity upon temperature.
2. Circular symmetry.
3. Negligible longitudinal heat conduction.
4. Adiabatic outer tube wall.
5. Negligible electrical capacitance and inductance effects.

Under experimental conditions the temperature drop through the tube wall was small. The first assumption was justified because over a limited temperature range these physical properties may be fitted with linear relationships. Assumption two was checked by inspection of random samples of the tube with a calibrated metallurgical microscope. The standard deviation of the wall thickness was less than 3%. The maximum error in the temperature of the inner wall arising from these variations was less than 0.1°F. Assumptions three and four were justified by measurements and calculations which indicated that the maximum axial heat conduction was less than 0.001% of the total heat input and the maximum radial heat loss to the surroundings was less than 1% of the total heat input. The minimum value of the measured power factor was 0.97, which substantiates assumption 5. With these assumptions the following

differential equation results:

$$\frac{1}{r}\frac{d}{dr}\left[r(1+\alpha T)\frac{dT}{dr}\right] = -\frac{E^2}{Vk_oR_o(1+\gamma T)} = -\frac{A}{(1+\gamma T)} ,$$

with the boundary conditions

$$T = T_o \text{ and } \frac{dT}{dr} = 0 \text{ at } r = r_o .$$

The temperature dependence of the electrical resistance and thermal conductivity were assumed to be

$$R = R_o(1+\gamma T) \text{ and } k = k_o(1+\alpha T) .$$

Under experimental conditions the temperature drop through the tube wall was small, not greater than 3°F. Therefore, the temperature may be expanded in a pertubation series in α and γ, and second-order terms may be neglected:

$$T = T(r,\alpha,\gamma) = \overset{0}{T}(r) + \alpha\overset{1}{T}(r) + \gamma\overset{2}{T}(r) + \cdots .$$

This relationship was substituted into the differential equation and boundary conditions. The coefficients of the first-order terms in α and γ on both sides of the equations were equated. The following linear differential equations and boundary conditions result:

$$\frac{1}{r}\frac{d}{dr}\left[r\frac{d\overset{0}{T}}{dr}\right] = -A \qquad \frac{d\overset{0}{T}}{dr} = 0;\ \overset{0}{T} = T_o \text{ at } r = r_o$$

$$\frac{d}{dr}\left[r\left\{\overset{0}{T}\frac{d\overset{0}{T}}{dr} + \frac{d\overset{1}{T}}{dr}\right\}\right] = 0 \qquad \frac{d\overset{1}{T}}{dr} = 0;\ \overset{1}{T} = 0 \text{ at } r = r_o$$

$$\frac{1}{r}\frac{d}{dr}\left[r\frac{d\overset{2}{T}}{dr}\right] = A\overset{0}{T} \qquad \frac{d\overset{2}{T}}{dr} = 0;\ \overset{2}{T} = 0 \text{ at } r = r_o$$

These differential equations were solved and substituted into the original pertubation series. The following relationship was obtained for the inner wall temperature:

$$T(r_i,\alpha,\gamma) = \overset{0}{T}(r_i) + \frac{\alpha}{2}\left[T_o^2-\overset{0}{T}{}^2(r_i)\right] + \gamma\left\{T_o^2-T_o\overset{0}{T}(r_i)\right.$$
$$- \frac{A^2r_o^4}{16}\ln\frac{r_o}{r_i} - \frac{A^2r_o^2r_i^2}{8}\ln\frac{r_o}{r_i} + \frac{A^2r_o^2}{16}(r_o^2-r_i^2)$$
$$\left. + \frac{A^2}{64}(r_o^4-r_o^4)\right\} + \cdots ,$$

with

$$\overset{0}{T} = \frac{A}{4}(r_o^2-r_i^2) - \frac{Ar_o^2}{2}\ln\frac{r_o}{r_i} + T_o .$$

Substituting the dimensions and physical properties of the stainless steel tube into the relationship, the final result was

$$T_o-T_i = 8.250 \cdot 10^{-7} A - 4.389 \cdot 10^{-10} T_oA$$
$$+ 1.810 \cdot 10^{-16} A^2 + \gamma\left\{8.250 \cdot 10^{-7} AT_o\right.$$
$$\left. + 0.016 \cdot 10^{-10} A^2\right\} + \cdots .$$

The second-order terms were obtained and proved to be 10% of the first-order terms. Since the first-order terms contributed a maximum of 0.3°F to the temperature, the justification of neglecting second-order terms was proven. The term which resulted from the dependence of the electrical resistance upon temperature was also negligible under these test conditions. The final result for the temperature drop through the tube wall was

$$T_o - T_1 = 8.250 \cdot 10^{-7} A - 4.389 \cdot 10^{-10} T_o A$$

$$+ 1.810 \cdot 10^{-16} A^2 .$$

Figure 26 is a plot of this equation which was made to facilitate the reduction of the experimental data.

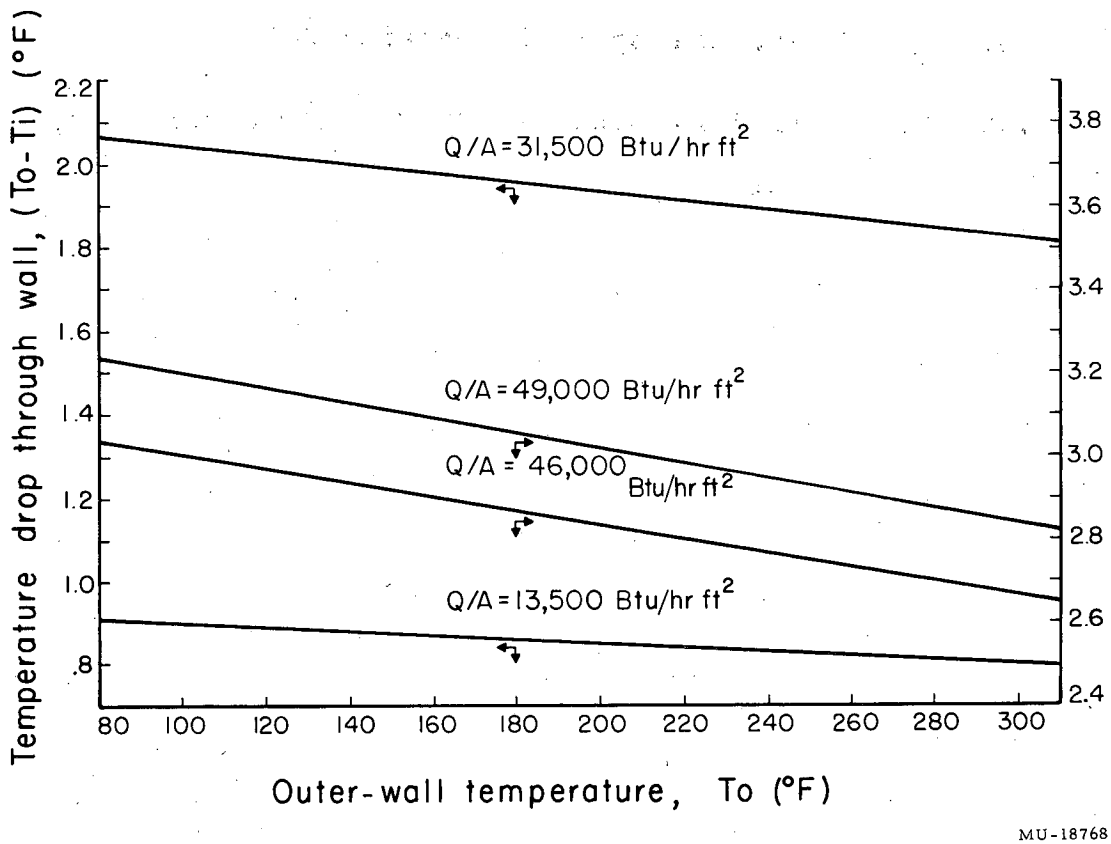

Fig. 26. Temperature drop through tube wall.

Table I. Nonboiling Heat Transfer Data

Run No.	T_{im} °F	T_{bm} °F	ΔT °F	G $\frac{lb}{sec\ ft^2}$	$q \cdot 10^{-1}$ $\frac{BTU}{hr\ ft^2}$	$h \cdot 10^{-1}$ $\frac{BTU}{hr\ ft^2\ °F}$	Nu	Re $\cdot 10^{-3}$	Pr	$\left(\frac{\mu_b}{\mu_w}\right)^{.14}$	k_b $\frac{BTU}{hr\ ft\ °F}$	μ_w c.p.	Heat Loss %
1	92.0	85.4	6.6	165	459	70	118	18.3	5.40	1.011	0.355	0.746	1.8
1-b	86.8	82.9	3.9	301	443	114	192	32.2	5.69	1.006	0.354	0.793	0.4
2	89.5	84.4	5.1	218	476	93	158	23.8	5.47	1.001	0.355	0.768	0.7
2-b	90.7	83.5	7.2	301	900	125	212	32.6	5.65	1.002	0.354	0.758	1.1
3	93.6	84.1	9.5	113	504	53	89.5	12.3	5.49	1.016	0.355	0.733	2.2
3-b	89.9	82.1	7.8	275	888	114	194	29.2	5.66	1.013	0.353	0.765	1.2
4	103.1	85.8	17.3	56.1	512	30	49.9	6.24	5.34	1.027	0.356	0.663	3.3
5	96.5	84.3	12.2	83.1	498	41	68.9	9.08	5.47	1.020	0.355	0.710	3.7
6	85.2	80.9	4.3	294	474	110	187	30.7	5.74	1.008	0.353	0.807	1.1
7	89.5	81.6	7.9	138	485	61	104	14.6	5.68	1.013	0.353	0.768	1.2
8	87.6	81.2	6.4	191	490	77	130	20.1	5.72	1.015	0.353	0.786	2.3
9	97.4	82.6	14.8	69.3	508	34	58.1	7.42	5.59	1.024	0.354	0.703	3.0
10	86.7	79.7	7.0	167	492	70	120	17.2	5.83	1.012	0.353	0.793	2.5
11	90.4	83.8	6.6	164	469	71	120	17.7	5.54	1.012	0.354	0.759	2.1
12	103.3	83.7	19.6	164	1454	74	126	17.7	5.54	1.031	0.354	0.663	1.7
13	107.8	85.0	22.8	136	1421	62	105	15.0	5.43	1.036	0.355	0.630	2.0
14	101.4	83.6	17.8	192	1479	83	141	20.8	5.53	1.028	0.354	0.674	1.2
15	99.1	83.5	15.6	220	1384	89	150	23.6	5.56	1.027	0.354	0.684	5.5
16	122.2	95.1	27.4	113	1521	56	92.4	13.9	4.78	1.040	0.360	0.548	3.0
17	95.1	81.5	13.6	205	1227	90	153	21.6	5.66	1.023	0.353	0.721	3.1
18	187.9	179.7	8.2	206	1057	129	200	52.7	2.57	1.008	0.388	0.329	1.8
19	187.6	183.5	4.1	269	665	162	250	70.9	2.09	1.003	0.389	0.330	1.4

Table II. Boiling Heat Transfer Data

ℓ ft	T_i °F	T_b °F	p psia	$h_B \cdot 10^{-1}$ $\frac{BTU}{hr ft^2 °F}$	$\frac{h_B}{h_\ell}$	x %	X_{tt}	$\left(\frac{dp}{d\ell}\right)_{tpt}$ $\frac{psia}{ft}$	$\frac{\left(\frac{dp}{d\ell}\right)_{tpt}}{\left(\frac{dp}{d\ell}\right)_\ell}$	$\frac{c\mu_\ell}{k_\ell}$	$\frac{h_B D}{k_\ell}$	$\frac{q}{h_{fg} G_T} \cdot 10^{+6}$	k_ℓ $\frac{BTU}{hr ft. °F}$	μ_ℓ c.p.	$\frac{G_T D}{\mu_\ell} \cdot 10^{-3}$
Run No. 5 m = 0.464 lb/sec G_T = 164.5 lb/sec ft^2 P = 4.32 kva q = 13800 BTU/hr ft^2															
1	228.4	224.2	18.73	329	2.89	1.57	1.576	.267	16.1	1.64	499	24.25	.394	.265	55.2
2	227.6	223.3	18.44	321	2.83	1.82	1.497	.302	18.3	1.66	488	24.23	.394	.267	54.8
3	226.8	222.3	18.10	308	2.72	2.08	1.200	.345	21.0	1.67	467	24.21	.394	.268	54.6
4	225.4	221.1	17.69	321	2.88	2.36	1.052	.468	28.6	1.68	488	24.19	.394	.270	54.2
5	223.2	219.3	17.14	354	3.18	2.67	0.928	.682	41.8	1.69	539	24.16	.394	.273	53.6
Run No. 5-b; m = 0.461 lb/sec; G_T = 163.5 lb/sec ft^2; p = 4.32 kva; q = 13,800 BTU/hr ft^2															
1	228.5	224.5	18.75	345	3.03	1.75	1.575	.275	16.8	1.64	524	24.39	.395	.265	54.9
2	227.8	223.7	18.45	337	2.97	2.00	1.271	.338	20.7	1.65	512	24.37	.394	.266	54.7
3	226.9	222.6	18.07	321	2.86	2.31	1.102	.400	24.7	1.66	488	24.35	.394	.268	54.3
4	225.4	221.2	17.59	321	2.88	2.57	.991	.503	31.1	1.68	488	24.33	.394	.270	53.9
5	223.1	219.4	17.03	373	3.36	2.90	.869	.724	45.0	1.69	568	24.30	.394	.273	53.3
Run No. 8; m = 0.466 lb/sec; G_T = 165.2 lb/sec ft^2; p = 4.32 kva; q = 13,800 BTU/hr ft^2															
1	229.6	225.8	19.33	288	2.53	2.07	1.224	.220	13.4	1.63	437	24.10	.395	.262	56.2
2	229.5	225.1	19.03	314	2.76	2.33	1.101	.363	22.1	1.64	477	24.08	.395	.264	55.8
3	228.4	223.7	18.58	294	2.60	2.61	0.986	.477	29.1	1.65	446	24.06	.394	.266	55.4
4	226.9	222.1	18.05	287	2.57	2.92	0.874	.578	35.6	1.67	437	24.04	.394	.268	55.0
5	224.8	220.1	17.42	294	2.65	3.26	0.776	.778	48.6	1.69	447	24.01	.394	.272	54.2

(Continued)

Table II (Continued-1)

ℓ ft	T_i °F	T_b °F	p psia	$h_B \cdot 10^{-1}$ $\frac{BTU}{hr ft^2 °F}$	$\frac{h_B}{h_\ell}$	x %	X_{tt}	$\left(\frac{dp}{d\ell}\right)_{tpt}$ $\frac{psia}{ft.}$	$\frac{\left(\frac{dp}{d\ell}\right)_{tpt}}{\left(\frac{dp}{d\ell}\right)_\ell}$	$\frac{c\mu_\ell}{k_\ell}$	$\frac{h_B D}{k_\ell}$	$\frac{q}{h_{fg} G_T} \cdot 10^{+6}$	k_ℓ $\frac{BTU}{hr ft °F}$	μ_ℓ c.p.	$\frac{G_T D}{\mu_\ell} \cdot 10^{-3}$
Run No. 9 ; m= 0.462 lb./sec.; G_T= 163.8 lb./sec.ft.^{2}; P= 4.32 KVA; q= 13,600 BTU/hr.ft.^{2}															
1	232.0	228.4	20.25	368	3.29	2.35	1.123	.415	25.7	1.60	559	24.09	.395	.258	56.5
2	229.9	227.2	19.75	368	3.23	2.64	.996	.518	32.3	1.61	559	24.04	.395	.260	56.0
3	229.7	225.6	19.20	336	2.98	2.96	.884	.637	39.7	1.63	511	24.02	.395	.263	55.4
4	228.1	223.6	18.55	302	2.70	3.32	.784	.687	42.4	1.65	460	23.99	.394	.266	54.8
5	225.3	221.2	17.80	340	3.08	3.70	.694	.783	49.0	1.68	518	23.97	.394	.270	54.0
Run No. 10 ; m= 0.464 lb./sec.; G_T= 164.5 lb./sec.ft.^{2}; P= 4.30 KVA; q= 13,740 BTU/hr.ft.^{2}															
1	235.1	231.8	21.55	416	3.59	2.92	.949	.497	30.8	1.57	631	24.12	.395	.253	58.1
2	233.7	230.4	20.95	416	3.62	3.24	.850	.637	39.7	1.58	631	24.10	.395	.255	57.6
3	232.1	228.6	20.25	392	3.45	3.57	.751	.768	47.9	1.60	595	24.06	.395	.258	57.0
4	230.0	226.5	19.42	392	3.49	3.93	.683	.842	53.0	1.63	596	24.03	.395	.262	56.1
5	227.1	223.5	18.51	381	3.44	4.38	.603	1.00	62.9	1.66	580	23.98	.394	.267	55.0
Run No. 11 ; m= 0.464 lb./sec.; G_T= 164.5 lb./sec.ft.^{2}; P= 4.32 KVA; q= 13,800 BTU/hr.ft.^{2}															
1	238.5	235.1	22.86	406	3.72	3.66	.769	.640	40.4	1.54	615	24.42	.396	.248	57.9
2	236.8	233.4	22.12	406	3.75	4.00	.711	.783	50.4	1.55	615	24.39	.395	.250	57.5
3	234.9	231.4	21.26	394	3.69	4.37	.646	.908	57.9	1.57	598	24.36	.395	.253	56.8
4	232.6	228.8	20.28	363	3.44	4.78	.579	1.03	66.1	1.60	551	24.32	.395	.258	55.7
5	229.4	225.5	19.21	354	3.44	5.22	.541	1.21	77.6	1.63	538	24.27	.395	.263	54.6

(Continued)

Table II (Continued-2)

ℓ ft	T_i °F	T_b °F	p psia	$h_B \cdot 10^{-1}$ $\frac{BTU}{hr.ft.^2 °F}$	$\frac{h_B}{h_\ell}$	x %	X_{tt}	$\left(\frac{dp}{d\ell}\right)_{tpt}$ $\frac{psia}{ft.}$	$\frac{\left(\frac{dp}{d\ell}\right)_{tpt}}{\left(\frac{dp}{d\ell}\right)_\ell}$	$\frac{c\mu_\ell}{k_\ell}$	$\frac{h_B D}{k_\ell}$	$\frac{q}{h_{fg} G_T} \cdot 10^{+6}$	k_ℓ $\frac{BTU}{hr.ft.°F}$	μ_ℓ c.p.	$\frac{G_T D}{\mu_\ell} \cdot 10^{-3}$
Run No. 12; m= 0.462 lb./sec.; G_T= 163.8 lb./sec.ft.^{2}; P= 4.38 KVA; q= 14,000 BTU/hr.ft.^{2}															
1															
2	240.8	237.4	23.83	412	3.80	5.34	.563	.965	62.3	1.51	624	24.89	.396	.244	60.4
3	238.6	234.9	22.75	378	3.52	5.75	.511	1.06	68.9	1.54	573	24.85	.396	.248	59.5
4	235.9	232.4	21.72	400	3.78	6.16	.469	1.17	76.3	1.56	606	24.81	.395	.252	58.5
5	232.0	228.9	20.35	451	4.34	6.66	.425	1.46	85.1	1.60	685	24.74	.395	.258	57.2
Run No. 13; m= 0.460 lb./sec.; G_T= 163.1 lb./sec.ft.^{2}; P= 4.32 KVA; q= 13,800 BTU/hr.ft.^{2}															
1	245.6	242.5	26.07	445	3.80	5.86	.553	1.09	73.9	1.47	674	24.77	.396	.238	60.9
2	243.3	240.1	25.02	431	3.72	6.25	.491	1.15	78.4	1.49	653	24.73	.396	.241	60.1
3	240.7	237.7	23.94	460	4.01	6.65	.457	1.24	80.8	1.51	697	24.69	.396	.244	59.4
4	237.7	234.7	22.73	460	4.07	7.05	.431	1.41	96.9	1.53	697	24.64	.396	.248	58.4
5	234.3	231.1	21.22	431	3.88	7.60	.379	1.87	129.3	1.57	655	24.62	.395	.254	57.1
Run No. 14; m= 0.463 lb./sec.; G_T= 164.2 lb./sec.ft.^{2}; P= 4.32 KVA; q= 13,800 BTU/hr.ft.^{2}															
1	224.0	219.0	16.85	276	2.46	.949	2.359	.143	8.5	1.69	420	24.19	.394	.273	53.5
2	223.9	218.5	16.69	256	2.28	1.16	1.979	.157	9.4	1.70	389	24.18	.394	.274	53.3
3	223.6	217.9	16.52	242	2.17	1.38	1.681	.202	12.1	1.71	368	24.17	.394	.275	53.1
4	222.5	217.2	16.28	260	2.34	1.61	1.441	.258	15.5	1.72	397	24.15	.394	.277	52.7
5	221.1	216.3	15.97	287	2.58	1.86	1.244	.386	23.3	1.73	438	24.14	.394	.278	52.5

(Continued)

Table II (Continued-3)

ℓ ft	T_1 °F	T_b °F	p psia	$h_B \cdot 10^{-1}$ $\frac{BTU}{hr ft^2 °F}$	$\frac{h_B}{h_\ell}$	x %	X_{tt}	$\left(\frac{dp}{d\ell}\right)_{tpt}$ $\frac{psia}{ft.}$	$\frac{\left(\frac{dp}{d\ell}\right)_{tpt}}{\left(\frac{dp}{d\ell}\right)_\ell}$	$\frac{c\mu_\ell}{k_\ell}$	$\frac{h_B D}{k_\ell}$	$\frac{q}{h_{fg} G_T} \cdot 10^{+6}$	k_ℓ $\frac{BTU}{hr ft. °F}$	μ_ℓ c.p.	$\frac{C_T D}{\mu_\ell} \cdot 10^{-3}$
Run No. 15; m= 0.478 lb./sec.; G_T= 169.5 lb./sec.ft.^{2}; P= 4.32 KVA; q= 13,800 BTU/hr.ft.^{2}															
1	241.0	237.8	24.00	431	3.69	4.30	.664	.75	45.9	1.51	653	23.73	.396	.244	61.8
2	239.1	235.8	23.17	418	3.61	4.66	.602	.87	53.3	1.53	634	23.70	.396	.247	61.1
3	237.0	233.5	22.21	394	3.45	5.05	.575	1.05	64.7	1.55	598	23.66	.395	.251	60.1
4	234.5	230.8	21.06	373	3.30	5.50	.545	1.15	71.3	1.57	566	23.61	.395	.254	59.4
5	230.9	227.6	19.83	418	3.77	5.96	.468	1.24	77.1	1.61	635	23.56	.395	.260	58.0
Run No. 16; m= 0.460 lb./sec.; G_T= 163.1 lb./sec.ft.^{2}; P= 15.6 KVA; q= 49,800 BTU/hr.ft.^{2}															
1	259.3	250.1	29.84	542	4.53	5.96	.559	1.00	67.8	1.41	820	89.81	.396	.228	63.7
2	257.0	249.0	28.73	623	5.27	6.75	.487	1.21	83.1	1.43	943	89.68	.396	.230	63.1
3	254.7	246.7	27.39	623	5.33	7.60	.434	1.45	101.1	1.44	943	89.50	.396	.233	62.3
4	250.6	242.7	25.90	631	5.52	8.50	.371	1.67	118.5	1.48	955	89.31	.396	.238	61.0
5	245.5	237.9	23.97	656	5.85	9.47	.322	2.14	153.9	1.51	993	89.04	.396	.244	59.5
Run No. 17; m= 0.462 lb./sec.; G_T= 163.8 lb./sec.ft.^{2}; P= 15.6 KVA; q= 49,800 BTU/hr.ft.^{2}															
1	248.1	229.9	20.73	274	2.34	.83	2.541	.057	3.43	1.58	416	88.23	.395	.256	56.9
2	247.7	229.6	20.59	275	2.37	1.47	1.744	.263	16.1	1.59	418	88.21	.395	.257	56.7
3	245.2	228.8	20.22	304	2.64	2.12	1.238	.437	27.0	1.60	461	88.16	.395	.258	56.4
4	239.9	227.4	19.73	399	3.49	2.83	.933	.563	35.2	1.61	606	88.08	.395	.260	56.0
5	236.7	225.3	19.00	445	3.96	3.64	.722	.985	62.4	1.63	676	87.96	.395	.263	55.4

(Continued)

Table II (Continued-4)

ℓ ft	T_i °F	T_b °F	p psia	$h_B \cdot 10^{-1}$ $\frac{BTU}{hr ft^2 °F}$	$\frac{h_B}{h_\ell}$	x %	X_{tt}	$\left(\frac{dp}{d\ell}\right)_{tpt}$ $\frac{psia}{ft.}$	$\frac{\left(\frac{dp}{d\ell}\right)_{tpt}}{\left(\frac{dp}{d\ell}\right)_\ell}$	$\frac{c\mu_\ell}{k_\ell}$	$\frac{h_B D}{k_\ell}$	$\frac{q}{h_{fg} G_T} \cdot 10^{+6}$	k_ℓ $\frac{BTU}{hr ft °F}$	μ_ℓ c.p.	$\frac{G_T D}{\mu_\ell} \cdot 10^{-3}$
Run No. 18; m= 0.462 lb./sec.; G_T= 163.8 lb./sec.ft.^{2}; P= 15.5 KVA; q= 49,500 BTU/hr.ft.^{2}															
1	258.8	234.2	22.42	339	2.87	1.61	1.665	.183	11.3	1.54	514	87.87	.395	.249	58.5
2	247.8	233.5	22.14	346	2.95	2.26	1.253	.297	18.5	1.55	525	87.82	.395	.250	58.2
3	245.8	232.3	21.69	366	3.16	2.94	.939	.415	26.1	1.56	556	87.76	.395	.252.	57.8
4	241.8	230.6	21.04	442	3.85	3.69	.751	.792	50.3	1.58	670	87.67	.395	.256	56.9
5	238.0	227.9	19.99	490	4.36	4.55	.602	1.32	85.2	1.61	744	87.50	.395	.260	56.0
Run No. 23; m= 0.461 lb./sec.; G_T= 163.5 lb./sec.ft.^{2}; P= 9.72 KVA; q= 31,100 BTU/hr.ft.^{2}															
1	248.2	240.1	25.86	383	3.61	4.20	.714	.815	53.0	1.49	580	55.56	.396	.241	60.3
2	246.2	239.1	24.96	437	3.73	4.73	.582	1.10	72.3	1.49	662	55.49	.396	.242	60.1
3	244.2	237.3	23.86	450	3.89	5.32	.567	1.16	77.1	1.51	682	55.39	.396	.244	59.6
4	241.1	234.6	22.60	478	4.18	6.00	.493	1.30	87.4	1.54	724	55.28	.395	.249	58.4
5	236.9	231.0	21.19	526	4.71	6.75	.426	1.49	101.1	1.57	799	55.15	.395	.254	57.2
Run No. 24; m= 0.462 lb./sec.; G_T= 163.8 lb./sec.ft.^{2}; P= 9.84 KVA; q= 31,400 BTU/hr.ft.^{2}															
1	252.0	245.9	27.72	515	4.36	5.65	.569	1.00	66.9	1.44	780	56.25	.396	.233	62.5
2	249.7	243.7	26.66	524	4.48	6.24	.510	1.18	79.9	1.46	793	56.16	.396	.237	61.5
3	247.3	241.0	25.39	493	4.26	6.91	.451	1.33	90.4	1.48	746	56.06	.396	.240	60.7
4	243.9	237.8	24.00	515	4.54	7.65	.398	1.48	101.6	1.51	780	55.93	.396	.244	59.7
5	239.4	234.0	22.48	582	5.23	8.47	.350	1.73	120.8	1.55	883	55.79	.395	.250	58.3

(Continued)

Table II (Continued-5)

ℓ ft	T_i °F	T_b °F	p psia	$h_B \cdot 10^{-1}$ $\frac{BTU}{hr ft^2 °F}$	$\frac{h_B}{h_\ell}$	x %	X_{tt}	$\left(\frac{dp}{d\ell}\right)_{tpt}$ $\frac{psia}{ft.}$	$\frac{\left(\frac{dp}{d\ell}\right)_{tpt}}{\left(\frac{dp}{d\ell}\right)_\ell}$	$\frac{c\mu_\ell}{k_\ell}$	$\frac{h_B D}{k_\ell}$	$\frac{q}{h_{fg} G_T} \cdot 10^{+6}$	k_ℓ $\frac{BTU}{hr ft °F}$	μ_ℓ c.p.	$\frac{G_T D}{\mu_\ell} \cdot 10^{-3}$
Run No. 25; m= 0.463 lb./sec.; G_T= 164.2 lb./sec.ft.^{2}; P= 9.90 KVA; q= 31,600 BTU/hr.ft.^{2}															
1	241.2	232.5	21.77	364	3.11	2.07	1.306	.265	16.3	1.56	551	55.93	.395	.252	58.0
2	240.0	231.1	21.38	355	3.07	2.55	1.057	.498	30.9	1.57	539	55.89	.395	.254	57.5
3	238.5	230.1	20.78	377	3.28	3.07	.891	.682	42.6	1.58	572	55.83	.395	.256	57.1
4	236.1	228.0	20.00	394	3.48	3.63	.750	.822	51.8	1.60	599	55.76	.395	.259	56.4
5	232.2	225.4	19.09	458	4.10	4.25	.635	.988	62.9	1.63	697	55.67	.395	.263	55.6
Run No. 26; m= 0.468 lb./sec.; G_T= 166.0 lb./sec.ft.^{2}; P= 9.84 KVA; q= 31,400 BTU/hr.ft.^{2}															
1	234.1	222.5	18.05	271	2.46	.77	2.945	.093	5.44	1.66	412	54.70	.394	.268	55.0
2	234.3	222.2	17.92	260	2.36	1.18	1.994	.168	9.90	1.66	395	54.48	.394	.268	55.0
3	233.8	221.6	17.72	258	2.36	1.61	1.499	.257	15.3	1.67	392	54.67	.394	.269	54.8
4	231.2	220.6	17.39	297	2.73	2.07	1.185	.400	23.9	1.68	451	54.63	.394	.271	54.4
5	227.9	219.2	16.91	361	3.36	2.58	.955	.480	28.9	1.69	550	54.57	.394	.273	54.0
Run No. 27; m= 0.464 lb./sec.; G_T= 164.5 lb./sec.ft.^{2}; P= 9.78 KVA; q= 31,200 BTU/hr.ft.^{2}															
1	245.3	237.4	23.80	396	3.37	3.47	.840	.592	37.5	1.51	599	55.37	.396	.244	59.9
2	243.6	236.0	23.16	411	3.52	3.75	.772	.732	46.7	1.53	623	55.31	.396	.247	59.2
3	241.9	234.0	22.33	296	3.43	4.08	.706	.770	49.3	1.54	600	55.24	.395	.249	58.8
4	239.0	231.4	21.28	411	3.61	4.56	.622	1.17	75.2	1.57	624	55.14	.395	.253	57.8
5	235.3	228.1	20.04	434	3.88	5.43	.528	1.30	84.7	1.60	659	55.02	.395	.259	56.5

(Continued)

Table II (Continued-6)

ℓ ft	T_i °F	T_b °F	p psia	$h_B \cdot 10^{-1}$ $\frac{BTU}{hr ft^2 °F}$	$\frac{h_B}{h_\ell}$	x %	X_{tt}	$\left(\frac{dp}{d\ell}\right)_{tpt}$ $\frac{psia}{ft.}$	$\frac{\left(\frac{dp}{d\ell}\right)_{tpt}}{\left(\frac{dp}{d\ell}\right)_t}$	$\frac{c\mu_\ell}{k_\ell}$	$\frac{h_B D}{k_\ell}$	$\frac{q}{h_{fg} G_T} \cdot 10^{+6}$	k_ℓ $\frac{BTU}{hr ft °F}$	μ_ℓ c.p.	$\frac{G_T D}{\mu_\ell} \cdot 10^{-3}$
Run No. 29; m= 0.466 lb./sec.; G_T= 165.2 lb./sec.ft.^{2}; P= 9.90 KVA; q= 31,600 BTU/hr.ft.^{2}															
1	251.9	246.0	27.89	536	4.53	5.83	.553	1.03	68.1	1.44	812	56.19	.396	.234	62.7
2	249.7	243.8	26.75	536	4.59	6.43	.469	1.21	81.0	1.46	812	56.11	.396	.236	62.2
3	247.4	241.2	25.50	510	4.41	7.06	.441	1.34	90.5	1.48	772	56.00	.396	.240	61.2
4	244.0	238.1	24.08	536	4.71	7.73	.394	1.47	100.5	1.51	812	55.87	.396	.244	60.2
5	239.2	234.1	22.43	620	5.57	8.46	.350	1.87	129.1	1.54	940	55.72	.395	.249	58.9
Run No. 30; m= 0.465 lb./sec.; G_T= 164.9 lb./sec.ft.^{2}; P= 9.84 KVA; q= 31,400 BTU/hr.ft.^{2}															
1	238.4	229.6	20.43	357	3.09	1.60	1.609	.241	14.6	1.59	542	55.29	.395	.257	57.0
2	237.5	228.8	20.13	361	3.13	2.05	1.271	.362	22.1	1.60	549	55.29	.395	.258	56.8
3	236.0	227.2	19.69	357	3.13	2.53	1.037	.497	30.6	1.62	543	55.22	.395	.261	56.1
4	233.7	225.5	19.10	388	3.46	3.06	.859	.656	40.6	1.63	590	55.16	.395	.263	55.6
5	230.4	223.3	18.31	443	3.97	3.64	.714	.920	57.5	1.66	673	55.08	.394	.267	54.8
Run No. 31; m= 0.598 lb./sec.; G_T= 212.1 lb./sec.ft.^{2}; P= 9.68 KVA; q= 30,900 BTU/hr.ft.^{2}															
1	243.0	233.7	22.27	333	2.53	1.14	2.450	.295	11.5	1.55	504	42.44	.395	.250	75.4
2	241.9	232.8	21.92	340	2.59	1.50	1.870	.418	16.3	1.56	515	42.42	.395	.252	74.8
3	240.5	231.6	21.42	347	2.93	1.92	1.307	.565	22.2	1.57	527	42.38	.395	.253	74.5
4	238.0	229.9	20.70	382	3.00	2.39	1.118	.677	26.8	1.58	579	42.33	.395	.256	73.6
5	234.7	227.5	19.81	430	3.43	2.90	.840	1.040	41.4	1.61	652	42.26	.395	.260	72.5

(Continued)

Table II (Continued-7)

ℓ ft	T_i °F	T_b °F	p psia	$h_B \cdot 10^{-1}$ $\frac{BTU}{hr ft^2 °F}$	$\frac{h_B}{h_\ell}$	x %	X_{tt}	$\left(\frac{dp}{d\ell}\right)_{tpt}$ $\frac{psia}{ft.}$	$\frac{\left(\frac{dp}{d\ell}\right)_{tpt}}{\left(\frac{dp}{d\ell}\right)_\ell}$	$\frac{c\mu_\ell}{k_\ell}$	$\frac{h_B D}{k_\ell}$	$\frac{q}{h_{fg} G_T} \cdot 10^{+6}$	k_ℓ $\frac{BTU}{hr ft °F}$	μ_ℓ c.p.	$\frac{G_T D}{\mu_\ell} \cdot 10^{-3}$
Run No. 32; m= 0.595 lb./sec.; G_T= 211.0 lb./sec.ft.^{2}; P= 9.84 KVA; q= 31,400 BTU/hr.ft.^{2}															
1	251.3	244.6	27.09	469	3.20	2.76	1.099	.695	28.3	1.46	710	43.65	.396	.235	79.8
2	249.6	242.9	26.29	469	3.26	3.22	.943	.870	35.7	1.48	710	43.60	.396	.238	78.8
3	247.8	240.7	25.27	443	3.17	3.73	.806	1.09	45.2	1.49	670	43.54	.396	.240	78.2
4	245.0	238.0	24.00	449	3.22	4.29	.686	1.37	57.1	1.51	680	43.44	.396	.244	76.9
5	240.7	234.2	22.54	484	3.53	4.91	.592	1.88	78.9	1.54	733	43.35	.395	.249	75.3
Run No. 33; m= 0.312 lb./sec.; G_T= 110.6 lb./sec.ft.^{2}; P= 9.78 KVA; q= 31,300 BTU/hr.ft.^{2}															
1	237.8	229.6	20.61	386	4.66	4.62	.596	.440	56.7	1.59	585	81.97	.395	.257	38.2
2	236.1	228.3	20.12	401	4.89	5.29	.526	.558	72.6	1.60	608	81.90	.395	.258	38.1
3	234.5	226.6	19.48	395	4.90	6.00	.474	.708	93.1	1.62	601	81.81	.395	.262	37.5
4	232.1	224.4	18.72	406	5.08	6.74	.403	.822	109.6	1.64	617	81.69	.394	.265	37.1
5	228.9	221.7	17.78	383	5.53	7.53	.346	1.10	148.0	1.67	582	81.56	.394	.269	36.5
Run No. 34; m= 0.313 lb./sec.; G_T= 111.0 lb./sec.ft.^{2}; P= 9.84 KVA; q= 31,400 BTU/hr.ft.^{2}															
1	242.2	235.1	22.90	443	5.40	7.76	.386	.793	108.0	1.53	671	82.52	.396	.248	39.8
2	240.0	233.3	22.05	469	6.33	8.51	.346	.882	121.9	1.55	712	82.39	.395	.251	39.3
3	237.7	230.8	21.08	456	5.71	9.28	.311	.968	135.2	1.57	691	82.25	.395	.254	38.9
4	234.8	228.1	20.02	469	6.04	10.01	.288	1.10	156.3	1.60	713	82.10	.395	.259	38.8
5	230.3	224.18	18.85	572	7.31	10.90	.252	1.33	191.1	1.64	869	81.92	.395	.264	37.4

(Continued)

Table II (Continued-8)

ℓ ft	T_i °F	T_b °F	p psia	$h_B \cdot 10^{-1}$ BTU/hr ft.^{2} °F	h_B/h_ℓ	x %	X_{tt}	$\left(\frac{dp}{d\ell}\right)_{tpt}$ psia/ft.	$\frac{\left(\frac{dp}{d\ell}\right)_{tpt}}{\left(\frac{dp}{d\ell}\right)_\ell}$	$\frac{c\mu_\ell}{k_\ell}$	$\frac{h_B D}{k_\ell}$	$\frac{q}{h_{fg} G_T} \cdot 10^{+6}$	k_ℓ BTU/hr ft. °F	μ_ℓ c.p.	$\frac{G_T D}{\mu_\ell} \cdot 10^{-3}$
Run No. 35; m= 0.313 lb./sec.; G_T= 111.0 lb./sec.ft.^{2}; P= 9.78 KVA; q= 31,200 BTU/hr.ft.^{2}															
1	240.6	233.5	22.17	440	5.32	6.37	.458	.612	81.0	1.55	667	81.83	.395	.250	39.5
2	238.7	231.7	21.43	446	5.46	7.08	.410	.796	106.9	1.57	677	81.67	.395	.253	39.0
3	236.7	229.5	20.53	434	5.39	7.85	.362	.948	128.7	1.59	659	81.60	.395	.257	38.4
4	233.9	226.9	19.50	446	5.65	8.65	.322	1.02	139.4	1.66	696	81.45	.395	.261	37.8
5	230.0	223.5	18.38	481	6.18	9.47	.286	1.28	177.5	1.70	750	81.28	.394	.267	37.0
Run No. 36; m= 0.312 lb./sec.; G_T= 110.6 lb./sec.ft.^{2}; P= 9.84 KVA; q= 31,400 BTU/hr.ft.^{2}															
1	238.7	230.8	21.06	398	4.81	5.16	.590	.523	67.8	1.57	604	82.39	.395	.254	38.8
2	238.1	229.8	20.51	379	4.63	5.84	.482	.632	83.1	1.58	575	82.32	.395	.256	38.4
3	235.5	227.5	19.80	393	4.87	6.57	.425	.737	97.9	1.61	597	82.21	.395	.260	37.9
4	232.8	225.1	18.98	408	5.14	7.32	.375	.878	117.9	1.64	620	82.09	.395	.264	37.3
5	229.2	222.3	18.01	456	5.83	8.12	.330	1.10	149.8	1.66	693	81.94	.394	.268	36.7
Run No. 37; m= 0.314 lb./sec.; G_T= 111.3 lb./sec.ft.^{2}; P= 9.84 KVA; q= 31,400 BTU/hr.ft.^{2}															
1	236.8	227.1	19.69	324	3.95	3.74	.722	.317	39.6	1.62	492	81.57	.395	.261	37.9
2	235.2	226.1	19.07	345	4.23	4.45	.612	.495	62.5	1.63	525	81.48	.395	.263	37.6
3	233.7	224.7	18.82	349	4.34	5.05	.535	.567	72.3	1.64	531	81.45	.395	.265	37.3
4	231.4	222.9	18.18	370	4.63	5.77	.459	.705	91.1	1.66	562	81.35	.394	.267	37.0
5	228.0	220.5	17.39	419	5.31	6.53	.399	.924	125.9	1.68	638	81.23	.394	.271	36.5

(Continued)

Table II (Continued-9)

ℓ ft	T_i °F	T_b °F	p psia	$h_B \cdot 10^{-1}$ BTU/hr.ft.^{2}°F	h_B/h_ℓ	x %	X_{tt}	$\left(\frac{dp}{d\ell}\right)_{tpt}$ psia/ft.	$\frac{\left(\frac{dp}{d\ell}\right)_{tpt}}{\left(\frac{dp}{d\ell}\right)_\ell}$	$c\mu_\ell/k_\ell$	$h_B D/k_\ell$	$\frac{q}{h_{fg}G_T} \cdot 10^{+6}$	k_ℓ BTU/hr.ft.°F	μ_ℓ c.p.	$G_T D/\mu_\ell \cdot 10^{-3}$
Run No. 38; m= 0.317 lb./sec.; G_T= 112.4 lb./sec.ft.^{2}; P= 9.84 KVA; q= 31,400 BTU/hr.ft.^{2}															
1	235.1	224.3	18.70	291	3.52	2.54	1.010	.198	23.7	1.64	443	80.89	.394	.265	37.7
2	233.9	223.6	18.45	305	3.79	3.15	.819	.318	38.0	1.65	464	80.86	.394	.266	37.5
3	232.2	222.5	18.06	321	3.95	3.80	.684	.458	56.0	1.66	488	80.80	.394	.268	37.3
4	230.1	221.1	17.54	349	4.34	4.48	.579	.592	73.1	1.68	531	80.70	.394	.271	36.9
5	227.1	219.3	16.92	403	5.06	5.20	.496	.592	73.9	1.69	613	80.62	.394	.273	36.6
Run No. 39; m= 0.314 lb./sec.; G_T= 111.3 lb./sec.ft.^{2}; P= 9.84 KVA; q= 31,400 BTU/hr.ft.^{2}															
1	233.8	222.1	17.83	269	3.26	2.02	1.224	.098	11.8	1.67	409	81.56	.394	.269	36.7
2	233.3	221.5	17.68	266	3.26	2.60	.967	.212	25.7	1.68	405	81.54	.394	.270	36.6
3	232.1	220.7	17.42	276	3.41	3.22	.787	.310	38.0	1.68	420	81.49	.394	.271	36.5
4	228.2	219.5	17.04	324	4.03	3.88	.656	.470	58.6	1.69	493	81.43	.394	.273	36.2
5	225.9	218.0	16.50	398	4.99	4.41	.571	.627	78.6	1.71	606	81.34	.394	.275	36.0
Run No. 40; m= 0.313 lb./sec.; G_T= 111.0 lb./sec.ft.^{2}; P= 14.4 KVA; q= 46,000 BTU/hr.ft.^{2}															
1	247.8	237.4	23.81	442	5.31	7.01	.433	.715	96.4	1.51	670	120.89	.396	.244	40.4
2	245.5	235.5	23.02	460	5.60	7.80	.384	.872	119.2	1.53	697	120.74	.396	.247	39.9
3	243.1	233.2	22.06	465	5.75	9.01	.326	1.02	141.7	1.56	705	120.55	.395	.251	39.3
4	239.5	230.3	20.94	500	6.32	10.07	.286	1.16	164.2	1.59	759	120.33	.395	.256	38.5
5	235.0	226.8	19.61	561	7.25	11.18	.251	1.50	217.3	1.62	853	120.04	.395	.261	37.8

(Continued)

Table II (Continued-10)

ℓ ft	T_i °F	T_b °F	p psia	$h_B \cdot 10^{-1}$ $\frac{BTU}{hr ft^2 °F}$	$\frac{h_B}{h_\ell}$	x %	x_{tt}	$\left(\frac{dp}{d\ell}\right)_{tpt}$ $\frac{psia}{ft.}$	$\frac{\left(\frac{dp}{d\ell}\right)_{tpt}}{\left(\frac{dp}{d\ell}\right)_\ell}$	$\frac{c\mu_\ell}{k_\ell}$	$\frac{h_B D}{k_\ell}$	$\frac{q}{h_{fg} G_T} \cdot 10^{+6}$	k_ℓ $\frac{BTU}{hr ft. °F}$	μ_ℓ c.p.	$\frac{G_T D}{\mu_\ell} \cdot 10^{-3}$
Run No. 41; m= 0.313 lb./sec.; G_T= 111.0 lb./sec.ft.^{2}; P= 14.4 KVA; q= 46,000 BTU/hr.ft.^{2}															
1	245.7	234.9	22.70	426	5.10	5.50	.534	.518	67.9	1.54	646	120.79	.396	.248	39.7
2	243.9	233.3	22.09	434	5.26	6.44	.454	.683	90.8	1.56	658	120.66	.395	.251	39.2
3	241.8	231.3	21.29	438	5.39	7.43	.382	.884	119.5	1.57	665	120.50	.395	.253	38.9
4	238.7	228.7	20.28	460	5.77	8.48	.334	1.13	156.0	1.60	698	120.30	.395	.258	38.2
5	234.9	225.5	19.07	489	6.26	9.57	.289	1.30	182.0	1.63	832	120.03	.395	.263	37.6
Run No. 42; m= 0.314 lb./sec.; G_T= 111.3 lb./sec.ft.^{2}; P= 14.4 KVA; q= 46,000 BTU/hr.ft.^{2}															
1	245.2	233.3	22.04	387	4.62	4.78	.603	.427	54.9	1.55	586	120.25	.395	.251	39.3
2	243.4	232.0	21.56	404	4.86	5.69	.506	.573	74.7	1.57	612	120.15	.395	.253	39.1
3	241.3	230.1	20.88	411	5.03	6.66	.430	.783	103.2	1.58	623	120.01	.395	.256	38.6
4	238.4	227.8	19.98	434	5.42	7.67	.366	.858	115.6	1.60	659	119.82	.395	.259	38.2
5	233.8	224.8	18.82	511	6.51	8.75	.314	1.34	182.9	1.64	777	119.57	.395	.264	37.5
Run No. 43; m= 0.316 lb./sec.; G_T= 112.1 lb./sec.ft.^{2}; P= 14.4 KVA; q= 46,000 BTU/hr.ft.^{2}															
1	243.7	229.5	20.63	324	3.87	3.20	.856	.200	24.5	1.59	492	119.11	.395	.257	38.7
2	241.5	228.8	20.33	362	4.37	4.07	.677	.437	54.4	1.60	550	119.04	.395	.258	38.6
3	238.9	227.3	19.74	397	4.85	5.02	.550	.704	89.2	1.61	603	118.91	.395	.260	38.3
4	236.0	225.3	18.99	430	5.34	6.00	.468	.796	102.7	1.63	653	118.75	.395	.263	37.9
5	233.2	222.8	18.18	442	5.60	7.00	.384	.980	128.0	1.66	744	118.58	.394	.267	37.3

(Continued)

Table II (Continued-11)

ℓ ft	T_i °F	T_b °F	p psia	$h_B \cdot 10^{-1}$ $\frac{BTU}{hr ft^2 °F}$	$\frac{h_B}{h_\ell}$	x %	X_{tt}	$\left(\frac{dp}{d\ell}\right)_{tpt}$ $\frac{psia}{ft.}$	$\frac{\left(\frac{dp}{d\ell}\right)_{tpt}}{\left(\frac{dp}{d\ell}\right)_\ell}$	$\frac{c\mu_\ell}{k_\ell}$	$\frac{h_B D}{k_\ell}$	$\frac{q}{h_{fg} G_T} \cdot 10^{+6}$	k_ℓ $\frac{BTU}{hr ft. °F}$	μ_ℓ c.p.	$\frac{G_T D}{\mu_\ell} \cdot 10^{-3}$
Run No. 44; m= 0.313 lb./sec.; G_T= 111.0 lb./sec.ft.^{2}; P= 14.4 KVA; q= 46,000 BTU/hr.ft.^{2}															
1	243.5	225.9	19.22	261	3.14	2.12	1.213	.145	17.6	1.62	397	119.87	.395	.262	37.7
2	242.1	225.4	19.04	275	3.34	2.96	.882	.275	34.0	1.63	419	119.83	.395	.263	37.5
3	239.1	224.4	18.68	313	3.82	3.86	.685	.458	57.5	1.64	476	119.74	.394	.265	37.3
4	235.1	223.0	18.21	380	4.71	4.78	.555	.560	71.3	1.66	578	119.66	.394	.267	37.0
5	231.0	221.1	17.55	465	5.83	5.76	.451	.730	94.5	1.68	707	119.51	.394	.271	36.4
Run No. 45; m= 0.313 lb./sec.; G_T= 111.0 lb./sec.ft.^{2}; P= 4.32 KVA; q= 13,800 BTU/hr.ft.^{2}															
1	235.2	231.9	21.51	418	5.17	7.72	.375	.785	106.9	1.57	635	36.16	.395	.253	38.9
2	233.1	229.9	20.70	431	5.36	8.16	.350	.817	112.2	1.58	655	36.12	.395	.256	38.5
3	231.0	227.6	19.87	406	5.12	8.60	.327	.862	118.8	1.61	616	36.06	.395	.260	37.9
4	228.5	225.1	18.99	406	5.19	9.06	.304	.917	127.2	1.64	617	36.00	.395	.264	37.3
5	226.6	222.4	17.99	329	4.26	9.56	.280	1.02	142.8	1.66	500	35.94	.394	.268	36.8
Run No. 46; m= 0.312 lb./sec.; G_T= 110.6 lb./sec.ft.^{2}; P= 4.32 KVA; q= 13,800 BTU/hr.ft.^{2}															
1	232.1	228.7	20.27	406	4.97	5.68	.497	.510	75.2	1.60	616	36.20	.395	.258	38.1
2	230.4	227.1	19.65	418	5.17	6.09	.465	.633	83.4	1.62	635	36.16	.395	.261	37.6
3	228.7	225.2	18.97	395	4.92	6.50	.420	.685	89.7	1.64	600	36.11	.395	.264	37.2
4	226.6	223.0	18.23	383	4.84	6.94	.392	.813	105.8	1.66	583	36.06	.394	.267	36.8
5	223.5	220.6	17.37	476	6.08	7.42	.356	.884	122.4	1.68	724	36.00	.394	.271	36.3

(Continued)

Table II (Continued-12)

ℓ ft	T_i °F	T_b °F	p psia	h_B $\cdot 10^{-1}$ BTU/hrft.^{2}°F	$\frac{h_B}{h_\ell}$	x %	X_{tt}	$\left(\frac{dp}{d\ell}\right)_{tpt}$ psia/ft.	$\frac{\left(\frac{dp}{d\ell}\right)_{tpt}}{\left(\frac{dp}{d\ell}\right)_\ell}$	$\frac{c\mu_\ell}{k_\ell}$	$\frac{h_B D}{k_\ell}$	$\frac{q}{h_{fg} G_T}$ $\cdot 10^{+6}$	k_ℓ BTU/hrft. °F	μ_ℓ c.p.	$\frac{G_T D}{\mu_\ell}$ $\cdot 10^{-3}$
Run No. 47; m= 0.314 lb./sec.; G_T= 111.3 lb./sec.ft.^{2}; P= 4.32 KVA; q= 13,800 BTU/hr.ft.^{2}															
1	229.7	225.8	19.18	354	4.33	4.38	.613	.277	53.8	1.62	538	35.86	.395	.262	37.8
2	228.5	224.5	18.69	345	4.25	4.75	.566	.532	66.8	1.64	524	35.83	.394	.265	37.4
3	227.0	222.9	18.13	337	4.19	5.15	.514	.580	74.2	1.66	512	35.79	.394	.267	37.1
4	225.3	221.1	17.54	329	4.12	5.55	.473	.615	80.2	1.68	500	35.75	.394	.271	36.5
5	222.6	219.0	16.88	380	4.85	5.98	.433	.672	85.8	1.69	578	35.70	.394	.273	36.3
Run No. 48; m= 0.311 lb./sec.; G_T= 110.3 lb./sec.ft.^{2}; P= 14.4 KVA; q= 46,000 BTU/hr.ft.^{2}															
1	247.8	238.3	24.41	495	5.94	7.59	.404	.470	100.5	1.50	749	121.58	.396	.243	40.4
2	245.2	236.3	23.61	517	6.31	8.62	.352	1.02	140.1	1.52	783	121.41	.396	.246	39.9
3	242.8	233.8	22.37	511	6.36	9.63	.308	1.23	169.4	1.55	775	121.17	.395	.250	39.3
4	239.5	230.9	21.14	535	6.78	10.73	.270	1.28	195.8	1.57	812	120.92	.395	.254	38.7
5	234.8	227.1	19.71	506	7.75	11.86	.237	1.52	225.4	1.62	769	120.61	.395	.261	37.6
Run No. 51; m= 0.314 lb./sec.; G_T= 111.3 lb./sec.ft.^{2}; P= 9.84 KVA; q= 31,400 BTU/hr.ft.^{2}															
1	241.3	234.9	22.74	491	5.96	7.39	.401	.683	102.1	1.53	745	82.27	.396	.248	39.9
2	238.9	232.9	21.93	524	6.44	8.13	.361	.837	115.1	1.56	795	82.15	.395	.252	39.2
3	236.8	230.5	21.01	499	6.23	8.86	.327	.978	131.4	1.58	757	82.03	.395	.256	38.6
4	234.1	227.9	19.94	507	6.45	9.69	.292	1.12	153.9	1.61	770	81.87	.395	.260	38.0
5	230.0	224.5	18.72	572	7.41	10.50	.261	1.33	199.2	1.64	869	81.68	.394	.265	37.3

(Continued)

Table II (Continued-13)

ℓ ft	T_i °F	T_b °F	p psia	$h_B \cdot 10^{-1}$ $\frac{BTU}{hr ft^2 °F}$	$\frac{h_B}{h_\ell}$	x %	X_{tt}	$\left(\frac{dp}{d\ell}\right)_{tpt}$ $\frac{psia}{ft.}$	$\frac{\left(\frac{dp}{d\ell}\right)_{tpt}}{\left(\frac{dp}{d\ell}\right)_\ell}$	$\frac{c\mu_\ell}{k_\ell}$	$\frac{h_B D}{k_\ell}$	$\frac{q}{h_{fg} G_T} \cdot 10^{+6}$	k_ℓ $\frac{BTU}{hr ft. °F}$	μ_ℓ c.p.	$\frac{G_T D}{\mu_\ell} \cdot 10^{-3}$
Run No. 52; m= 0.144 lb./sec.; G_T= 51.1 lb./sec.ft.^{2}; P= 9.84 KVA; q= 31,400 BTU/hr.ft.^{2}															
1	231.3	222.1	17.92	342	8.26	9.13	.291	.290	153.6	1.67	520	177.23	.394	.269	15.4
2	229.9	221.2	17.57	361	8.87	10.39	.257	.367	196.3	1.68	549	177.12	.394	.271	15.1
3	228.5	219.9	17.16	365	9.10	11.68	.226	.404	219.0	1.69	550	176.97	.394	.272	14.8
4	226.6	218.5	16.68	388	9.85	12.99	.200	.495	270.8	1.70	591	176.79	.394	.274	14.7
5	223.9	216.7	16.12	436	11.18	14.33	.177	.626	345.7	1.72	664	176.59	.394	.277	14.1
Run No. 54; m= 0.460 lb./sec.; G_T= 163.1 lb./sec.ft.^{2}; P= 9.84 KVA; q= 31,400 BTU/hr.ft.^{2}															
1	234.7	222.6	18.08	260	2.28	.837	2.751	.050	1.88	1.66	395	55.56	.394	.267	54.5
2	235.3	222.4	18.00	244	2.15	1.23	1.942	.110	4.18	1.66	371	55.56	.394	.268	54.3
3	234.4	221.9	17.83	252	2.23	1.65	1.481	.237	9.06	1.67	383	55.54	.394	.269	54.1
4	231.9	221.0	17.53	288	2.56	2.11	1.171	.385	14.7	1.68	438	55.51	.394	.271	53.7
5	228.1	219.7	17.10	374	3.47	2.66	.934	.447	21.7	1.69	570	55.46	.394	.273	53.3
Run No. 55; m= 0.459 lb./sec.; G_T= 162.8 lb./sec.ft.^{2}; P= 9.84 KVA; q= 31,400 BTU/hr.ft.^{2}															
1	241.4	232.3	21.66	345	2.95	2.29	1.182	.357	22.5	1.56	524	59.12	.395	.252	57.4
2	240.3	231.3	21.26	349	3.01	2.76	.991	.493	31.4	1.57	530	59.07	.395	.253	57.1
3	238.6	229.8	20.66	357	3.12	3.29	.828	.650	41.4	1.59	542	59.00	.395	.257	56.3
4	235.9	227.7	19.92	383	3.40	3.85	.706	.836	56.5	1.61	582	58.93	.395	.260	55.6
5	232.6	225.3	19.00	431	3.86	4.46	.600	1.05	67.8	1.63	652	58.83	.395	.263	55.0

(Continued)

Table II (Continued-14)

ℓ ft	T_i °F	T_b °F	p psia	$h_B \cdot 10^{-1}$ $\frac{BTU}{hr ft^2 °F}$	$\frac{h_B}{h_\ell}$	x %	X_{tt}	$\left(\frac{dp}{d\ell}\right)_{tpt}$ $\frac{psia}{ft.}$	$\frac{\left(\frac{dp}{d\ell}\right)_{tpt}}{\left(\frac{dp}{d\ell}\right)_\ell}$	$\frac{c\mu_\ell}{k_\ell}$	$\frac{h_B D}{k_\ell}$	$\frac{q}{h_{fg} G_T} \cdot 10^{+6}$	k_ℓ $\frac{BTU}{hr ft. °F}$	μ_ℓ c.p.	$\frac{G_T D}{\mu_\ell} \cdot 10^{-3}$
Run No. 56; m= 0.455 lb./sec.; G_T= 161.4 lb./sec.ft.^{2}; P= 9.84 KVA; q= 31,400 BTU/hr.ft.^{2}															
1	247.0	239.7	24.78	431	3.62	4.05	.754	.698	46.2	1.49	652	56.85	.396	.242	59.3
2	245.1	237.9	24.04	437	3.75	4.59	.648	.830	55.4	1.51	661	56.78	.396	.244	58.8
3	243.1	235.7	23.07	424	3.68	5.19	.571	1.010	68.0	1.53	642	56.69	.396	.247	58.1
4	240.0	233.0	21.94	449	3.95	5.84	.499	1.235	84.2	1.55	681	56.60	.395	.251	57.2
5	236.1	229.5	20.60	476	4.28	6.53	.436	1.510	103.7	1.59	723	56.46	.395	.257	55.8
Run No. 57; m= 0.464 lb./sec.; G_T= 164.5 lb./sec.ft.^{2}; P= 9.84 KVA; q= 31,400 BTU/hr.ft.^{2}															
1	252.2	245.8	27.68	491	4.16	5.96	.540	.995	66.2	1.44	744	55.99	.396	.234	62.6
2	250.0	243.5	26.62	484	4.15	6.54	.485	1.144	77.1	1.46	732	55.89	.396	.237	61.8
3	247.6	240.8	25.38	462	4.01	7.17	.433	1.314	89.5	1.48	700	55.81	.396	.240	61.0
4	243.9	237.8	23.98	515	4.54	7.83	.389	1.516	104.2	1.51	781	55.66	.396	.244	60.0
5	239.3	233.9	22.30	582	5.25	8.55	.347	1.808	125.4	1.54	883	55.51	.395	.249	58.8
Run No. 58; m= 0.312 lb./sec.; G_T= 110.6 lb./sec.ft.^{2}; P= 9.84 KVA; q= 31,400 BTU/hr.ft.^{2}															
1,	233.6	219.3	16.98	220	2.68	1.42	1.648	.050	3.77	1.69	336	81.84	.394	.273	36.1
2	233.9	219.1	16.91	212	2.61	1.99	1.211	.107	8.13	1.69	323	81.82	.394	.273	36.1
3	232.4	218.7	16.78	230	2.83	2.57	.955	.178	13.7	1.70	349	81.80	.394	.274	36.0
4	229.7	218.0	16.52	269	3.33	3.20	.773	.320	24.9	1.71	409	81.75	.394	.275	35.8
5	225.9	216.9	16.16	349	4.36	3.85	.641	.413	32.5	1.72	532	81.69	.394	.277	35.6

(Continued)

Table II (Continued-15)

ℓ ft	T_i °F	T_b °F	p psia	h_B $\cdot 10^{-1}$ $\frac{BTU}{hr ft^2 °F}$	$\frac{h_B}{h_\ell}$	x %	X_{tt}	$\left(\frac{dp}{d\ell}\right)_{tpt}$ $\frac{psia}{ft.}$	$\frac{\left(\frac{dp}{d\ell}\right)_{tpt}}{\left(\frac{dp}{d\ell}\right)_\ell}$	$\frac{c\mu_\ell}{k_\ell}$	$\frac{h_B D}{k_\ell}$	$\frac{a}{h_{fg} G_T}$ $\cdot 10^{+6}$	k_ℓ $\frac{BTU}{hr ft. °F}$	μ_ℓ c.p.	$\frac{G_T D}{\mu_\ell}$ $\cdot 10^{-3}$
Run No. 61; m= 0.313 lb./sec.; G_T= 111.0 lb./sec.ft.^{2}; P= 9.84 KVA; q= 31,400 BTU/hr.ft.^{2}															
1	232.6	218.0	16.53	215	2.61	0.85	2.520	.027	3.19	1.71	328	81.47	.394	.275	35.9
2	233.9	217.9	16.49	197	2.41	1.41	1.628	.061	7.26	1.71	299	81.47	.394	.275	35.9
3	232.9	217.6	16.39	205	2.53	1.98	1.063	.124	14.9	1.71	313	81.42	.394	.276	35.8
4	229.8	217.0	16.20	246	3.05	2.58	.926	.202	24.5	1.72	374	81.42	.394	.277	35.6
5	225.7	216.1	15.94	327	4.23	3.20	.758	.286	35.1	1.73	499	81.39	.394	.278	35.5
Run No. 62; m= 0.312 lb./sec.; G_T= 110.6 lb./sec.ft.^{2}; P= 10.0 KVA; q= 32,000 BTU/hr.ft.^{2}															
1	233.6	220.2	17.27	239	2.91	1.60	1.482	.063	7.47	1.69	364	83.40	.394	.272	36.2
2	234.1	220.0	17.18	227	2.78	2.18	1.107	.137	16.7	1.69	345	83.38	.394	.272	36.2
3	232.6	219.4	16.99	243	2.99	2.79	.882	.237	29.3	1.69	369	83.35	.394	.273	36.0
4	229.6	218.5	16.70	288	3.58	3.43	.719	.346	43.0	1.70	439	83.30	.394	.274	35.9
5	226.0	217.2	16.30	364	4.56	4.11	.603	.489	61.5	1.72	554	83.22	.394	.277	35.5
Run No. 63; m= 0.310 lb./sec.; G_T= 109.9 lb./sec.ft.^{2}; P= 9.84 KVA; q= 31,400 BTU/hr.ft.^{2}															
1	234.7	224.2	18.61	299	3.64	2.84	.909	.244	30.6	1.64	455	82.69	.394	.265	36.8
2	233.7	223.5	18.38	308	3.78	3.45	.749	.375	47.5	1.65	469	82.66	.394	.266	36.7
3	232.3	222.4	17.99	318	3.92	4.11	.630	.526	67.3	1.66	483	82.61	.394	.268	36.4
4	229.9	220.9	17.49	349	4.36	4.81	.537	.741	97.8	1.68	531	82.53	.394	.271	36.0
5	226.7	219.0	16.85	403	5.08	5.54	.462	.812	106.6	1.69	613	82.42	.394	.273	35.8

(Continued)

Table II (Continued-16)

ℓ ft	T_i °F	T_b °F	p psia	$h_B \cdot 10^{-1}$ $\frac{BTU}{hr ft^2 °F}$	$\frac{h_B}{h_\ell}$	x %	X_{tt}	$\left(\frac{dp}{d\ell}\right)_{tpt}$ $\frac{psia}{ft.}$	$\frac{\left(\frac{dp}{d\ell}\right)_{tpt}}{\left(\frac{dp}{d\ell}\right)_\ell}$	$\frac{c\mu_\ell}{k_\ell}$	$\frac{h_B D}{k_\ell}$	$\frac{q}{h_{fg} G_T} \cdot 10^{-6}$	k_ℓ $\frac{BTU}{hr ft. °F}$	μ_ℓ c.p.	$\frac{G_T D}{\mu_\ell} \cdot 10^{-3}$
Run No. 64; m= 0.308 lb./sec.; G_T= 109.2 lb./sec.ft.^{2}; P= 9.78 KVA; q= 31,300 BTU/hr.ft.^{2}															
1	237.0	228.3	20.14	359	4.35	4.22	.647	.384	49.9	1.60	545	82.79	.395	.258	37.7
2	235.6	227.1	19.71	368	4.49	4.90	.558	.500	66.0	1.62	558	82.73	.395	.261	37.2
3	233.9	225.5	19.12	372	4.60	5.62	.483	.624	82.9	1.63	565	82.63	.395	.263	37.0
4	231.6	223.6	18.41	391	4.89	6.38	.421	.754	101.6	1.65	594	82.53	.394	.266	36.5
5	228.6	221.2	17.55	422	5.36	7.18	.367	.894	121.7	1.68	642	82.39	.394	.271	35.9
Run No. 65; m= 0.311 lb./sec.; G_T= 110.3 lb./sec.ft.^{2}; P= 9.84 KVA; q= 31,400 BTU/hr.ft.^{2}															
1	238.9	230.5	21.00	374	4.52	5.03	.561	.532	69.1	1.58	568	82.74	.395	.256	38.3
2	237.3	229.0	20.41	379	4.63	5.73	.488	.625	82.6	1.60	575	82.66	.395	.258	38.0
3	235.6	227.2	19.72	374	4.64	6.45	.429	.741	98.7	1.62	568	82.56	.395	.261	37.6
4	233.0	225.0	18.91	393	4.93	7.19	.380	.871	117.2	1.64	597	82.43	.395	.264	37.1
5	229.4	222.3	17.97	443	5.65	8.00	.333	1.029	140.7	1.66	673	82.29	.394	.268	36.6
Run No. 66; m= 0.313 lb./sec.; G_T= 111.0 lb./sec.ft.^{2}; P= 9.84 KVA; q= 31,400 BTU/hr.ft.^{2}															
1	239.4	231.9	21.51	419	5.06	5.59	.511	.560	72.8	1.57	636	83.06	.395	.253	39.1
2	237.7	230.4	20.92	431	5.29	6.29	.453	.668	87.6	1.58	654	82.34	.395	.256	38.6
3	235.8	228.4	20.18	425	5.27	7.02	.400	.800	106.6	1.60	645	81.96	.395	.258	38.3
4	233.0	225.9	19.28	443	5.58	7.79	.355	.960	129.8	1.62	673	81.83	.395	.262	37.7
5	229.3	223.0	18.23	499	6.39	8.61	.313	1.195	162.8	1.66	759	81.68	.394	.267	37.0

(Continued)

Table II (Continued-17)

ℓ ft	T_i °F	T_b °F	p psia	$h_B \cdot 10^{-1}$ $\frac{BTU}{hr ft^2 °F}$	$\frac{h_B}{h_\ell}$	x %	X_{tt}	$\left(\frac{dp}{d\ell}\right)_{tpt}$ $\frac{psia}{ft.}$	$\frac{\left(\frac{dp}{d\ell}\right)_{tpt}}{\left(\frac{dp}{d\ell}\right)_\ell}$	$\frac{c\mu_\ell}{k_\ell}$	$\frac{h_B D}{k_\ell}$	$\frac{q}{h_{fg} G_T} \cdot 10^{+6}$	k_ℓ $\frac{BTU}{hr ft. °F}$	μ_ℓ c.p.	$\frac{G_T D}{\mu_\ell} \cdot 10^{-3}$
Run No. 67; m= 0.316 lb./sec.; G_T= 112.1 lb./sec.ft.^{2}; P= 9.84 KVA; q= 31,400 BTU/hr.ft.^{2}															
1	241.2	234.2	22.41	449	5.44	6.95	.423	.714	94.2	1.54	681	81.64	.395	.249	40.0
2	239.4	232.3	21.71	443	5.44	7.66	.380	.814	108.7	1.56	671	81.54	.395	.252	39.5
3	237.0	230.1	20.83	463	5.68	8.41	.341	.942	126.6	1.58	703	81.45	.395	.256	38.9
4	234.0	227.4	19.83	476	6.00	8.92	.312	1.100	149.3	1.61	724	81.28	.395	.260	38.3
5	230.1	224.2	18.92	533	6.91	9.94	.276	1.211	167.2	1.65	810	81.14	.394	.266	37.4

Appendix C - Sample Calculations

The experimental data were partially reduced by taking the thermocouple emf and tranducer emf and converting these into temperatures and pressures respectively. These were then plotted versus length from the entrance of the heated section, and a smooth curve was placed through these points. The bulk fluid temperature was then determined from the saturation pressure, and it was also plotted. Five heat-transfer coefficients were determined per run. Starting one foot from the entrance of the heat section, heat-transfer coefficients were determined at one-foot intervals. Figures 27 and 28 are plots of experimental data from run 57. A sample calculation will be made for run 57 at a point which is five feet from the entrance of the heated section.

a. Vapor Mass Fraction

The vapor mass fraction, x, was determined by assuming a homogeneous model and writing a total energy balance on the fluid from before the flashing valve to the position of interest in the test section. As a first approximation, the kinetic energy terms were assumed negligible. This resulted in the following:

$$\overset{o}{x} = \frac{h_1 - h_f + \left(\frac{Q_T}{mL}\right)\ell - \frac{1}{J}(z - z_1)}{h_{fg}} ,$$

where

h_1 = enthalpy of liquid before flashing valve, BTU/lb,

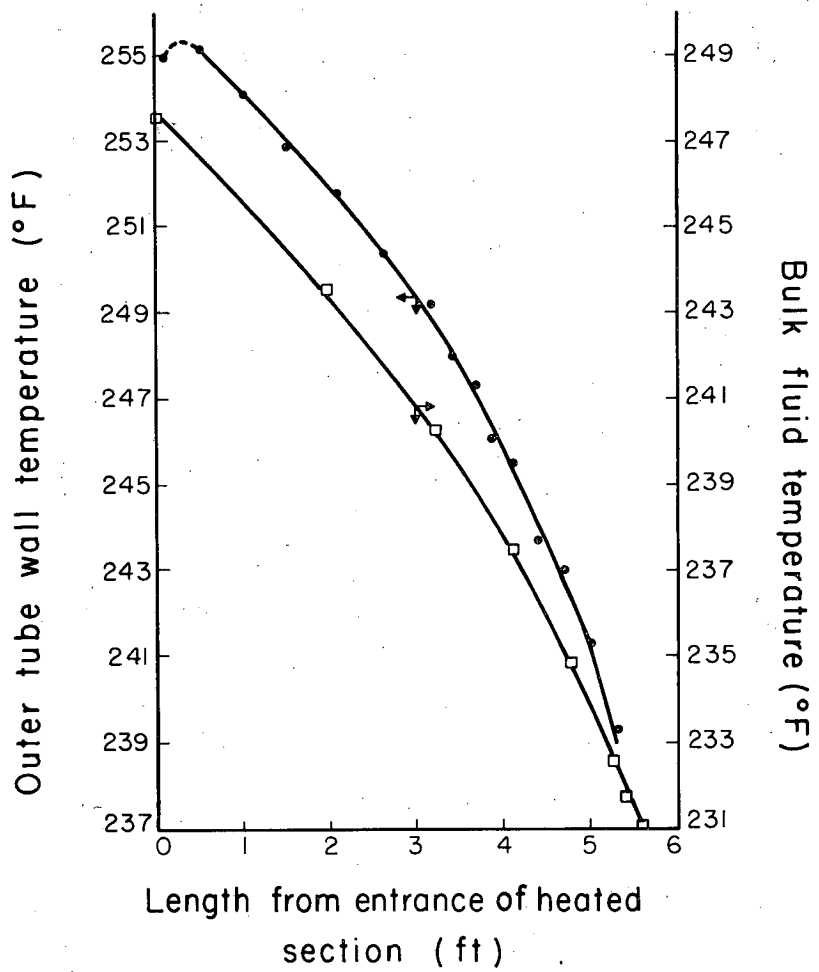

MU-18770

Fig. 27. Outer wall and bulk fluid temperatures for Run 57.

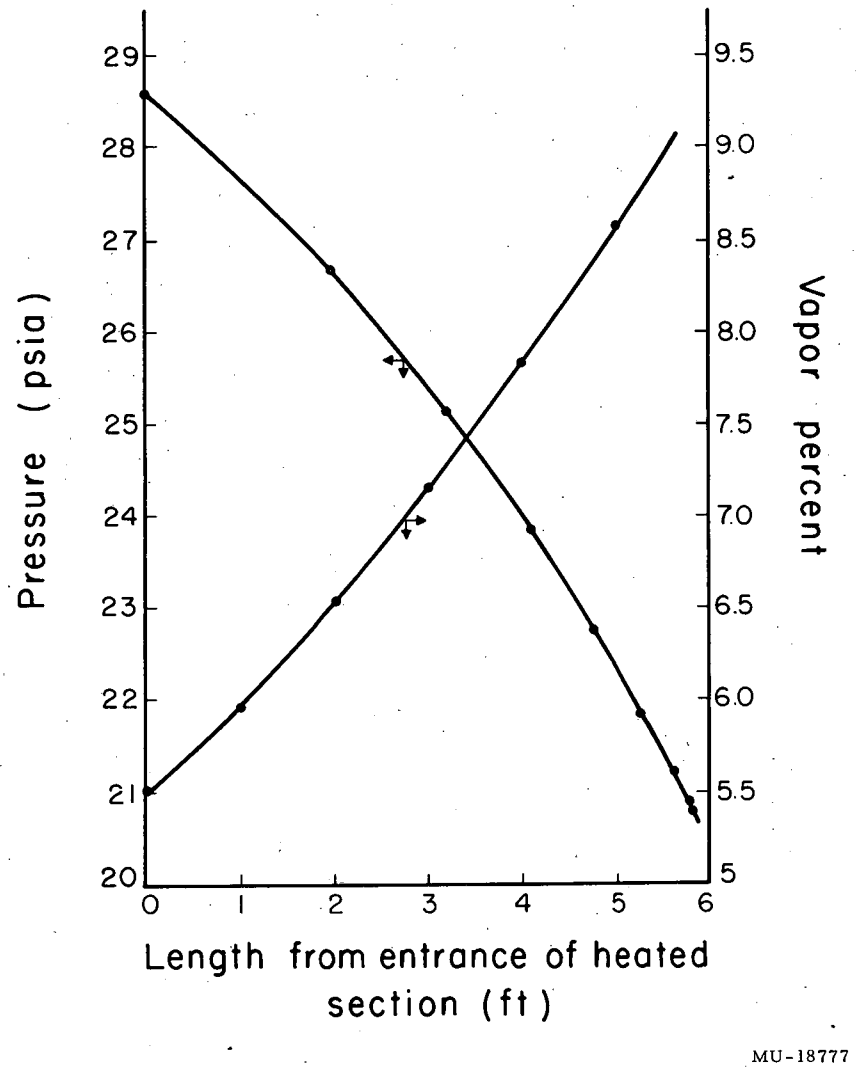

MU-18777

Fig. 28. Local static pressure and quality for Run 57.

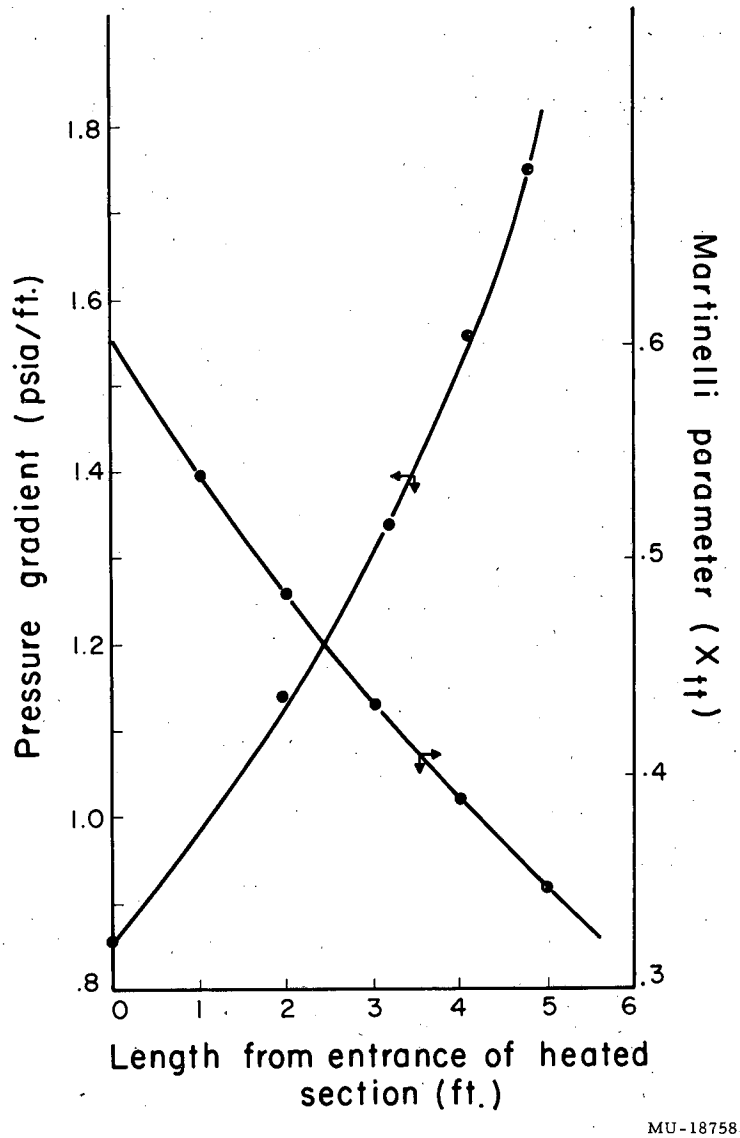

Fig. 29. Pressure gradient and Martinelli parameter for Run 57.

h_f = local enthalpy of liquid, BTU/lb,

m = mass flow rate, lb /sec,

L = total length of heated section, ft,

$(z-z_1)$ = vertical distance from flashing valve to point of interest, ft,

h_{fg} = heat of vaporization, BTU/lb.

This vapor mass fraction was then used to calculate the kinetic energy change. The kinetic energy of the liquid preceding the flashing valve was considered negligible.

$$\Delta(K.E.) = \frac{G_T^2 V^2}{2gJ} = \frac{G_T^2}{2gJ}\left(V_f + \overset{0}{X}\, V_{fg}\right)^2$$

This kinetic energy term was substituted into the complete energy equation to obtain a second approximation of x,

$$\overset{1}{x} = \frac{h_{fg}x - \Delta(K.E.)}{h_{fg}} .$$

This converged very rapidly. Since all the experimental runs of interest in this study were made at low qualities, one iteration was all that was required.

The following values were obtained from the reduced-data sheet for run 57 and the Keenan and Keyes steam tables (7):

T_o = 298.0°F	m = 0.464 lb/sec	G_T = 164.5 lb/sec ft^2
T_b = 233.9°F	ℓ = 5 ft	P = 9.84 KVA
V_f = 0.01687 ft^3/lb	$(z-z_1)$ = -7 ft	h_1 = 267.5 BTU/lb
V_g = 18.12 ft^3/lb	L = 5.67 ft	h_f = 202.1 BTU/lb
V_{fg} = 18.10 ft^3/lb		h_{fg} = 956.3 BTU/lb

Therefore:

$$\overset{0}{x} = \frac{267.5-202.1+\frac{(9.84)(3412)(5)}{(0.464)(5.67)(3600)} + \frac{7}{778}}{956.3} = 0.0869,$$

$$\Delta(K.E.) = \frac{(164.5)^2}{(2)(32.17)(778)}\left[0.01687 + (18.10)(0.0869)\right]^2 = 1.37,$$

$$\overset{1}{x} = \frac{(956.3)(0.0869) - 1.37}{956.3} = 0.0855.$$

b. Martinelli Parameter

The Martinelli parameter, X_{tt}, was calculated from the defining equation,

$$X_{tt} = \left(\frac{V_f}{V_g}\right)^{0.5}\left(\frac{u_f}{u_g}\right)^{0.1}\left(\frac{1-x}{x}\right)^{0.9} .$$

From the reduced-data sheet and from quantities previously calculated, the following results:

$$X_{tt} = \left(\frac{0.01687}{18.12}\right)^{0.5}\left(\frac{0.249}{0.01301}\right)^{0.1}\left(\frac{1-0.0855}{0.0855}\right)^{0.9} = 0.347.$$

c. Boiling Heat Transfer Coefficients

The heat transfer coefficient was calculated from the definition

$$h_B = \frac{q}{(T_i - T_b)} ,$$

where

q = local heat flux at inner wall, BTU/hr ft^2,

T_i = inner wall temperature as computed from the measured outside wall temperature, T_o, and figure 26,

T_b = bulk fluid temperature, which was assumed to be the temperature of saturated liquid at the pressure, which was obtained from figure 27.

For this particular run and tube position the following quantities were obtained from Figures 27 and 28:

$$T_o = 241.2°F, \quad T_b = 233.9°F, \quad q = 31{,}400 \text{ BTU/hr ft}^2.$$

From Figure 26 the drop through the wall for this particular heat input and outer wall temperature is 1.9°F. Therefore,

$$T_i = T_o - 1.9 = 241.2 - 1.9 = 239.3°F$$

and

$$h_B = \frac{31{,}400}{(239.3-233.9)} = 5820 \text{ BTU/hr ft}^2\,°F.$$

d. Nonboiling Heat Transfer Coefficient (Boiling Runs)

The nonboiling heat transfer coefficients were calculated from the Dittus-Boelter correlation,

$$Nu_\ell = 0.023\, Re_\ell^{0.8}\, Pr_\ell^{0.4}.$$

The Reynolds number and Prandtl number were calculated on the basis of local liquid flow and not on total mass flow. All fluid properties were assumed to be those of the fluid state evaluated at the local saturation temperature. From the reduced-data sheet we have

$$Re_T = 58{,}800, \quad Pr_\ell = 1.54, \quad k_\ell = 0.395 \text{ BTU/hr ft °F}.$$

Therefore

$$Re_\ell = Re_T(1-x) = (58,800)(0.9131) = 53,690$$

and

$$h_\ell = \frac{(0.023)(0.395)}{5.996 \cdot 10^{-2}} (1.54)^{0.4}(53,690)^{0.8} = 1110.$$

The nondimensional ratio of heat transfer coefficients may now be calculated:

$$\frac{h_B}{h_\ell} = \frac{5820}{1110} = 5.25,$$

$$\frac{Nu_B}{Re_\ell^{0.8} Pr_\ell^{1/3}} = \frac{h_B}{h_\ell} (0.023) \frac{Pr^{0.4}}{Pr^{1/3}} = 0.124 .$$

e. Boiling Number

The boiling number was calculated from the defining equation

$$Bo = \left(\frac{q}{h_{fg} G_T}\right).$$

From the reduced-data sheet and the Keenan and Keyes tables (6) we have

$$q = 31,400 \text{ BTU/hr ft}^2,$$

$$G_T = 164.5 \text{ lb/sec ft}^2,$$

$$h_{fg} = 956.3 .$$

Therefore

$$B_o = \frac{31,400}{(956.3)(164.5)(3600)} = 55.5 \cdot 10^{-6} .$$

X. BIBLIOGRAPHY

1. D. E. Dengler, "Heat Transfer and Pressure Drop for Evaporation of Water in a Vertical Tube," Chem. Eng. Progr. Sym. Series 52, 95-103 (1956).

2. R. G. Deissler, "Analysis of Turbulent Heat Transfer and Flow in the Entrance Regions of Smooth Passages," NACA TN3016.

3. F. W. Dittus and L. M. K. Boelter, "Heat Transfer in Automobile Radiators of the Tubular Type," University of California Publication in Engineering, 2, 443 (1930).

4. R. G. Eckert, "Introduction to the Transfer of Heat and Mass " (McGraw-Hill Book Co., Inc., 1950), p. 115.

5. R. G. Eckert, A. J. Diaguila, and A. N. Curren, "Experiments on Mixed-Free and Forced Convective Heat Transfer Connected with Turbulent Flow Through a Short Tube," NACA TN 2974.

6. L. M. Grossman and V. E. Schrock, "Local Pressure Gradients in Forced Vaporization," Nuclear Science and Engineering 3, 245-250 (1959).

7. J. H. Keenan and F. G Keyes, "Thermodynamic Properties of Steam " (John Wiley and Sons, Inc., New York, Twenty-Sixth Printing, 1954).

8. D. L. Linning, "The Adiabatic Flow of Evaporating Fluids in Pipes of Uniform Bore," Proc. Inst. Mech. Eng. (B) 1B, 64 (1952).

9. R. W. Lockhart and R. C. Martinelli, "Proposed Correlation of Data for Isothermal Two-Phase, Two-Component Flow in Pipes," Chem. Eng. Progr. 45, 39 (1949).

10. R. C. Martinelli and D. B. Nelson, "Prediction of Pressure Drop During Forced-Circulation Boiling of Water," Trans. ASME 70, 695 (1948).

11. J. F. Mumm, "Heat Transfer to Boiling Water Forced Through a Uniformly Heated Tube," Argonne National Lab. Report ANL-5276.

12. P. J. Schneider, "Effect of Axial Fluid Conduction on Heat Transfer in the Entrance Regions of Parallel Plates and Tubes " (Heat Transfer and Fluid Mech. Inst., Stanford University Press, 1956).

BIBLIOGRAPHY(Continued)

13. V. E. Schrock and L. M. Grossman, "Local Heat Transfer Coefficients and Pressure Drop in Forced Convection Boiling," Submitted to University of California Radiation Lab., Livermore, California, Sept. 30, 1957.

14. V. E. Schrock, Personal Communication.

15. E. N. Sieder and G. E. Tate, "Heat Transfer and Pressure Drop of Liquids in Tubes," Ind. Eng. Chem. 28, 1429-1436 (1936).

16. R. Siegel and E. M. Sparrow, "Turbulent Flow in a Circular Tube with Arbitrary Internal Heat Sources and Wall Heat Transfer," Trans. ASME Journal of Heat Transfer 81, 280-290 (1959).

This report was prepared as an account of Government sponsored work. Neither the United States, nor the Commission, nor any person acting on behalf of the Commission:

A. Makes any warranty or representation, expressed or implied, with respect to the accuracy, completeness, or usefulness of the information contained in this report, or that the use of any information, apparatus, method, or process disclosed in this report may not infringe privately owned rights; or

B. Assumes any liabilities with respect to the use of, or for damages resulting from the use of any information, apparatus, method, or process disclosed in this report.

As used in the above, "person acting on behalf of the Commission" includes any employee or contractor of the Commission, or employee of such contractor, to the extent that such employee or contractor of the Commission, or employee of such contractor prepares, disseminates, or provides access to, any information pursuant to his employment or contract with the Commission, or his employment with such contractor.